

Udd
73756

UMTRI-86-35/III

The Influence of Weights and Dimensions on the Stability and Control of Heavy Duty Trucks in Canada

Final Report

Volume III - Appendices C-F

Robert D. Ervin
Yoram Guy

July, 1986

UMTRI The University of Michigan
Transportation Research Institute

Technical Report Documentation Page

1. Report No.		2. Government Accession No.		3. Recipient's Catalog No.	
4. Title and Subtitle THE INFLUENCE OF WEIGHTS AND DIMENSIONS ON THE STABILITY AND CONTROL OF HEAVY-DUTY TRUCKS IN CANADA - VOL. III - APPENDICES				5. Report Date July 1986	
				6. Performing Organization Code 388762	
7. Author(s) Robert D. Ervin, Yoram Guy				8. Performing Organization Report No. UMTRI-86-35/III	
9. Performing Organization Name and Address The University of Michigan Transportation Research Institute 2901 Baxter Road Ann Arbor, Michigan 48109				10. Work Unit No. (TRAIS)	
				11. Contract or Grant No.	
12. Sponsoring Agency Name and Address Canroad Transportation Research Corporation 1765 Saint Laurent Boulevard Ottawa, K1G 3V4, CANADA				13. Type of Report and Period Covered Final 5/84 - 7/86	
				14. Sponsoring Agency Code	
15. Supplementary Notes					
16. Abstract <p>The stability and control characteristics of heavy-duty truck combinations used in Canada were determined as an aid for the development of new regulations on the weights and dimensions of vehicles in interprovincial trucking. Truck combinations which are currently in use in Canada were first identified through a survey activity. Parameters describing these vehicles were evaluated and an extensive computerized analysis of dynamic performance characteristics was conducted. Full-scale tests were run as a supplement to the computerized study for three of the selected vehicles.</p> <p>The results serve to classify the contrasting dynamic performance qualities of some 22 vehicle configurations, distinguished by number and placement of axles, number of trailers, and type of hitching mechanisms. Also, the sensitivity of the dynamic behavior of each configuration to variations in weights and dimensions, as well as certain component properties, is determined. Novel measures of performance were developed for characterizing (1) the dynamic stability of roll-coupled trailer combinations and the offtracking overshoot in a rapid path-change maneuver, and (2) the potential for low-speed jackknife while towing a trailer with multiple-wide-spread axles around a tight turn. Generalized performance evaluation techniques are outlined for future use in examining prospective new vehicle combinations.</p>					
17. Key Words trucks, safety, stability, control, offtracking, size and weight, regulation			18. Distribution Statement UNLIMITED		
19. Security Classif. (of this report) NONE		20. Security Classif. (of this page) NONE		21. No. of Pages 125	22. Price

TABLE OF CONTENTS

APPENDIX	<i>Page</i>
C Algorithms for Computing Performance Measures.....	1
D Presentation of Simulation Matrix.....	28
E Demonstartion Test Program.....	60
F Data-Base of Simulation Results.....	102

APPENDIX C

ALGORITHMS FOR COMPUTING PERFORMANCE MEASURES

Maneuver "a"

Maneuver "a" serves for the calculation of three performance measures:

- a(1) - Static Rollover Threshold
- a(2) - Steady-State Yaw Stability
- a(3) - Steady-State High Speed Off-Tracking.

The maneuver consists of a constant-radius turn of 10 seconds duration, intended to maintain a lateral acceleration of 0.2 G's at 100 km/hr, then switching to a constant-rate ramp-steer, producing a spiral path of slowly-increasing curvature and lateral acceleration up to vehicle rollover. The first, constant radius portion of the maneuver is simulated with closed-loop control, the driver model parameters being specified for optimum tracking precision. For the second, ramp-steer (spiral) portion of the maneuver, the steering control is switched to open-loop, with a constant-rate steer of 2.0 deg/sec being applied at the steering wheel, starting from the final steer condition left by the driver model at $t = 10$ sec.

The constant-radius portion serves for the evaluation of the high speed off-tracking measure, and closed-loop control is required here in order to achieve and maintain the specified turning radius with vehicles differing widely in their steady-state steer properties (path curvature gains). The spiral portion of the maneuver serves for the evaluation of the combination's static rollover threshold and the tractor's yaw stability. The latter must be simulated in open-loop mode in order to prevent any driver intervention. Such intervention would mask the tractor's basic steering response, as well as introduce undesirable oscillations. In order to provide for smooth and quick stabilizing of the vehicle in its constant-radius, 0.2 G condition after the start of the simulation run, during the first 2 seconds the vehicle is made to negotiate a quasi-spiral entry section consisting of 3 tangentially-matching path segments of equal duration, and constant, but distinct, radii. The three radii are set sequentially to yield nominal lateral acceleration values of 0.05, 0.10 and 0.15 G's, respectively. The final, fourth radius (corresponding to 0.2 G's) is encountered at $t = 2.0$ sec. The steer-input damping provided by the driver model helps smooth-out the transitions between the segments and contributes to minimize the undesirable oscillations and response-overshoot associated with stepped inputs. The

driver-model control parameters found to provide optimum tracking performance in this maneuver were: Transport Lag = 0.0 sec, Preview Interval = 0.3 sec.

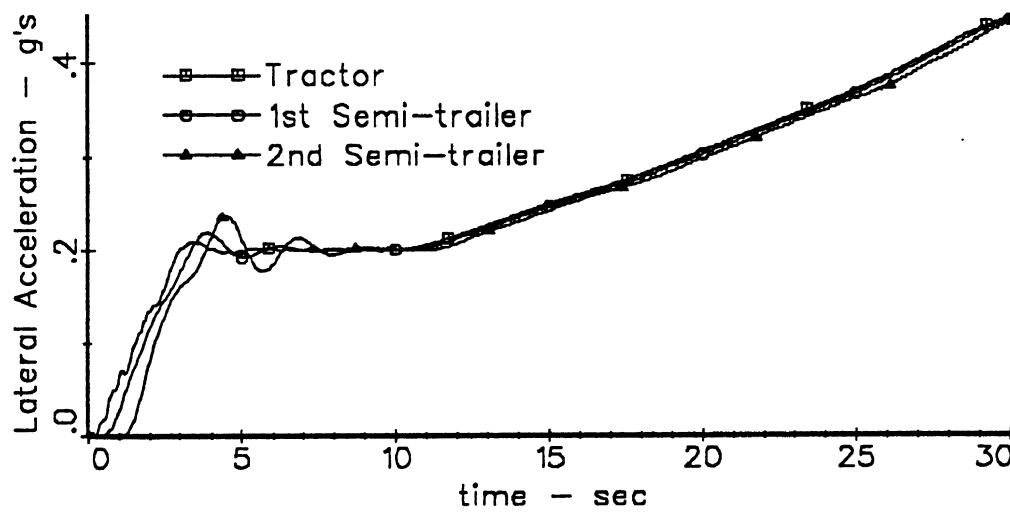
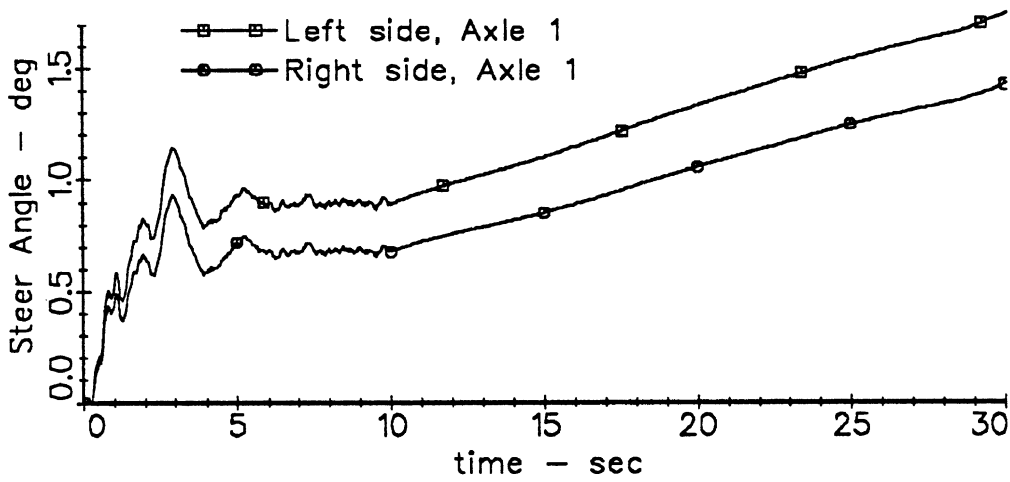
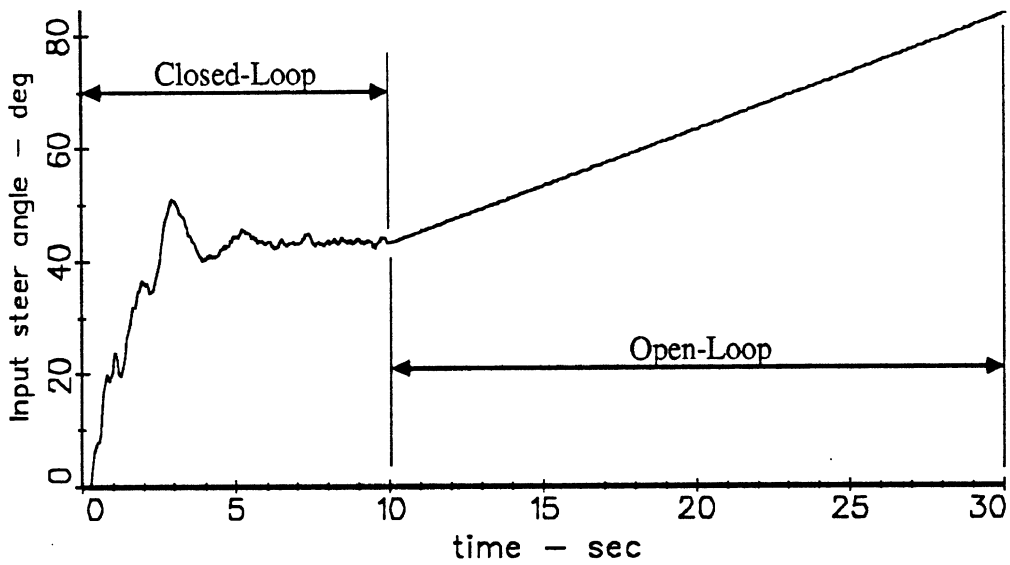
Typical time-histories, characteristic of maneuver "a", are presented in Figures C.0. Detailed discussions of the evaluation algorithms, as applied on these time-histories for the derivation of each of the "a" measures, follow. Note, that because of their oscillatory response, triples were not subjected to the ramp-steer portion of the maneuver, but rather to an extended constant-steer, "nominally 0.2 G's" condition resulting from freezing the steering wheel angle at $t = 12.0$ sec, and maintaining its value until $t = 20.0$ sec.

a(1) - Static Rollover Threshold

An open-loop, constantly increasing ramp-steer input of 2.0 deg/sec at the steering wheel is imposed from an initial steady-state condition of 0.2 G. Based on its hitch types, the combination is divided into separate roll-uncoupled sections ("roll-units") by way of identifying the first and last axles and articulation-units of each roll-unit. For example, an 8-axle A-train double with tandem axles at all positions except at the tractor steering axle and at the dolly would be divided into two roll-units - the first roll unit would include the tractor and the lead semitrailer (articulation units No. 1 and 2, axle No. 5 is last), and the second roll-unit would comprise the dolly and the rear semitrailer (articulation units No. 3 and 4, axle No. 6 is first). An equivalent C-train double would be considered one roll-unit.

The objective of this algorithm is to identify the time-step at which a complete lift-off has first occurred at all wheels on one side of any roll-unit, indicating the steady-state rollover threshold for the combination at the corresponding lateral acceleration. At each time-step, the vertical ground loads of all axles for each roll-unit are being screened separately for each side. The lead steer axle is never included, since its own roll stiffness is so low relative to that of any of the load carrying axles, that it would experience lift-off only long after the onset of a terminal rollover condition. The time-step is incremented until first total lift-off on one side at any roll-unit has occurred, as indicated when all vertical loads on that side equal to zero for the first time. At that time-step, the lateral acceleration of the last articulation-unit within the roll-unit that experienced lift-off is recorded as the combination's rollover threshold.

The actual acceleration value is obtained from an arithmetic average of that articulation-unit's lateral acceleration values over the period of ± 0.15 sec about the actual time-step of lift-off. This is done in order to locally smooth-out high-frequency noise in the acceleration time history. From the first lift-off time-step, the above outlined screening



RTAC 8 axle A-train Doubles (49t/108k GCW), conf. 2.1, var. 2.02

Figure C.0 - Maneuver "a"

procedure is continued for another 0.2 sec in order to verify, that the condition is actually a sustained lift-off, and not a local wheel-hop. If within the 0.2 sec the lift-off assumption is violated (evidenced by one or more zero ground loads becoming positive), the lift-off is ignored and the screening procedure is continued as described above.

a(2) - Tractor Steady-State Yaw Stability

This measure involves the continuous computation of the tractor's understeer-coefficient (or understeer-gradient) along the time history of the same low-rate ramp-steer maneuver that serves for extracting measure a(1). The goals of this computation are - 1) to obtain the tractor's understeer-coefficient at a nominal steady-state lateral acceleration of 0.25 G's, and - 2) to detect the onset of tractor yaw divergence, if taking place prior to rollover. The steady-state understeer-coefficient U is a non-dimensional differential function (to be precise, it has the units of radians/G), defined as follows:

$$U = d(\delta_{sw}/n - L\rho) / d(A_y) \quad (C.1)$$

where: δ_{sw} - Steering-wheel angle, radians

n - Overall steering ratio, steering-wheel-radians/front-wheel-radians

L - Tractor wheelbase, ft

ρ - Tractor path curvature, 1/ft

A_y - Lateral acceleration, G's

d - The differential operator.

In this formulation, the influences of roll-steer (and/or suspension compliance, if any) on the tractor's steady-state steer characteristics are implicitly accounted for, and by using steering-wheel angles (and steering ratio) rather than front wheel angles, any steering-system compliance effects are also included in the understeer-coefficient calculation. Figure C.1 illustrates schematically this analytical definition of the understeer-coefficient and its derivation from numerical data.

In order to discretize the analytical function (C.1) so as to perform numerical differentiation (obtain the slope of A_y at some point j) on the output data, one may assume some two actual output steps, i and k , that bracket point j , and which are sufficiently distant from each other so as to minimize inaccuracy in calculating the slope due to numerical noise, yet sufficiently close to j so as to minimize inaccuracy due to curvature (local changes in the "real" value of U in the vicinity of these three points). In other words -

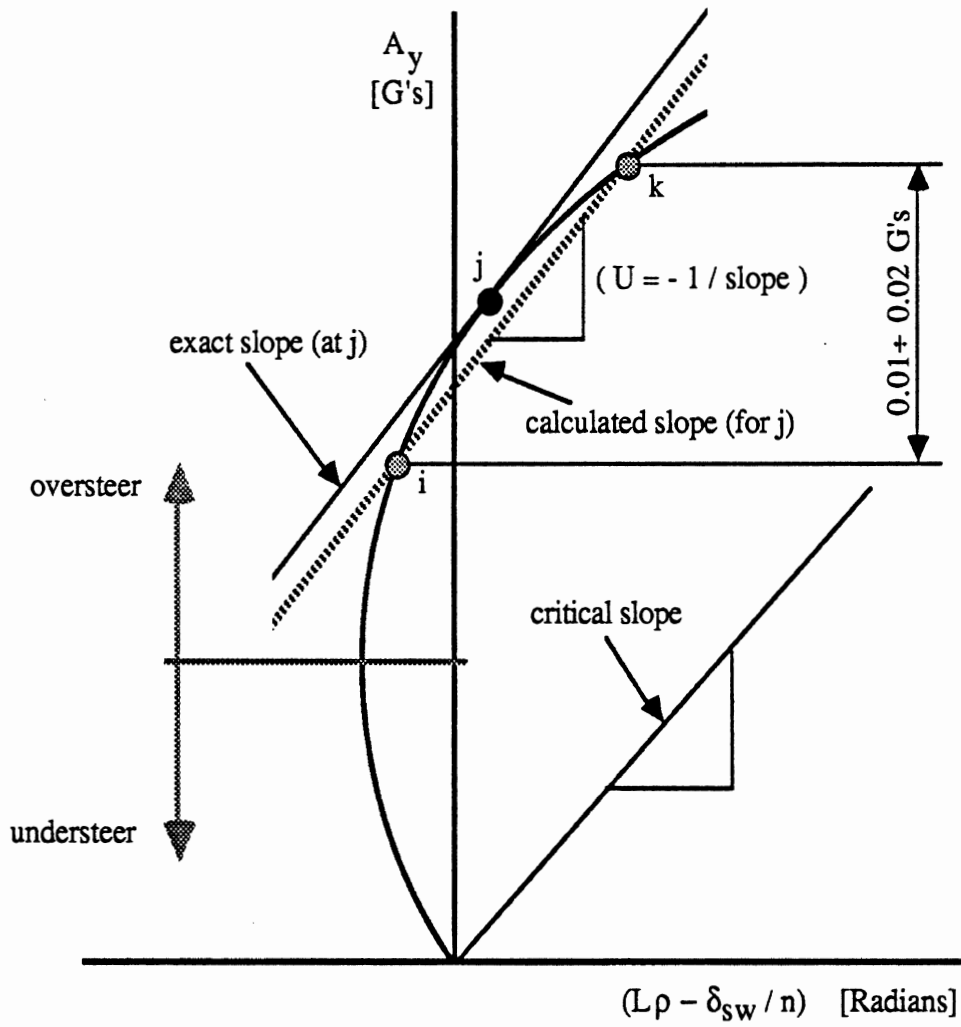


Figure C.1 - Handling diagram and numerical derivation of understeer-coefficient

referring again to Figure C.1 - any point j , at which the understeer-coefficient is to be computed, will have associated with it a pair of i,k points bracketing it, and defining the understeer-gradient near it. The change in the value $(\delta_{sw}/n - L\rho)$ in the numerator for a corresponding change in the value of lateral acceleration A_y in the denominator is strongly dependent upon the effects of lateral load transfer over the tractor tandem axles and tractor roll angle, both affected mostly by the lead semitrailer. Hence, the lateral acceleration values actually employed in the denominator were the semitrailer's, rather than the tractor's, and will be denoted A_{ys} . (this may be superfluous, since, as can be seen from the bottom plot of Figure C.0, the slopes of all the A_y curves are very close at the vicinity of 0.25 G's.) Also, since the actual time history of the tractor's path curvature, ρ , was found to be not quite smooth enough for the purpose of this calculation, it was approximated instead by: $\rho \approx A_{yt} G / V^2$, where A_{yt} denotes the tractor's lateral acceleration (in G's), and V is the forward velocity (in ft/sec).

Using the symbols and subscripts defined above, the tractor's understeer-coefficient U at point j , in discretized and approximated formulation, is:

$$U_j \approx \{ [(\delta_{sw} / n - L A_{yt})_k - (\delta_{sw} / n - L A_{yt})_i] / [(A_{ys})_k - (A_{ys})_i] \} G / V^2 \quad (C.2)$$

As can be seen from equation (C.2), the simulation variables whose time histories serve for the computation are the steering-wheel angle δ_{sw} , the tractor lateral acceleration A_{yt} , and the lead semitrailer lateral acceleration A_{ys} . Figure C.2 shows schematically an example time-history segment for any one of the above, and serves to support the following discussion. In order to accurately yet efficiently process these time histories, it is necessary to select - 1) the appropriate "time-differential", ΔT_{ik} , between the points i and k , - 2) the appropriate "computation-interval", ΔT_j , between successive U calculations (that is, between successive samplings of i,k pairs), and - 3) an adequate averaging or smoothing scheme, that would provide reliable numerical values for each of the variables sampled at each point.

Based on a rather considerable trial-and-error-type search, a time-differential, ΔT_{ik} , of 1.0 sec, and a computation-interval, ΔT_j , of 0.5 sec were selected, "sec" referring to simulated maneuver seconds. The value of the variable sampled at each point was established by averaging its recorded values over the sampling-interval ΔT_s of ± 0.5 sec about the nominal point. This method afforded reasonable computational efficiency by taking advantage of the $(\Delta T_s / 2)$ overlap shared by successive sampling-intervals ΔT_s (for averaging, summations over "second-half" of each ΔT_s are stored and recalled for "first-half" of next ΔT_s). Further advantage was taken of the fact that, basically, only the end-point, k , out of every i,k pair has to be evaluated per each computation-step j , since its

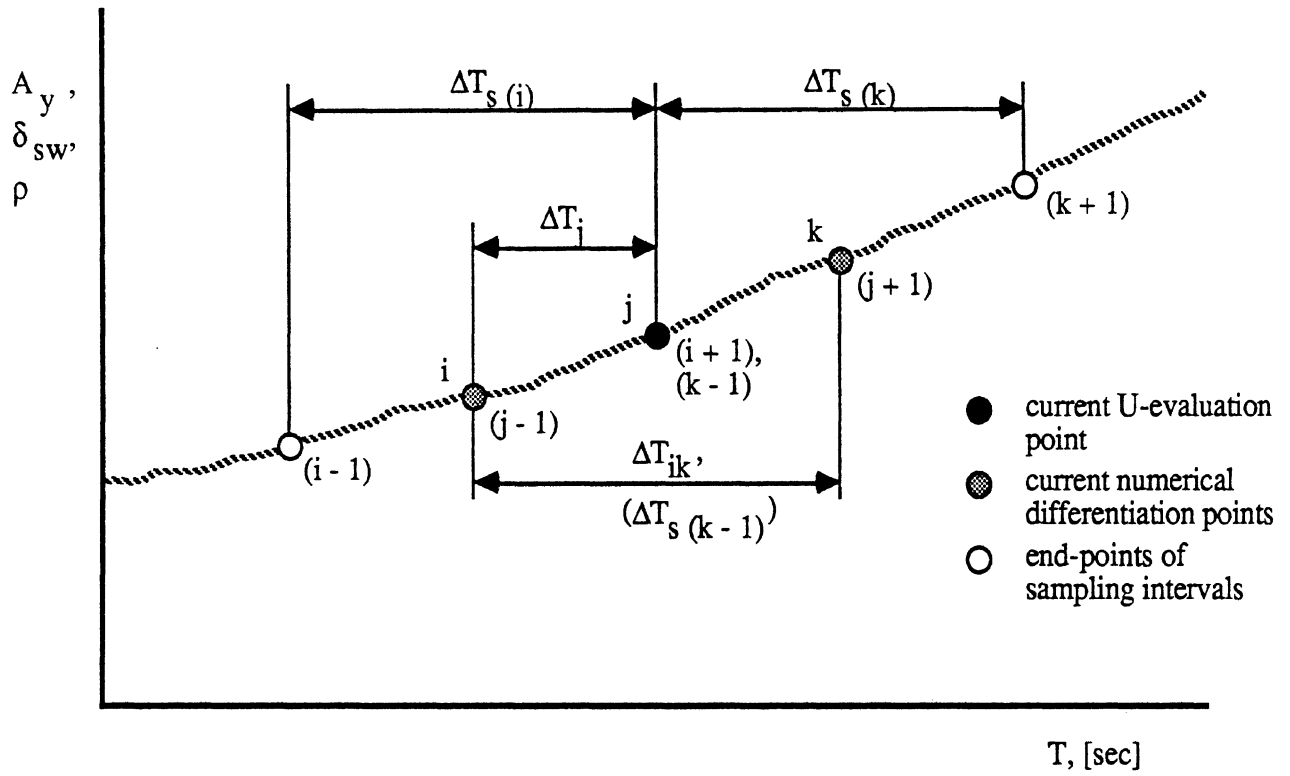


Figure C.2 - Sampling scheme of time-histories used in derivation of understeer-coefficient

start-point, i , has been evaluated as the end-point $k - 2$ of computation step $j - 2$. Figure C.2 should be consulted for clarity of the above discussion.

The selected ramp-steer rate of 2.0 deg/sec at the steering wheel yields an approximate rate of increase in lateral acceleration between 0.01 and 0.02 G's per second, depending on vehicle. The simulation output frequency selected was 20 steps/sec. To speed-up the processing, the computation begins at the time-step at which the lead-semitrailer's instantaneous (non-smoothed) value of lateral acceleration first exceeds 0.22 G's. From this point on, the averaging (smoothing) scheme described above is employed, and the understeer-coefficient is successively computed. The nominal 0.25 G condition is considered as the iteration-step j for which the $(A_y)_k$ value first equals or exceeds 0.25, while the corresponding $(A_y)_i$ value is less than 0.25 (referring to (C.2)).

In order to detect an onset of yaw-divergence, if any, the critical understeer-coefficient for a given speed, V , (100 km/hr here) can be readily computed, using the same symbols as before, from the equation:

$$U_{\text{critical}} = - LG / V^2 \quad (\text{C.3})$$

This calculation is performed before the start of the successive U -computation process, and later, at each iteration, the following condition: $U > U_{\text{critical}}$, is checked. If this inequality is violated, yaw-divergence is declared, the corresponding lead-semitrailer lateral acceleration is recorded, and further processing is halted. The lateral acceleration value recorded, $(A_y)_j$, is actually $(A_y)_{k-1}$ - calculated for end-point k of the previous iteration, ($j - 1$).

a(3) - Steady-State High-Speed Off-Tracking

This performance measure was evaluated at 100 km/hr at a nominal lateral acceleration of 0.2 G's. The maneuver was closed-loop (driver-model control) turning along a path of a constant radius equal to 393.3 m (1290.3 ft). The high-speed off-tracking measure evaluates the lateral distance between the path trajectories of the lead- and last-axle centerpoints in the above maneuver. These trajectories are obtained from the simulation as time histories of X-Y coordinates in the road axis system (inertial frame). The high-speed steady-state off-tracking measure is actually defined as an average lateral displacement between these two path trajectories, computed along portions of their time histories which satisfy certain steady-state criteria. Hence, the evaluation of this measure involves two

phases - locating of a satisfactory steady-state subrange within the simulation time-histories, and (if steady-state subrange successfully located) the actual off-tracking calculation.

Steady-State Definition: The criteria used for identifying a subrange of time-steps as satisfying the steady-state condition are: --

- 1) Lateral acceleration of last unit: For triples, the instantaneous value must remain without interruption within ± 0.015 G's of the nominal value of 0.2 G's. For all other combinations - within ± 0.005 G's of the nominal 0.2 G's. The wider tolerance range for triples was necessitated by their very oscillatory and under-damped transient behavior in Phase-4 simulations of this maneuver, a behavior which in some C-train cases prevented approaching steady-state cornering prior to the onset of numerical instability, and required an extended maneuver duration -- up to 20 seconds of constant radius turning.
- 2) Duration (length-overlap of steady-state path-portions of lead and last axles): Initially, the last uninterrupted sequence of time-steps within the whole time-history, during which criterion 1) remained valid, is identified by the sequential numbers of its limit-steps, $Step_{start}$ and $Step_{end}$. The number of time-steps, N_L , corresponding to the combination's overall wheelbase, is calculated by rounding-off the result of the expression:

$$N_L = (X_1 - X_L) / (V \Delta t) \quad (C.4)$$

where: X_1 - X-coordinate of lead axle at time-step #1, ft

X_L - X-coordinate of last axle at time-step #1, ft

V - Vehicle forward velocity, ft/sec

Δt - Step-size, sec.

The first necessary, but not sufficient, condition then required for declaring the achievement of a steady state for the purpose of this measure is stated by the inequality:

$$(Step_{end} - Step_{start} + 1) > (2 N_L + 0.1 / \Delta t) \quad (C.5)$$

where all symbols are as defined previously. Inequality (C.5) requires, basically, that the respective time-period during which criterion 1) is continuously satisfied exceed that needed by the vehicle to travel a forward distance equalling twice the overall wheelbase, plus 0.1 sec. Next, the step-range is reduced by moving its both limit-steps "inwards" by N_L steps each, such that $Step_{start}$ becomes $Step_{start} + N_L$, and $Step_{end}$ becomes $Step_{end} - N_L$. With 20 output-steps/sec, there will be at least 3 contiguous output-steps in the subrange $Step_{start}$ to $Step_{end}$. If the corresponding reduced time-period is found to exceed

0.5 sec, $Step_{start}$ is moved further forward, towards $Step_{end}$, so as to limit the time-period to 0.5 sec, according to the inequality:

$$(Step_{end} - Step_{start} + 1) \leq 0.5 / \Delta t \quad (C.6)$$

The corresponding number of steps is thus no more than 11. This is done in order to limit the amount of resulting computation.

Off-Tracking Calculation: Only if both steady-state criteria are fulfilled, is the actual off-tracking calculation invoked. The calculation is based on the averaging of off-tracking values for all output-steps within the portion of the last-axle trajectory which is contained between $Step_{start}$ and $Step_{end}$, as shown schematically in Figure C.3. The following discussion describes the evaluation of the local off-tracking OT_j of the last axle relative to the lead axle at some last-axle $Step_j$ between $Step_{start}$ and $Step_{end}$. The term "Step" above corresponds to a time-history output pair of X-Y coordinates, specifying an instantaneous location of the last-axle center in the inertial (road) frame. The first required action is to locate the particular lead-axle output-step, whose road X-Y point is the nearest to that of $Step_j$. This particular, "nearest" lead-axle point is indicated as $Step_{nearest}$ in Figure C.3. It is important to note here, that $Step_j$ and $Step_{nearest}$ are not adjacent or successive in time, but in the respective instantaneous positions on the road of the lead- and last-axle centers. In the time domain, $Step_j$ took place approximately N_L time-steps after $Step_{nearest}$, N_L having been calculated by equation (C.4).

Hence, the search for $Step_{nearest}$ will start at a lead-axle $Step_j - N_L - 2$, by successively calculating its road-distance D_j from last-axle $Step_j$, and then incrementing the lead-axle step until a minimum value for D_j was encountered (when the distance C_j associated with lead-axle $Step_{nearest} + 1$ is for the first time larger than the current D_j). The final notion is to evaluate the minimum distance of the road-point defined by lead-axle $Step_{nearest}$ from the path-trajectory of the last-axle. Having to deal with discrete numerical steps rather than with a continuous function, the last-axle path-trajectory at the vicinity of lead-axle $Step_{nearest}$ is approximated by the line-segment S_j . Using the relationship:

$$OT_j = D_j \cos(\theta), \quad \text{where: } \theta = \arctan(D_x / D_y) + \arctan(S_y / S_x), \quad (C.7)$$

the local off-tracking OT_j is readily calculated (see Figure C.3). If C_j is shorter than the distance P_j previously calculated for $Step_{nearest} - 1$, then previous last-axle $Step_j - 1$ is taken, instead of the next $Step_j + 1$, for the purpose of defining the last-axle path segment S_j and its slope S_y / S_x . Actually, only the squares of the intermediate-result distances (P_j , C_j) to

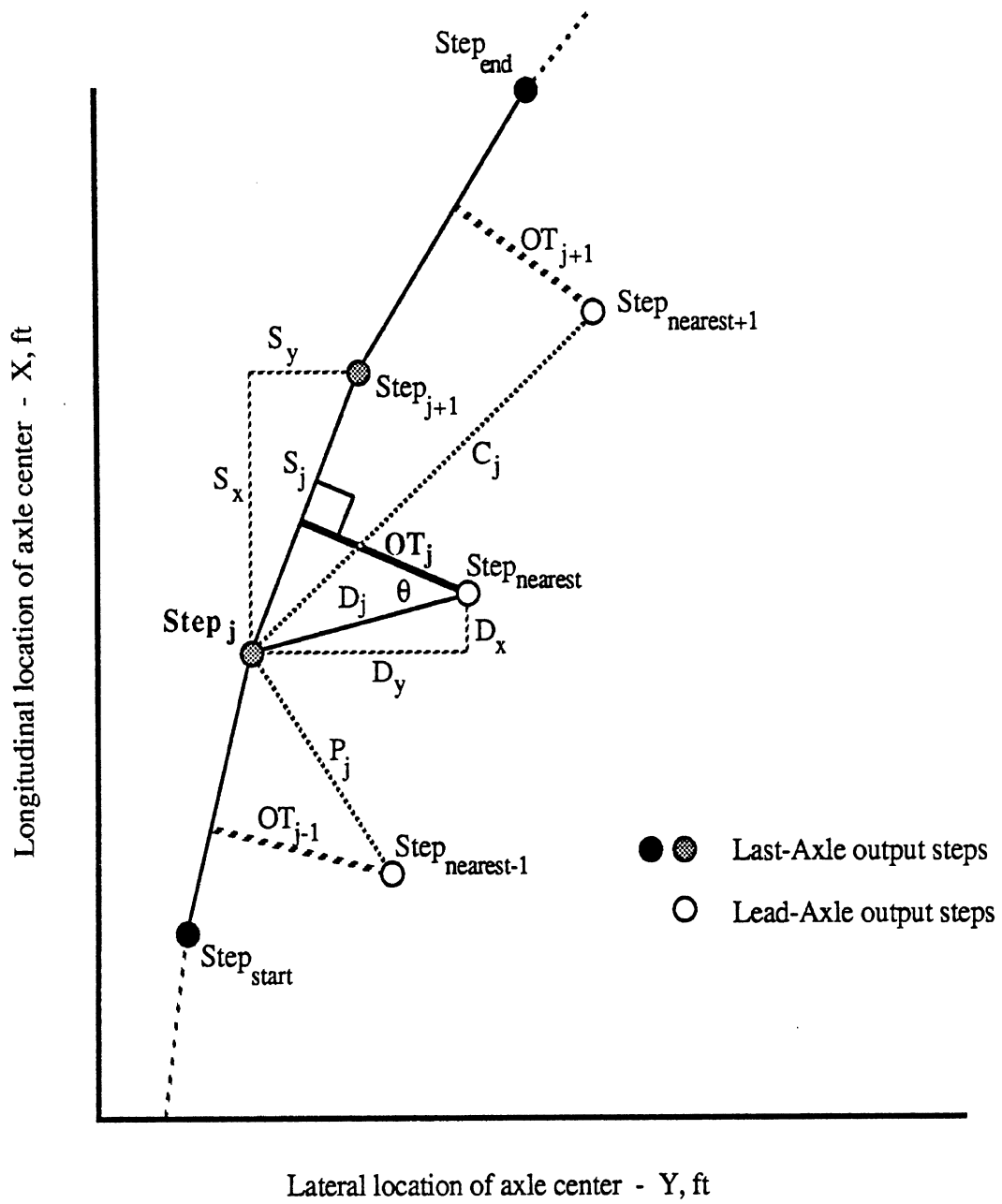


Figure C.3 - Steady-State High-Speed Off-Tracking Calculation Method

be compared in each nearest-step search are calculated (based on the Pythagorean Theorem), and no square roots are evaluated, so as to improve efficiency. The local off-tracking (OT_j) calculation is repeated for each last-axle Step_j from Step_{start} to Step_{end}, as defined above, and the final off-tracking measure is the arithmetic average of all resulting OT_j values.

Maneuver "b"

Maneuver "b" serves for the calculation of two performance measures, both associated with the rearward-amplification phenomenon, namely:

b(1) - Dynamic Rollover Threshold

b(2) - Transient High Speed Off-Tracking.

The maneuver consists of a rapid path change, intended to produce sinusoidal lateral acceleration at the tractor of 0.15 G's amplitude at 100 km/hr. Since rearward amplification is frequency-sensitive, and since vehicles vary in their peak-rearward-amplification frequencies, the maneuver is repeated for sine periods of 2.0, 2.5 and 3.0 seconds, in order to find and record for each combination its "worst" response. The simulation is performed in closed-loop control, aimed to allow reasonably precise tracking of road X-Y paths which were calculated to produce the specified tractor A_y time-histories. The equation used to generate these X-Y paths is given by:

$$Y = A B \{ X / v - B \sin [X / (v B)] \} \quad (C.8)$$

where: Y - Lateral coordinate of path-point in road reference frame, ft

X - Longitudinal coordinate of path-point in road reference frame, ft

v - Forward velocity, ft/sec.

A - Lateral-Acceleration Amplitude, ft / sec²

B = T / (2π), T being the sine period, sec.

A very short, straight entry segment requiring 0.5 sec at 100 km/hr leads into the above path-change segment, and a long exit straight follows. The total maneuver duration is normally 8.0 sec, 10.0 sec for triples and some lightly damped doubles. The driver-model control parameters found to provide optimum tracking performance in this maneuver were: Transport Lag = 0.0 sec, Preview Interval = 0.3 sec.

Typical time-histories, characteristic of maneuver "b", are presented in Figures C.4. Detailed discussions of the evaluation algorithms, as applied on these time-histories for the derivation of each of the "b" measures, follow.

b(1) - Dynamic Rollover Threshold

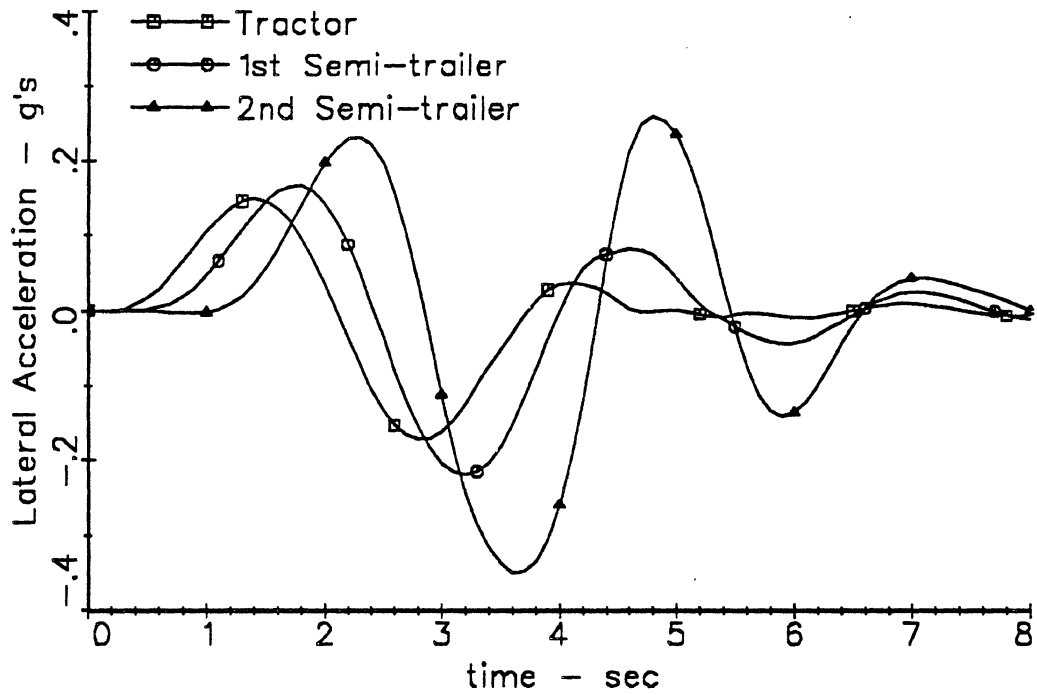
This objective of this measure is to identify and quantify the one instantaneous condition during the maneuver, at which any or all portions of the combination were the nearest to rollover. As a first step, any "uncoupled-in-roll" portions ("roll-units") in the combination are identified by their respective first- and last-axle positions and the total number of axles in the combination, and also by the first and last articulating-unit numbers in the sequence of all articulating units in the combination. This is done in exactly the same way as in the evaluation of measure a(1) - the static rollover threshold.

Two distinct, complementary performance measures were defined in order to accomplish the above objective. The primary measure is the "Load Transfer Ratio" (LTR), and the secondary one is the "Roll Margin" (RM). Their derivation algorithms are described below:

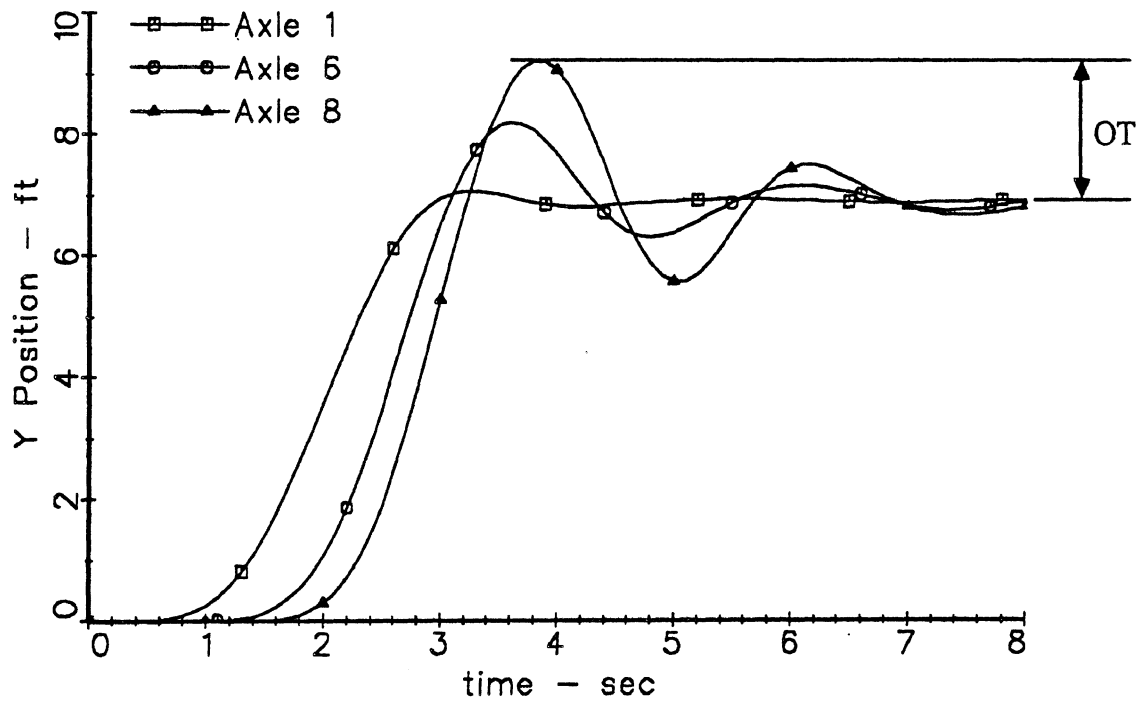
Load Transfer Ratio (LTR) - The LTR measure serves to indicate the instantaneous (and peak) amount of lateral transfer of tire vertical loads which took place between the two sides of each roll-unit during the maneuver. The definition of the LTR measure is:

$$\text{LTR} = | \Sigma (F_L - F_R) | / \Sigma (F_L + F_R) \quad (\text{C.9})$$

where F_L and F_R indicate vertical ground loads under the left- and right-hand-side tires of an axle, and Σ indicates summation over all the roll-unit's axles. For the roll-unit which includes the tractor, the summation always skips over the lead axle, as explained for measure a(1). At each time-step, beginning at $t = 1.0$ sec, and ending at the end of the simulation-run's time-history (usually at $t = 8.0$ sec), or with the detection of rollover, an LTR value is separately calculated for each roll-unit per equation (C.9). A symmetrical roll-unit at rest will yield an LTR value of 0.0 (zero load transfer). When a complete lift-off at any roll-unit has just occurred, the value of its LTR becomes 1.0 (100% load transfer), the corresponding time-step number is stored, and the RM calculation is then invoked for that roll-unit. During the maneuver, each roll-unit will experience two peaks of roll and lateral load transfer directly in response to the two peaks in curvature of the negotiated path trajectory. Usually, several subsequent peaks of decreasing magnitude will



RTAC two-semi 8 axle B-train (56.5t/125k GCW), conf. 3.1, var. 2.11



RTAC two-semi 8 axle B-train (56.5t/125k GCW), conf. 3.1, var. 2.11

Figure C.4 - Maneuver "b"

follow during the decay period along the exit path, and, occasionally, peaks of increasing magnitude will appear, indicating a divergent, unstable vehicle behavior. Also, there will always be considerable time-lag between the occurrences of roll-peaks in different roll-units.

Hence, for each roll-unit, the following procedure is separately pursued: At each time-step, the previous-step LTR value is compared with the current one, and the larger value is stored as the last-encountered LTR peak. After an actual LTR peak has been reached, each subsequent LTR peak encountered is compared with the previous one for relative magnitude, so that at the end of the iterating along the time-history, the largest LTR peak is retained as a maximum LTR value for that roll-unit. Finally, after the iteration process has ended, and if no RM values have been calculated, all the individual roll-unit LTR peaks are compared, and a maximum LTR for the whole maneuver and combination is identified and displayed together with its corresponding roll-unit number and time of occurrence.

In vehicle combinations which consist of just one roll-unit (such as tractor-semitrailers, B- and C-trains), the RM calculation is never invoked. Rather, a rollover is declared, and further processing abandoned, if the condition: $LTR > .999$ is continuously satisfied during a period longer than 0.4 seconds. In such cases, the lateral acceleration of the last unit in the combination at the first time-step of lift-off (leading to the rollover) is displayed. This time-step was stored, as described above.

Roll Margin (RM) - The RM measure was devised to quantify, in cases of complete but not terminal lift-off, how near was the roll-unit which experienced it to actual rollover. A schematic illustration of the concept behind the RM measure is provided in Figure C.5.a. The corresponding formulation and calculation scheme are illustrated in Figure C.5.b. Referring first to Figure C.5.a, the RM of a roll-unit is defined as:

$$RM = Y / H \quad (C.10)$$

where Y and H specify the instantaneous C.G. location of its total-mass in the roll-plane. Any articulation angle effects on roll statics are neglected in this algorithm. Thus, the main task is to find Y and H through evaluation of that total-mass C.G. location. Differences in heights of individual sprung-mass C.G.'s and roll-centers, and in track widths for each axle within the roll-unit must be accounted for. This is accomplished by defining and computing virtual total-masses and C.G. locations separately for each axle, and then calculating a weighted average C.G. location for the whole roll-unit. Prior to the start of the actual "per-time-step" RM computation sequence, all the relevant static parameters are

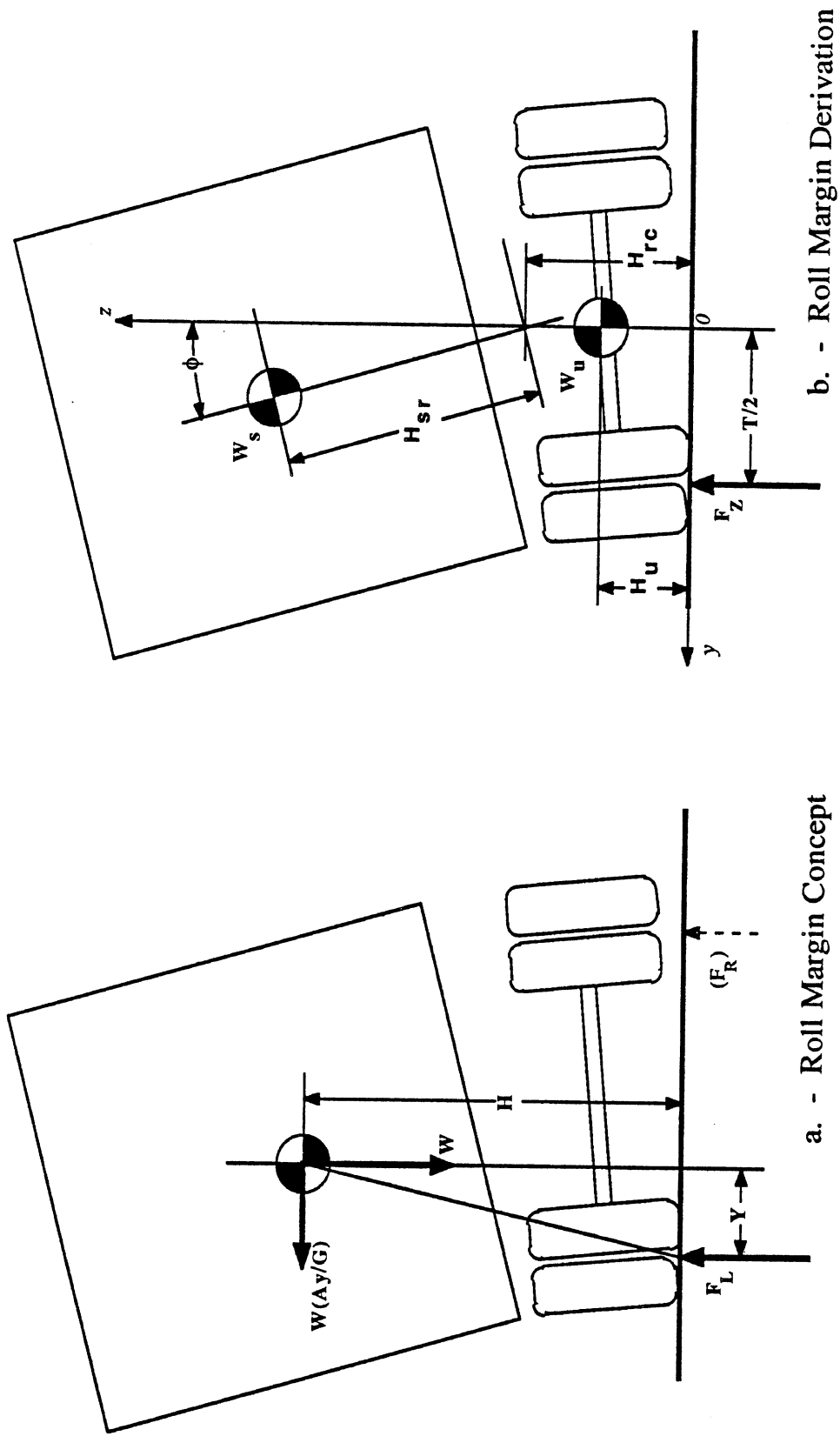


Figure C.5 - Performance Measure b(1) - Dynamic Rollover Threshold

extracted or calculated (and stored in arrays indexed by axle number) for each axle from the initial condition recorded at time-step = 1. This includes: -

1) W_S , the axle's virtual sprung weight, obtained from: $W_S = F_Z - W_U$, where $F_Z = F_L + F_R$ (the total static load on the axle), and W_U is the axle unsprung-weight (2500 lb for a rear axle of unit 1, 1500 lb for any trailer axle), and -

2) H_{SR} , the C.G. height of the virtual sprung weight, W_S , above the roll center, obtained by subtracting the given axle's roll-center height from the relevant unit's actual sprung-mass C.G. height, H_S . If any dollies are present, a combined sprung-mass C.G. height for each "full trailer" (dolly + following semitrailer) is first calculated based on the respective H_S values of its individual units, and the H_{SR} values for all of the full trailer's axles are evaluated from this combined H_S .

Defining a non-rolling, "non-SAE" coordinate frame $y-z$ in the roll plane, with its origin at the track center at road level, and neglecting axle roll effects on the displacements of the roll-center and the unsprung mass C.G. (relative to their initial positions) and on track width, the C.G. location- coordinates, y and z , of the virtual total-weight, W , for each axle under roll are:

$$y = [W_S H_{SR} \sin \phi] / W \quad (C.11)$$

$$z = [W_U H_U + W_S (H_{RC} + H_{SR} \sin \phi)] / W \quad (C.12)$$

where all symbols are as indicated in Figure C.5. Denoting the given axle's track-width as T , these results can be expressed in terms of axle-specific Y and H :

$$Y = T / 2 - [W_S H_{SR} \sin \phi] / W \quad (C.13)$$

$$H = [W_U H_U + W_S (H_{RC} + H_{SR} \sin \phi)] / W \quad (C.14)$$

Applying equation (C.10) for each axle along the roll-unit, an "overall" RM can be calculated for the whole roll-unit from all the individual "axle-RM" values. This is accomplished by averaging their values, after having them weighted by their axle total weights, W . Using the subscript j to denote individual axles, and the summation symbol, Σ , to indicate a summation over all the axles of a roll-unit, the RM value for the given roll-unit is thus computed by:

$$RM = \frac{\sum [W_j (Y/H)_j]}{\sum W_j} \quad (C.15)$$

The RM calculation is invoked for a roll-unit at every time-step, for which that roll-unit's LTR value is greater than .999. If this condition, namely, $LTR > .999$, remains continuously true for the same roll-unit during a period of more than 1.0 second, OR if the RM value for that roll-unit becomes negative (implying a lateral displacement of the roll-unit's total C.G. location beyond the equivalent track width), rollover is declared and further processing abandoned. Otherwise, each successive RM value is compared to that of the immediately preceding time-step for the same roll-unit, until a minimum, "limit-RM" value is encountered. Each limit-RM value is stored indexed by the roll-unit number, the sequential lift-off number for that roll-unit, and the time-step at which it was encountered. After scanning of the whole time history is completed, the lowest limit-RM is selected and displayed with its corresponding roll-unit number and time of occurrence. If the RM calculation was ever invoked in the processing of a given time history, subsequent LTR peaks are not stored, and no sorting of LTR peaks is performed for that run.

b(2) - High-Speed Transient Off-Tracking

Mesasure b(2) is shown as the dimension OT on the lower plot of Figure C.4. It involves the evaluation of the difference between {the peak lateral displacement in the path of the rearmost axle in the combination} and {the final average lateral displacement of the path of the lead axle}, both displacements given at axle centers. The lateral displacement of the lead axle is averaged over the last one second of time-history (involving the last 21 time-steps), yielding a value denoted as Y_1 . The time history of the lateral displacement of the rearmost axle is scanned from $t = 1.0$ sec through the last time-step for the largest instantaneous value, this being denoted as Y_p . The high-speed transient off-tracking dimension, OT, is then calculated from: $OT = Y_p - Y_1$. (Note, that the selected maneuvers impose on the vehicle a swerve to its right, which by SAE convention results in positive axle displacement values as shown in Figure C.4.) The largest off-tracking values were obtained always for the 3.0 second steer period, hence these were the only cases of interest.

Maneuver "c"

Maneuver "c" serves for the calculation of two performance measures, both associated with the low-speed tight turn, namely:

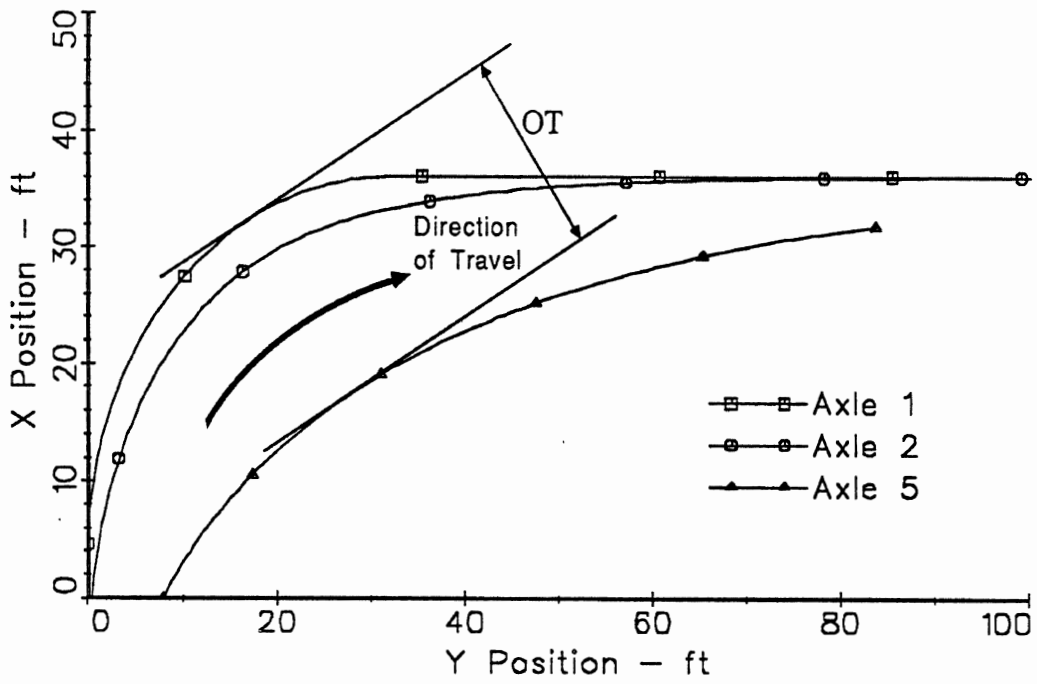
c(1) - Low-Speed Off-Tracking

c(2) - Tight-Turn Friction Demand.

The maneuver is conducted at very low speed (8.25 km/hr -- 5.11 mph) in closed-loop (path-follower control), and involves the negotiating of an "intersection turn", with the lead-axle center point tracking an arc of 90.0 degrees and 9.8 m (32.15 ft) radius, followed by a long tangent exit straight. This is approximately equivalent to an outside front-wheel path-radius of 11 m (36 ft).. Three representative axle-center-point trajectories obtained from an actual simulation run are shown in Figure C.6, in which Axle 1 refers to the path-following lead (steering) axle, Axle 2 is the leading drive axle on the tractor's tandem rear suspension, and Axle 5 is the center (innermost-tracking) one in the semitrailer's tridem-axle group. The duration of the maneuver is 20.0 seconds, the output time-step interval is 0.05 sec (equivalent to 0.11 m -- 4.5 inches along the lead-axle path), and the turn is preceded by a straight 1.22 m (4.0 ft) entry segment tangent to the arc, necessary for smooth control by the driver model. The driver-model control parameters found to provide optimum tracking performance in this maneuver were: Transport Lag = 0.0 sec, Preview Interval = 0.25 sec.

c(1) - Low-Speed Off-Tracking

The maximum off-tracking measure, OT, shown in Figure C.6, is defined as the maximum distance between the path-trajectories of the lead and the "innermost-tracking" axles. It can be proven mathematically, that the maximum distance, OT, is the only finite-length straight-line segment intersecting both trajectories perpendicularly to their respective tangents at the intersection points. However, since the path trajectories are specified in discrete form (coordinates at each time-step), a closed-form, analytical processing of the data is not feasible. Also, the lead-axle trajectory is not a pure circular arc, but only a close approximation to it, as resulting from the discrete-path-follower driver model which was employed in the simulation. These two facts necessitated devising a rather elaborate numerical-processing algorithm in order to reliably calculate the maximum off-tracking measure. Following is a description of this algorithm, supported by Figure C.7.



RTAC tractor-semi (45t/99k GCW), configuration 1.2, variation 1.00

Figure C.6 - Maneuver "c"

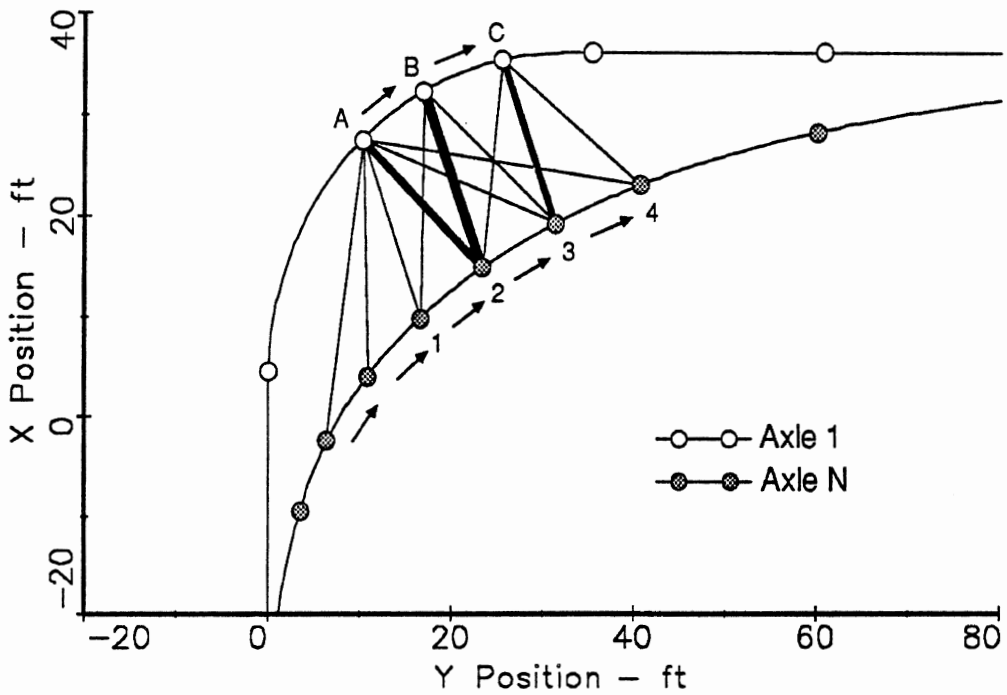


Figure C.7 - Maximum Low Speed Off-Tracking Calculation

Prior to the start of actual time-history scanning and processing, the "innermost-tracking" axle (the displacements of which will be used in the calculation) is selected by the following logic:

If the number of axles of the last articulating unit is 1, the rearmost axle is selected, else the axle next to the rearmost one (axle# "Last - 1") is selected as the innermost-tracking axle. This logic may not be true for all possible vehicle configurations, but it was found appropriate for the whole range of vehicle configurations and axle-spread variations covered in the RTAC study.

Denoting the lead axle and the innermost-tracking axle as "Axle-1" and "Axle-N", respectively, the numerical evaluation of the maximum off-tracking is based on the simple following scheme:

For each Axle-1 X-Y path point, there can be located one Axle-N X-Y path point, which is the nearest of all Axle-N points to the given Axle-1 point (in terms of distance on the pavement). This "nearest" Axle-N point is located by iterating along Axle-N X-Y output steps, computing for each X-Y point its distance from the Axle-1 point, and searching for the minimum distance. (This "minimum distance" may be viewed as the instantaneous or "local" off-tracking of the combination relative to the given Axle-1 X-Y path point.) Once found, this Axle-1 path point is incremented by one output-step, the whole process repeated, and a new minimum distance is found from some Axle-N point to the next Axle-1 point. These "minimum distances", corresponding to successive Axle-1 points, are sorted for the largest among them, which is the maximum off-tracking value desired. The actual determination of the above minimum and maximum distances is simplified by the well-behaved, quasi-hyperbolic shape of the Axle-N X-Y path, characterized by a monotonously decreasing gradient throughout. Also, since the distances between consecutive X-Y points along each axle path are very small (approximately 0.1 m) compared to the off-tracking values evaluated (in the range of 3 to 10 m), no interpolation between such consecutive points was used, thereby simplifying the algorithm. This scheme yields two iteration loops -- at two levels: An outer loop, iterating on Axle-1 X-Y points and executed just once, and an inner (nested) loop, iterating on Axle-N X-Y points and executed once for every Axle-1 point (each time on a new subrange of Axle-N points).

Many preliminary simulation results have shown, that maximum off-tracking in the selected maneuver always takes place at last-unit heading angles (and Axle-1 path heading angles) within the range of 30.0 to 60.0 degrees. Also, as indicated above, the Axle-1 path was (arbitrarily) selected for the outer-loop. Hence, the following logic was applied in determining the range of iteration, so as to minimize CPU time: Beginning at $t = 2.0$ sec, the instantaneous sums of (Lead Unit Heading Angle) + (Lead Axle Steer Angle) were

evaluated at 0.1 sec intervals, until the sum exceeded 30.0 deg. The time-step at which this condition was first encountered was set as the starting step for the Axle-1 X-Y point iteration (first step of outer-loop). Then, the time step at which that sum first exceeded 60.0 deg was set as a safety-stop for the Axle-1 iteration loop (default last-step of outer-loop), if a maximum off-tracking value was not found yet for any reason. Finally, the first iteration step along the Axle-N path was determined similarly by scanning the last-unit heading angle values, again beginning at $t = 2.0$ sec and proceeding at 0.1 sec intervals. The first time-step, for which the last-unit heading angle exceeded 30.0 deg, yielded the first iteration step for Axle-N (first step of first inner-loop).

Referring now to Figure C.7, let points "A" and "3" denote a pair of iteration points along the Axle-1 and Axle-N paths, respectively. The distance between these points, denoted here as " $|A3|$ ", is calculated from their X-Y coordinates, as was " $|A2|$ " at the previous Axle-N iteration (point "2"). Other distances mentioned in this discussion will be denoted accordingly. The difference, DD, between the squares of these distances -- $DD = |A2|^2 - |A3|^2$ -- will then serve to determine the next Axle-N time-step, corresponding to point "4" (the next Axle-N iteration step, if any), as follows:

- 1) If $DD > 100 \text{ ft}^2$, then the time-step recorded the nearest to 0.4 sec after that of point "3" will correspond to point "4" (an empirically developed accelerated-iterating scheme), else --
- 2) If $DD > 20 \text{ ft}^2$, then the time-step recorded the nearest to 0.1 sec after that of point "3" will correspond to point "4" (empirical, as above), else --
- 3) If $DD > 0$, then the successive time-step to the one of point "3" will correspond to point "4", else --
- 4) $|A2|^2 \leq |A3|^2$, implying that a minimum distance, $|A2|$, has been found from the nearest Axle-N point ("2", in this case) to the current Axle-1 point "A". In this case, the minimum distance, $|A2|$, is stored, and the Axle-1 point incremented by one time-step, from "A" to "B". It remains, however, to establish the new Axle-N point, whose distance from "B" will be first evaluated. This is accomplished by a comparison of those two already-calculated distances, which bracket the minimum distance, $|A2|$, -- namely, $|A3|$ and $|A1|$. The scheme involves the following logic: If $|A3| \leq |A1|$, then the last Axle-N point evaluated for "A", namely, "3", will remain as the first Axle-N point to be evaluated for "B", and the corresponding first distance evaluated for "B" will be $|B3|$. However, if $|A3| > |A1|$, then, figuratively, point "3" tends already to "precede" point "A", and this may cause the eventual missing of the maximum off-tracking distance. Hence, in such cases, the current Axle-N step is backed-up by 2 time-steps, and, assuming that points "1", "2"

and "3" correspond to three consecutive time-steps, then point "1" becomes the first Axle-N point for "B".

The process described above for "A" is now repeated for "B", until a minimum distance from some Axle-N point to "B" is found. Assuming this distance to be $|B2|$, it is then compared to the previous minimum distance, $|A2|$ (it is coincidental that both employ the same Axle-N point, "2", and it could conceivably be $|B3|$ vs. $|A2|$, or $|B1|$ vs. $|A2|$, or $|B4|$ vs. $|A2|$, etc.). If $|B2| \geq |A2|$, then the outer-loop iteration sequence continues with the next Axle-1 point, "C", in the same manner as described for the move from "A" to "B", eventually yielding some corresponding minimum distance such as $|C3|$, and so on. If, however, $|B2| < |A2|$, then $|A2|$ is assumed to represent the maximum off-tracking value attained in the simulation, and the iteration process is halted. Actually, from the step at which an Axle-N point of minimum distance from the very first Axle-1 point was found, most of the iteration process involves a "zig-zag"-like progress, with one single Axle-N iteration per each Axle-1 iteration. This process can be visualized on Figure C.7 as involving an iteration-sequence: 1 - A - 2 - B - 3 - C - 4 - ..., with the resulting corresponding sequence of distance evaluations: $|A1| < |A2| < |B2| < |B3| < |C3| < |C4|$. This usually continues to the vicinity of maximum off-tracking, where the proximity of gradients between the Axle-1 and Axle-N paths would force the backing-up scheme of Axle-N steps described above. Also, the actual implementation of the whole algorithm specifies only the evaluation and comparison of squares of distances, since these are the values directly obtained from X-Y point coordinates by the Pythagoras theorem. The square-root function is called only once, at the very end, in order to evaluate the final result. These last two characteristics help somewhat to improve the computational efficiency relative to its apparent low level.

c(2) - Tight-Turn Friction Demand

This performance measure is evaluated in response to the same 90 degree turn of 9.8-meter radius defined as maneuver "c". The degree of susceptibility to jackknife during a tight turn on a slippery surface is quantified by the peak frictional coefficient (" μ -peak") which is demanded at the tractor drive wheels in order to achieve the described maneuver. This measure is evaluated by continuous calculation during the maneuver of the non-dimensional quantity given by the ratio of {the sum of drive-wheel side forces F_y divided by the cosine of the tractor/semitrailer articulation angle Γ } divided by {the sum of the

drive-wheel vertical loads F_z to yield a friction-coefficient-type result. Referring to Figure C.8, the instantaneous frictional coefficient, μ , demanded at a given time-step is:

$$\mu = (\Sigma F_y / \cos \Gamma) / \Sigma F_z \quad (C.16)$$

Division by the cosine of the articulation angle Γ is intended to approximately yield the effective resultant of longitudinal and lateral shear forces at the tractor rear tires (since the longitudinal tire force, F_x , is not expressly computed in the simulation model). This computation assumes that the total resultant shear force between the drive-wheels and the road acts perpendicular to the semitrailer longitudinal axis and just counteracts the total horizontal king-pin force, F_{kp} , applied by the semitrailer at the tractor's fifth wheel. The king-pin force, F_{kp} , is caused by the yaw-resisting moment created by the semitrailer's widely spread axles, whose tires are subjected to high slip angles and thus generate large side forces, F_t . (This calculation neglects tire rolling resistance, and would be absolutely accurate, had the tire/road shear forces at the tractor front wheels also been zero. The measure provides good approximation, however, since the location of the fifth wheel is very near that of the combined centroid of the drive-wheel shear forces.) Hence, the Tight-Turn Friction Demand measure is defined as the minimum frictional-coefficient necessary to avoid saturation of the tractor drive-wheel tires during the given maneuver, and the higher its value, the lesser will be the tractor's resistance to jackknife in tight turns on slippery surfaces.

The actual processing begins at the time-step of 2.0 seconds, and is repeated for all consecutive time-steps throughout the duration of the maneuver. At each step, the instantaneous frictional coefficient, μ , is calculated according to equation (C.16), and its value compared with the maximum value, " μ -peak", obtained and stored before this step. If $\mu > \mu$ -peak, then this last μ becomes the new μ -peak, and its corresponding time-step is stored with it. At the end of scanning throughout the time history, the stored μ -peak will be the maximum value encountered along the whole maneuver.

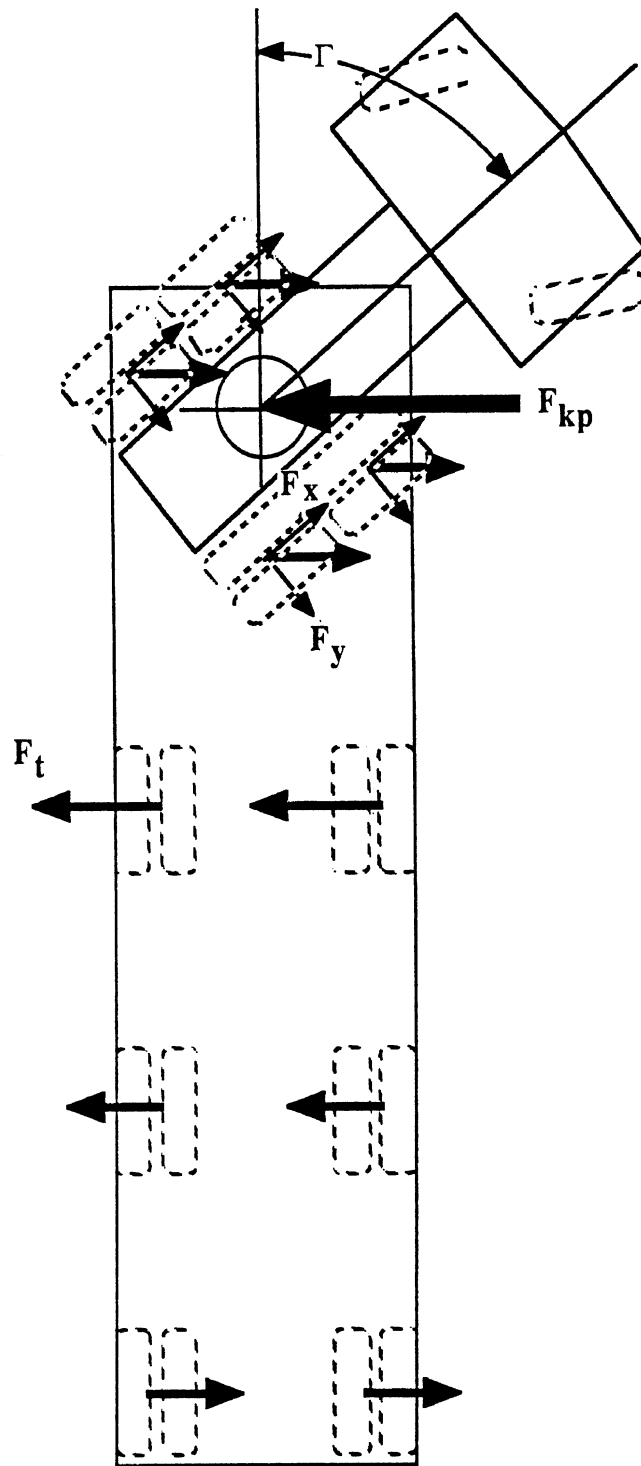


Figure C.8 Performance Measure c(2) - Tight Turn Friction Demand

e - Braking Efficiency

Braking Efficiency is defined as the percentage of available tire/road friction limit that can be utilized in achieving an emergency stop without incurring wheel lockup. In other words, it is the ratio of the deceleration level, in G's, divided by the highest friction coefficient required by any axle, if no lockup is allowed. For example, a vehicle achieves a 50% braking efficiency level when wheel lockup first occurs at 0.2 G's of deceleration on a surface having a tire/road friction level of 0.4. The braking efficiency measure is calculated by the Simplified Braking program which computes the relationship between delivered brake torques and instantaneous wheel loads at each axle of a combination, over the wide range of deceleration levels, assuming unlimited available friction. Although results are produced covering the deceleration range corresponding to brake-application pressures between 10 and 100 psi, the braking efficiency measure is reported only for decelerations of 0.1 and 0.4 G's which illustrates braking performance in nominally low and high level braking conditions.

The calculation is based on the repetitive closed-form solution (as opposed to a numerical simulation) of a set of quasi-static linear equations defining a steady-state braking condition (constant deceleration) for the vehicle combination. The analytical model is documented in detail in [1] (pp. 26-33). The equations neglect suspension and tire compliance and any related pitch-plane displacements, as well as any timing issues, but account for all inter-axle and inter-unit load transfer effects. The equations are solved for each 1.0 psi increment in brake application pressure, with linear pressure-torque gains specified for all brakes along the vehicle. The gains used in this study were 1000 in-lb / psi for each lead-axle brake, and 1500 in-lb / psi for each brake of a "load-carrying" dual-wheel axle. Since brake application pressure is the independent variable, and the resulting deceleration level is a dependent variable, the whole range of recorded deceleration levels (obtained by 1.0 psi increments in pressure) has to be scanned, and the nearest values to the nominal 0.1 and 0.4 G ones serve to locate and display the corresponding braking efficiencies.

f - Simplified Low-Speed Off-Tracking

Low Speed Off-tracking for A-train triples was evaluated using the simplified kinematic model. This model served also to correlate the Yaw/Roll model suitability for low speed, tight turn simulation. The maneuver and the extracted measure are in essence the same as those described in c(1), except that the computation is purely kinematic, involving a simplified, approximated formulation, and does not require a driver model. The formulation is not based on the "instantaneous turning center" approach, but rather on the "cord" approximation fully documented in [1] (pp. 24-26). Essentially, this approximation implies that, upon updating the vehicle's position at each path increment t , the rear-axle centerpoint, " R_t ", of a given articulating unit is moved forward along a "cord" defined by R_t and the updated location of the front articulation-point of the same unit, " F_{t+1} ", until the distance $|F_{t+1} - R_{t+1}|$ equals to the unit's wheelbase. The updated location of the front articulation point, F_{t+1} (which doubles as the rear articulation point of the unit in front), was computed previously by defining similarly the updated position, $t+1$, of the preceding unit. Since this scheme uses a kinematically-defined circular input path with a predefined center for its lead axle, the off-tracking measure is calculated based on the distance of the last-axle path points from the known lead-axle turning center.

References for Appendix C

1. Mathew, A. "Simple Models -- User's Manual." UMTRI, February 1986.

APPENDIX D

PRESENTATION OF SIMULATION MATRIX

This appendix provides structured specification sets for all the vehicle configurations by their relevant parameter values and variations and the performance measures of interest. Each specification set covers one axle configuration from each vehicle category, and consists of three parts:

- The first part presents a schematic drawing of the vehicle illustrating the relevant geometric and load parameters, and indicates their reference values.

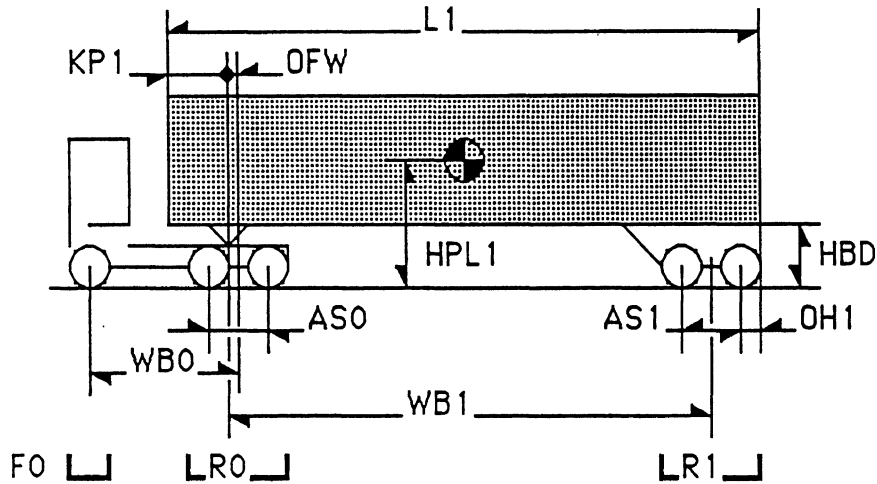
- The second part contains a series of notes explaining the rationale behind the choice of parametric values and variations.

- The third part shows the simulation matrix. The top row contains the code-letters (and numbers, if applicable) of the various performance measures (see Table 1), and the left-most column itemizes all the parameter variations to be investigated, in numbered groups. Entries in the matrix, indicating a simulation run, are specified by the letter "Y" (Yes) for "non-dolly" vehicle categories 1 & 3, and by either "A" or "C" (A- or C-train, respectively) for "dolly-type" categories 2 & 4.

Each simulation matrix has a number corresponding to the given configuration number. The numbers preceding individual notes in the second part of each specification set correspond to the numbers of the respective variation groups in the matrix following the notes.

Category 1. TRACTOR/SEMITRAILER

Configuration 1.1 - Baseline Semi



Weights: [Tonnes]

Tractor Tare	8.2
Trailer Tare	6.3
Payload	25.0
GCW	39.5

Axle Loads: [Tonnes]

F0	5.5
R0	17.0
R1	17.0

Tractor Dimensions:

WB0	Wheelbase	190"
AS0	Tandem Spread	60"
DFW	Fifth Wheel Offset	~15"

Trailer Dimensions:

WB1	Wheelbase	486"
AS1	Tandem Spread	48"
KP1	Kingpin Setback	36"
L1	Bed/Van Length	48'
OH1	Rear Overhang	30"
HPL1	Payload C.G. Height	~79"
HBD	Bed Floor Height	54"

Tires: Michelin XZA 11.00R22.5-G, full tread depth, @ 100 psi.

NOTES (Pertaining to the simulation matrix 1.1 which follows)

- 1) The "reference" case, specified above, indicates the generally most common combination of geometric and load parameters for this vehicle configuration - in this case, a 48' tandem-axle van semitrailer with 48" axle spacing hitched to a tandem-axle tractor of 190" wheelbase and 60" axle spacing. As in this case, the reference vehicle is generally subjected to the complete simulation set, in order to establish all its performance measures in comparison with results obtained from any subsequent cases of the same configuration, as well as from reference cases of any other configurations and categories.
The fifth-wheel offset (~15") is not a predetermined value, but rather is calculated based on the specified vehicle tare weight and axle loads.
The reference payload (25.0 Tonnes) and its longitudinal position are also determined from given tare weights and axle loads, while its approximate reference CG height of 79" results from the assumption of a uniform density load of 34 lb/ft³ and from the given typical bed height and floor area.
- 2) In varying the vehicle lengths (actually, their wheelbases), the load density and axle loads are held at reference values. Vehicle tare weights, payload, payload CG longitudinal and vertical location and associated moments of inertia are all modified to reflect the length and wheelbase changes, and the fifth-wheel offset is adjusted to maintain the reference axle loads.
- 3) Variations of tractor and semitrailer tandem spreads AS0 and AS1 are shown as sets of their respective values, separated by a slash /.
The tandem-spreads are chosen to cover all common values in use. The separate long-spread variations of 3.2) feature increased tandem axle loads to the maximum Canadian allowance (20.0 Tonnes), serving to illustrate the utilization of the longer spreads for higher loads.
- 4) Fifth wheel offset and trailer rear overhang (bogie location) are varied at reference-payload (all payload parameters are set equal to those determined in the reference case), causing changes in axle loads as may occur in service.
- 5) Tractor suspension types were determined from the actual relative popularity of the different models and load ratings in use.
The only alternative trailer suspension type investigated is the Neway air (model AR-95-17), since virtually no other suspension types were found commonly in use beside it and the Reyco 21b.
- 6) Tandem axle loads are varied over the range of load allowances bound by the most restrictive and the most permissive across provinces.
- 7) The 105" value serves as a practical upper bound for payload CG height, as well as a common fixed parameter allowing closer comparison between vehicles from other configurations and categories. This case is a useful supplement to the other runs in which load variations with constant freight density automatically cause changes in payload CG height, hence introducing an additional dependent parameter.

- 8) The 1/2 payload condition is defined by specifying a payload of the same freight density, width and CG height as in the reference case, but of 1/2 the weight, length, and roll moment of inertia.

The new payload CG is then placed once at a distance of 1/4 bed length from its front end, and once at 3/4 bed length, thus simulating front-half-full and rear-half-full trailer loadings, respectively.

- 9) Worn radials possess higher cornering stiffness than the reference (full-tread) ones, while bias-ply tires possess considerably lower cornering stiffness than the reference tires. Variation 9.2) is intended to represent to levels of deterioration of the tractor's directional stability - one with worn radials in front and full tread (reference) radials in the rear, and one with worn radials in front and bias-ply tires in the rear.
- 10) The 102" tractor width case accounts for increases in wheel tracks and spring spacings, but neglects any changes in frame torsional stiffness (roll-stiffness distribution).

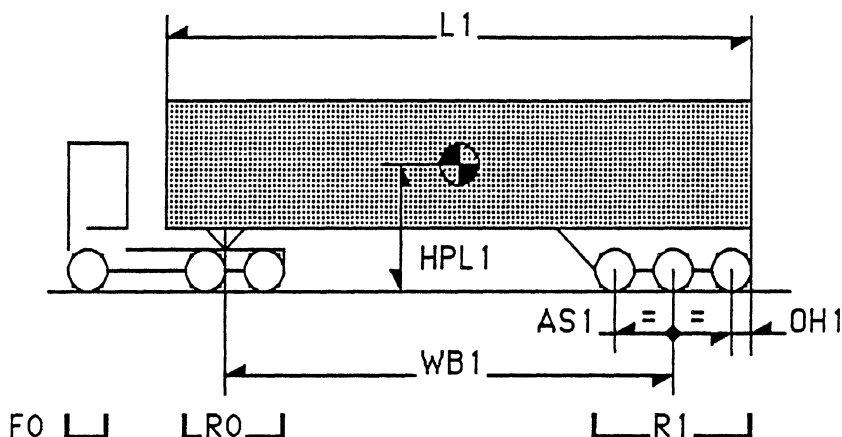
RTAC SIMULATION MATRIX 1.1

<u>VEHICLE VARIATIONS</u>	<u>PERFORMANCE MEASURES</u>			
	<u>a(1,2,3)</u>	<u>b(1,2)</u>	<u>c(1,2)</u>	<u>e</u>
1.00) <u>Reference Vehicle</u>	Y	Y	Y	Y
1.01) Ref. Vehicle - Empty	-	-	-	Y
2) <u>Lengths</u>				
2.1) - <u>Tractor Wheelbase [in.]:</u>				
2.11) WB0 = 150	Y(1,3)	-	Y	Y
2.12) WB0 = 210	Y(1,3)	-	Y	Y
2.13) WB0 = 250	Y(1,3)	-	Y	Y
2.2) - <u>Semitrailer Length [ft.]:</u>				
2.21) L1 = 40	Y(1,3)	-	Y	Y
2.22) L1 = 54	Y(1,3)	-	Y	Y
2.23) L1 = 60	Y(1,3)	-	Y	Y
3) <u>Tandem Spreads AS0/AS1 [in.]</u>				
3.1) - @ R0 = R1 = 17. Tonnes:				
3.11) 60/60	Y(1,3)	-	Y	-
3.12) 60/72	Y(1,3)	-	Y	-
3.13) 60/96	Y(1,3)	-	Y	-
3.14) 60/108	Y(1,3)	-	Y	-
3.15) 48/48	Y(1,3)	-	Y	Y
3.16) 72/48	Y(1,3)	-	Y	Y
3.2) - @ R0 = R1 = 20. Tonnes:				
3.21) 72/72	Y(1,3)	-	Y	Y
3.22) 72/96	Y(1,3)	-	Y	Y
3.23) 72/108	Y(1,3)	-	Y	Y
4) <u>Hitch & Bogie Location [in.]</u>				
4.1) - <u>Fifth Wheel Offset:</u>				
4.11) OFW = (ref) + 12.	Y	-	Y(2)	Y
4.12) OFW = 0.	Y	-	Y(2)	Y
4.13) OFW = (ref) - 12.	Y	-	Y(2)	Y
4.2) - <u>Trailer Rear Overhang:</u>				
4.21) OH1 = (ref) + 24.	Y(1,3)	-	Y	Y
4.22) OH1 = (ref) + 60.	Y(1,3)	-	Y	Y
4.23) OH1 = (ref) + 96.	Y(1,3)	-	Y	Y
5) <u>Suspension Type</u>				
5.1) <u>Tractor Rear Suspension:</u>				
5.11) Hendrickson RTE380	Y	-	-	Y
5.12) Mack Camelback 38k	Y	-	-	Y
5.13) Neway Air 44k	Y	-	-	-
5.20) <u>Trailer Rear Suspension:</u>				
Neway Air 44k	Y	Y	-	-
5.30) <u>All Around:</u>				
Neway Air 12k/44k/44k	Y	Y	-	-
6) <u>Tandem Axle Loading [Tonnes]</u>				
6.01) R0= R1= 16.	Y	-	-	Y
6.02) R0= R1= 18.	Y	-	-	Y
6.03) R0= R1= 19.	Y	-	-	Y
6.04) R0= R1= 20.	Y	-	-	Y

RTAC SIMULATION MATRIX 1.1 (con'd)

<u>VEHICLE VARIATIONS</u>	<u>PERFORMANCE MEASURES</u>			
	<u>a(1,2,3)</u>	<u>b</u>	<u>c(1,2)</u>	<u>e</u>
7) <u>High Payload</u> HPL1=105[in.]				
7.01) 96" Tractor Width (ref)	Y	Y	-	Y
7.02) 102" Tractor Width	Y	Y	-	-
8) <u>Partial & Bias Loading</u> 0.5 Payload, its X_{CG} @ :				
8.01) .25*L1	Y(1,3)	-	Y(2)	Y
8.02) .75*L1	Y(1,3)	-	Y(2)	Y
9) <u>Tire Selection</u>				
9.1) - <u>Uniform</u> (all around):				
9.11) Worn Radials	Y	-	-	-
9.12) Bias Ply's	Y	-	-	-
9.2) - <u>Tractor Front</u> : Worn Radials				
9.21) @ Rear: Radials (ref)	Y	-	-	-
9.22) @ Rear: Bias Ply's	Y	-	-	-
10.00) <u>102" Tractor Width</u>	Y	Y	-	-

Configuration 1.2 - Tridem Axle Semi



Weights: [Tonnes]

Tractor Tare	8.2
Trailer Tare	7.3
Payload	29.5
GCW	45.0

Axle Loads: [Tonnes]

F0	5.5
R0	17.0
R1	22.5

Trailer Dimensions:

WB1	Wheelbase	462"
AS1	Tridem Spreads	48+48"
KP1	Kingpin Setback	36"
L1	Bed/Van Length	48'
OH1	Rear Overhang	30"
HPL1	Payload C.G. Height	~81"

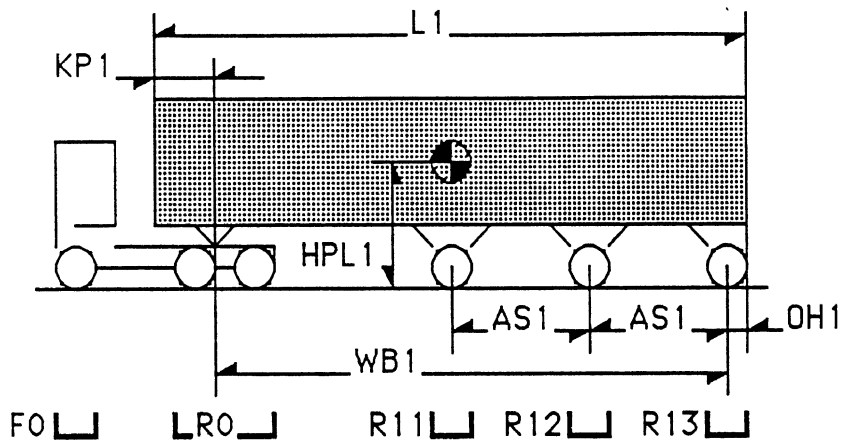
NOTES

- 1) Tridem Spreads (Interaxle spacing) of 48" reflect a common, closely spaced axle set. The approximate payload CG height of 81" (vs. 79" for the baseline semitrailer) reflects the increased payload of 29.5 Tonnes (vs. 25.0 for the baseline) at a constant density of 34 lb/ft³, on an identical bed.
- 2) Tridem group load of 22.5 Tonnes reflects a moderate load condition generally allowable across all provinces, varied later up to 27.0 Tonnes -- close to the highest allowable tridem load in Canada.

RTAC SIMULATION MATRIX 1.2

<u>VEHICLE VARIATIONS</u>	<u>PERFORMANCE MEASURES</u>			
	<u>a(1,3)</u>	<u>b</u>	<u>c</u>	<u>e</u>
1.00) <u>Reference Vehicle</u>	Y	Y	-	-
2) <u>Tridem Loading</u> [Tonnes]				
2.01) R1 = 17.	Y	Y	-	-
2.02) R1 = 24.	Y	Y	-	-
2.03) R1 = 27.	Y	Y	-	-
3.00) <u>High Payload</u> HPL1=105[in.]	Y	Y	-	-

Configuration 1.3 - Three Axle Semi



Weights: [Tonnes]

Tractor Tare	8.2
Trailer Tare	7.3
Payload	34.0
GCW	49.5

Axle Loads: [Tonnes]

F0	5.5
R0	17.0
R11	9.0
(= R12 = R13)	

Trailer Dimensions:

WB1	Wheelbase	510"
AS1	Axle Spreads	96+96"
KP1	Kingpin Setback	36"
L1	Bed/Van Length	48'
OH1	Rear Overhang	30"
HPL1	Payload C.G. Height	~83"

NOTES

1) Axle Spreads of 96" between adjacent trailer axles reflect rather closely spaced separate axles, which are not a tridem (no load equalization) -- these spreads are later uniformly increased up to a condition which provides approximately uniform spacing, starting from the tractor's rearmost axle.

Approximate payload CG height of 83" reflects the increase in payload weight to 34.0 Tonnes -- see configuration 1.2, note 1) above.

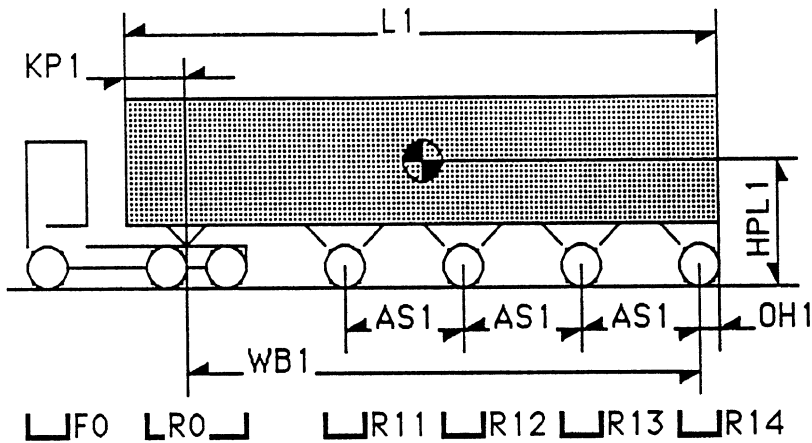
2) The individual trailer axle loads (9.0 Tonnes/axle) reflect roughly the load allowance of various bridge formulae and tables for the 96" axle spreads.

These axle loads are varied both down to the tridem reference value of 7.5 Tonnes/axle and up to the highest allowable single axle load of 10.0 Tonnes/axle.

RTAC SIMULATION MATRIX 1.3

<u>VEHICLE VARIATIONS</u>	<u>PERFORMANCE MEASURES</u>			
	<u>a(1.3)</u>	<u>b(1.2)</u>	<u>c(1.2)</u>	<u>e</u>
1.00) <u>Reference Vehicle</u>	Y	Y	Y	-
2) <u>Rear Axle Loading</u> [Tonnes]				
2.01) R11 = R12 = R13 = 7.5	Y	Y	Y(2)	-
2.02) R11 = R12 = R13 = 10.0	Y	Y	Y(2)	-
3) <u>Rear Axle Spread</u> [in.]				
3.01) AS1 = 108.	Y	Y	Y	-
3.02) AS1 = 120.	Y	Y	Y	-
3.03) AS1 = 132.	Y	Y	Y	-
3.04) AS1 = 144.	Y	Y	Y	-
4.00) <u>High Payload</u> HPL1=105[in.]	Y	Y	-	-

Configuration 1.4 - Four Axle Semi



<u>Weights: [Tonnes]</u>		<u>Axle Loads: [Tonnes]</u>	
Tractor Tare	8.2	F0	5.5
Trailer Tare	8.0	R0	16.0
Payload	41.3	R11	9.0
GCW	57.5	(= R12= R13= R14)	

Trailer Dimensions:

WB1	Wheelbase	510"
AS1	Axle Spreads	3x114"
KP1	Kingpin Setback	36"
L1	Bed/Van Length	48'
OH1	Rear Overhang	30"
HPL1	Payload C.G. Height	~85"

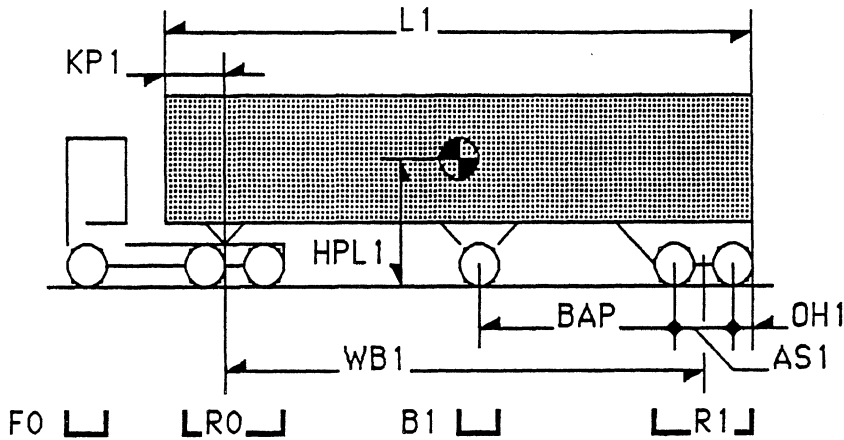
NOTES

- 1) Axle Spreads of 114" between adjacent trailer axles yield close-to-uniform axle spacing, starting from the tractor's rearmost axle.
Approximate payload CG height of 85" reflects the increase in payload weight to 41.3 Tonnes -- see configuration 1.2, note 1) above.
- 2) The individual trailer axle loads (9.0 Tonnes/axle) reflect roughly the load allowance of various bridge formulae and tables for the 114" axle spreads.
These axle loads are varied up to the highest allowable single axle load of 10.0 Tonnes/axle.

RTAC SIMULATION MATRIX 1.4

<u>VEHICLE VARIATIONS</u>	<u>PERFORMANCE MEASURES</u>			
	<u>a(1.3)</u>	<u>b(1.2)</u>	<u>c(1.2)</u>	<u>e</u>
1.00) <u>Reference Vehicle</u>	Y	Y	Y	-
2.01) <u>Axle Loading</u> [Tonnes] R0 = 18.0 R1(i) = 10.0	Y	Y	Y(2)	-
3.00) <u>High Payload</u> HPL1=105[in.]	Y	Y	-	-

Configuration 1.5 - Belly Axle Semi



Weights: [Tonnes]

Tractor Tare	8.2
Trailer Tare	7.3
Payload	33.0
GCW	48.5

Axle Loads: [Tonnes]

F0	5.5
R0	17.0
B1	9.0
R1	17.0

Trailer Dimensions:

WB1	Wheelbase	486"
AS1	Axle Spread	48"
BAP	Belly Axle Position	240"
KP1	Kingpin Setback	36"
L1	Bed/Van Length	48'
OH1	Rear Overhang	30"
HPL1	Payload C.G. Height	~83"

NOTES

- 1) The belly axle is the CESCHI self-steering, air-suspension type, with the steering locked (disabled), except in variation 4) below.
- 2) Belly vs. tandem axle load distribution is varied such that the total load remains constant, and the tandem loads on both tractor and semitrailer tandem loads are equal in each case, simulating variation of belly-axle air-spring pressure.
Slashes / are used to separate the respective R0, B1 and R1 values of each load condition.
- 3) Belly axle location is varied from a point approximately midships between the tractor's and semi's tandems (which is the reference) rearwards, until relatively near (120") the semi's first tandem axle.
- 4) The "Enabled-Steering" variations cover two conditions of castering action: A "Reference" condition, as specified for the C-train (B-dolly) reference case of configuration 2.1, with intermediate friction and self-centering stiffness values, and an extreme "Free Castering" condition representing the case when no side-force is generated by the belly axle. See a more detailed discussion below for variation 7) of configuration 2.1).

RTAC SIMULATION MATRIX 1.5

<u>VEHICLE VARIATIONS</u>	<u>PERFORMANCE MEASURES</u>			
	<u>a(1,3)</u>	<u>b(1,2)</u>	<u>c(2)</u>	<u>e</u>
1.00) <u>Reference Vehicle</u>	Y	Y	Y	-
2) <u>Axle Loads R0/B1/R1 [Tonnes]</u>				
2.01) 18/7/18	Y	Y	Y	-
2.02) 19/5/19	Y	Y	Y	-
2.03) 20/3/20	Y	Y	Y	-
3) <u>Belly Axle Position [in.]</u>				
3.01) BAP = 200.	Y	Y	Y	-
3.02) BAP = 160.	Y	Y	Y	-
3.03) BAP = 120.	Y	Y	Y	-
4) <u>Belly Axle Steer Enabled</u>				
4.01) Reference Properties	Y	Y	Y	-
4.02) Free Castering	Y	Y	Y	-
5.00) <u>High Payload HPL1=105[in.]</u>	Y	Y	-	-

NOTES

- 1) The basic configuration chosen, namely, 27' trailers with 48" tandem axles and a single axle converter dolly, reflects a normally legal and very common hardware combination across most provinces. Based on common practice, the kingpin setback value for both short 27' semitrailers is 24", and not the usual 36" of longer trailers. Tandem axle loads are low, to reflect a mildly-biased loading scheme constrained by the dolly's usual single axle limit (9.0 Tonnes). Approximated payload CG heights reflect payload density of 34 lb/ft³ and specified bed floor plan (27' x 8.5') and height (54").
The reference properties of the B-dolly self-steering axle are selected based on intermediate values approximating the CESCHI model (which was seen to exhibit rather "average" centering behavior). Longitudinal CG location of payload on each trailer is determined from the specified axle loads, these in turn being set to reflect realistic, close to uniform (mildly-biased) loading scenarios (rather than some generally unlikely optimal utilization of axle capacity, which would often require highly biased, unequal-density payloads).
The type of train configuration to be simulated is indicated in the simulation matrices by the respective letter/s - A or C (in lieu of the "Y" designation used in Categories 1 & 3).
- 2) Trailer lengths are varied up to 60' only to illuminate their effect on yaw and roll stability, not reflecting any common hardware.
- 3) The dolly's fifth wheel is kept directly over the dolly axle, and the drawbar length of 72" is increased in 3.1) up to 150" (pushing the second trailer backwards), as in some U.S. west-coast practices. The front trailer's tandem load is increased in 3.2) by varying the overhang -- in these cases the pintle-hook remains flush with the end plane of the trailer, and the drawbar length remains at 72". Pintle-hooks for both A- and B-dollies are assumed to be within the rear-end plane of the reference trailers, except when moved according to variation 3.3) -- the drawbar length then is held at 120" to accommodate the case of a far-forward pintle-hook position.
(Note that the PH dimension is measured from the centerline of axle #5 to the pintle hook.)
- 4) Simultaneously increasing all tandem loads to 20.0 Tonnes results in exceeding normal GCW limits and is of "academic" nature.
- 5) 1/2 payload scheme is as described for variation 8) in configuration 1.1), with two cases, respectively combining the loads near and away from the dolly, with an additional case of a fully loaded rear trailer and an empty front one.
- 6) Bias-ply tires on all axle positions serve to aggravate the vehicle's rearward-amplification and high-speed off-tracking tendencies.
- 7) Actual parameter values for each self-steer characteristic are set at the two extreme ("Lo" & "Hi") values obtained from the three self-steering B-dollies measured, the reference case providing an intermediate condition. The "6. deg." condition for hitch lash pertains to a total lash at each pintle hook of 1.5 inches.

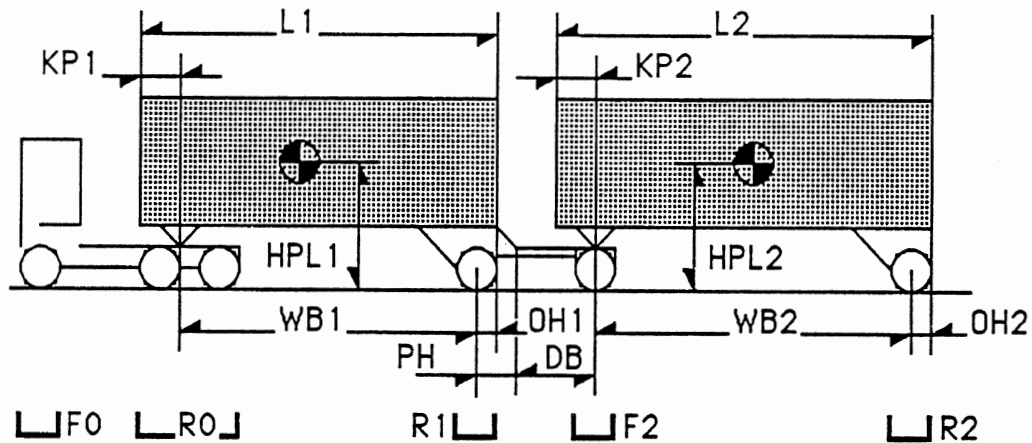
RTAC SIMULATION MATRIX 2.1

<u>VEHICLE VARIATIONS</u>	<u>PERFORMANCE MEASURES</u>				
	<u>a(1)</u>	<u>a(3)</u>	<u>b(1,2)</u>	<u>c(1)</u>	<u>e</u>
1.00) <u>Reference Vehicle</u>	A	A,C	A,C	A,C	A
1.01) Ref. Vehicle - Empty	-	-	-	-	A
2) <u>Semitrailer Lengths</u> [ft.]					
2.01) L1 = L2 = 22.	A	A,C	A,C	A,C	A
2.02) L1 = L2 = 32.	A	A,C	A,C	A,C	A
2.03) L1 = L2 = 40.	A	A,C	A,C	A,C	A
3) <u>Hitch & Bogie Location</u> [in.]					
3.1) - Drawbar Length:					
3.11) DB = 96.	A	A,C	A,C	A,C	A
3.12) DB = 108.	A	A,C	A,C	A,C	A
3.13) DB = 120.	A	A,C	A,C	A,C	A
3.14) DB = 150.	A	A,C	A,C	A,C	A
3.2) - Trailer Rear Overhang:					
3.21) OH1 = 48.	A	A,C	A,C	A,C	A
3.22) OH1 = 72.	A	A,C	A,C	A,C	A
3.23) OH1 = 96.	A	A,C	A,C	A,C	A
3.24) OH2 = 48.	A	A,C	A,C	A,C	A
3.25) OH2 = 72.	A	A,C	A,C	A,C	A
3.26) OH2 = 96.	A	A,C	A,C	A,C	A
3.3) - Pintle Hook Location					
@ DB=120 [in.]:					
3.31) PH = 0.	A	A,C	A,C	A,C	A
3.32) PH = 48.	A	A,C	A,C	A,C	A
3.33) PH = 96.	A	A,C	A,C	A,C	A
4) <u>Axle Loading</u> [Tonnes]					
4.01) R(i) = 14.	A	A,C	A,C	-	A
4.02) R(i) = 16.	A	A,C	A,C	-	A
4.03) F0= 5.5 R(i) = 18.	A	A,C	A,C	-	A
4.04) F0= 5.5 F2= 10. R(i)= 20.	A	A,C	A,C	-	A

RTAC SIMULATION MATRIX 2.1 (con'd)

<u>VEHICLE VARIATIONS</u>	<u>PERFORMANCE MEASURES</u>				
	<u>a(1)</u>	<u>a(3)</u>	<u>b(1,2)</u>	<u>c(1)</u>	<u>e</u>
5) <u>Partial & Bias Loading</u>					
5.10) Trailer#1 Empty	A	A,C	A,C	-	A
5.11) Trailer#2 Empty	-	-	-	-	A
5.2) 0.5 Payloads @ :					
5.21) 0.25*L1/0.75*L2	A	A,C	A,C	-	A
5.22) 0.75*L1/0.25*L2	A	A,C	A,C	-	A
6.00) <u>Tire Selection:</u>					
- Bias Ply tires all around	A	A,C	A,C	-	-
7) <u>B-Dolly Characteristics</u>					
7.1) - @ DB = 72 [in.]:					
7.11) Steering Friction - Low	-	C	C	-	-
7.12) Steering Friction - High	-	C	C	-	-
7.13) Steering Stiffness - Low	-	C	C	-	-
7.14) Steering Stiffness - High	-	C	C	-	-
7.15) Hitch Lash (Yaw) - 6. deg.	-	C	C	-	-
7.16) Hitch Roll Stiffness - Lo	-	C	C	-	-
7.17) Hitch Roll Stiffness - Hi	-	C	C	-	-
7.18) Free-Castering Dolly Axle	-	C	C	-	-
7.19) Dolly Axle Steer Disabled	-	C	C	-	-
7.2) - @ DB = 120 [in.]:					
7.21) Steering Friction - Low	-	C	C	-	-
7.22) Steering Friction - High	-	C	C	-	-
7.23) Steering Stiffness - Low	-	C	C	-	-
7.24) Steering Stiffness - High	-	C	C	-	-
7.25) Hitch Lash (Yaw) - 6. deg.	-	C	C	-	-
7.26) Hitch Roll Stiffness - Lo	-	C	C	-	-
7.27) Hitch Roll Stiffness - Hi	-	C	C	-	-
7.28) Free-Castering Dolly Axle	-	C	C	-	-
7.29) Dolly Axle Steer Disabled	-	C	C	-	-
8.00) <u>Air Suspension @ Trailer #2</u>	A	A,C	A,C	-	-
9.00) <u>High Payload</u> HPL=105[in.]	A	A,C	A,C	-	-

Configuration 2.2 - Single Axle Trailers



Weights: [Tonnes]

GCW	43.0	
Dolly Tare	1.1	
Semitrailer #	1	2
Tare	3.2	3.2
Payload	13.6	13.7

Axle Loads: [Tonnes]

F0	4.5
R0	11.5
R1	9.0
F2	9.0
R2	9.0

Semitrailer Dimensions:

		#1	#2
HPL#	Payload C.G. Height	~77"	~77"
WB#	Wheelbase	270"	270"
KP#	Kingpin Setback	24"	24"
L#	Bed/Van Length	27'	27'
OH#	Rear Overhang	30"	30"
PH	Pintle Hook Location	30"	--

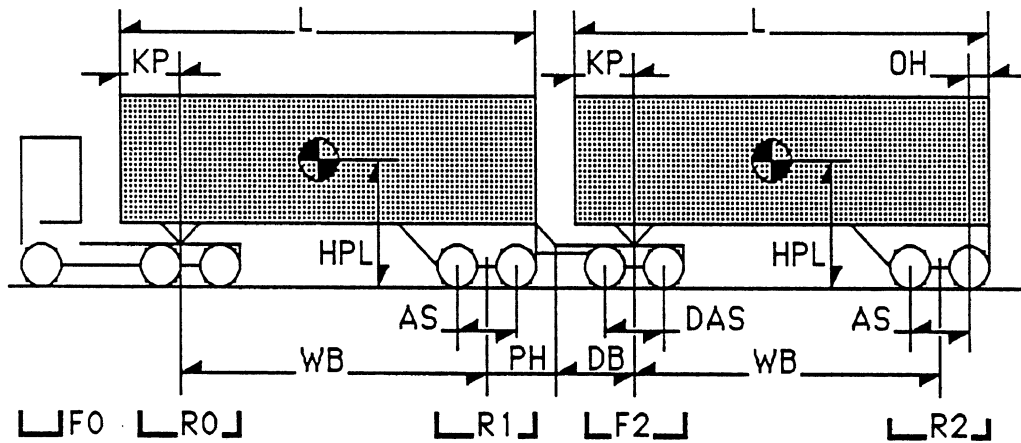
NOTES

- 1) Trailer bed floor plan and height is same as in configuration 2.1 (popular "short" semitrailers).
- 2) Tractor tandem axle load is set in each case at 2.5 Tonnes more than trailer single axles, to represent equal-weight, uniform payloads in both trailers while also accounting for the tractor's tare weight, and front axle light load.
- 3) The partial and bias loading variations specified are aimed to cover the practical boundaries of achievable rearward amplification values as well as B-dolly steering and/or braking response modes. The scheme is thus identical to the one described above for configuration 2.1, 5).

RTAC SIMULATION MATRIX 2.2

<u>VEHICLE VARIATIONS</u>	<u>PERFORMANCE MEASURES</u>				
	<u>a(1)</u>	<u>a(3)</u>	<u>b(1,2)</u>	<u>c(1)</u>	<u>e</u>
1.00) <u>Reference Vehicle</u>	A	A,C	A,C	A,C	A
1.01) Ref. Vehicle - Empty	-	-	-	-	A
2) <u>Axle Loading</u> [Tonnes]					
2.01) R0=10.5 R1= F2= R2= 8.	A	A,C	A,C	-	A
2.02) R0=12.5 R1= F2= R2=10.	A	A,C	A,C	-	A
3) <u>Partial & Bias Loading</u>					
3.10) Trailer#1 Empty	A	A,C	A,C	-	A
3.2) - 0.5 Payloads @ :					
3.21) 0.25*L1/0.75*L2	A	A,C	A,C	-	A
3.22) 0.75*L1/0.25*L2	A	A,C	A,C	-	A
4.00) <u>High Payload</u> HPL=105[in.]	A	A,C	A,C	-	A

Configuration 2.4 - Turnpike Doubles



Weights: [Tonnes]

GCW	56.0	
Dolly Tare	2.0	
Semitrailer #	1	2
Tare	6.3	6.3
Payload	16.5	16.7

Axle Loads: [Tonnes]

F0	4.5
R0	14.0
R1	12.5
F2	12.5
R2	12.5

Semitrailer Dimensions (#1 & 2):

HPL	Payload C.G. Height	~76"
WB	Wheelbase	486"
AS	Tandem Spread	48"
KP	Kingpin Setback	36"
L	Bed/Van Length	48'
OH	Rear Overhang	30"
PH	Pintle Hook Location	54"

Dolly Dimensions:

DB	Drawbar Length	96"
DAS	Dolly Tandem Spread	48"

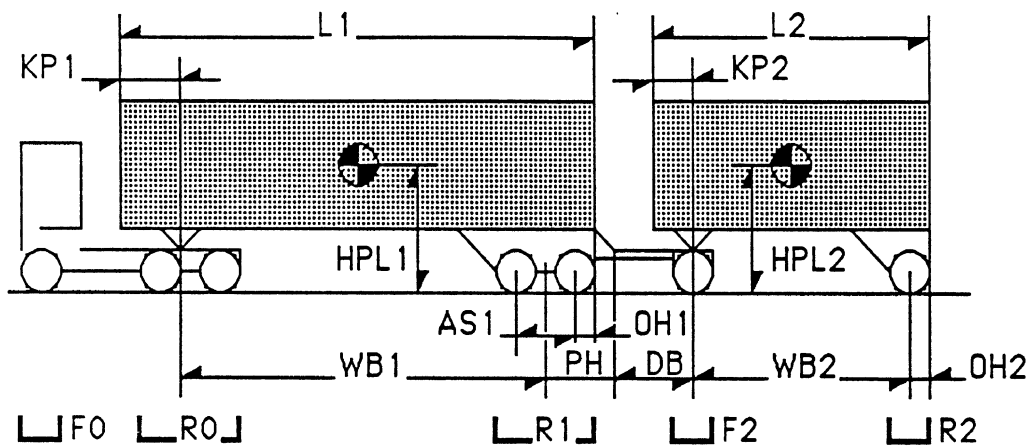
NOTES

- 1) Dolly tandem spread (48") and drawbar length (96") represent common values found in Canadian practice. Note that C-train cases are not represented for the turnpike double, since rearward amplification is known to be minimal for this long-trailer combination.
- 2) Uniform tandem axle loads are assumed, normally limited by the GCW allowance, a common value of 57.5 Tonnes serving as reference. Tandem axle loads are increased simultaneously up to the highest theoretical limit of 20.0 Tonnes/tandem, yielding a purely "academic" GCW of 85.5 Tonnes.

RTAC SIMULATION MATRIX 2.4

<u>VEHICLE VARIATIONS</u>	<u>PERFORMANCE MEASURES</u>			
	<u>a(1,3)</u>	<u>b(1,2)</u>	<u>c(1)</u>	<u>e</u>
1.00) <u>Reference Vehicle</u>	A	A	A	A
1.01) Ref. Vehicle - Empty	-	-	-	A
2) <u>Axle Loading</u> [Tonnes]				
2.01) R0= 16.5 R1= F2= R2= 15.0	A	A	-	-
2.02) F0= 5.0 F2= R(i)= 17.5	A	A	-	-
2.03) F0= 5.5 F2= R(i)= 20.0	A	A	-	-
3.00) <u>High Payload</u> HPL=105[in.]	A	A	-	A

Configuration 2.5 - Rocky Mountain Doubles



Weights: [Tonnes]		Axle Loads: [Tonnes]	
GCW	53.5	F0	5.5
Dolly Tare	1.1	R0	15.0
Semitrailer #	<u>1</u>	R1	15.0
Tare	6.3	F2	9.0
Payload	21.0	R2	9.0
		<u>2</u>	
		Tare	3.2
		Payload	13.7

Semitrailer Dimensions:		#1	#2
HPL#	Payload C.G. Height	~77"	~77"
WB#	Wheelbase	486"	270"
AS#	Tandem Spread	48"	--
KP#	Kingpin Setback	36"	24"
L#	Bed/Van Length	48'	27'
OH#	Rear Overhang	30"	30"
PH	Pintle Hook Location	54"	--

NOTES

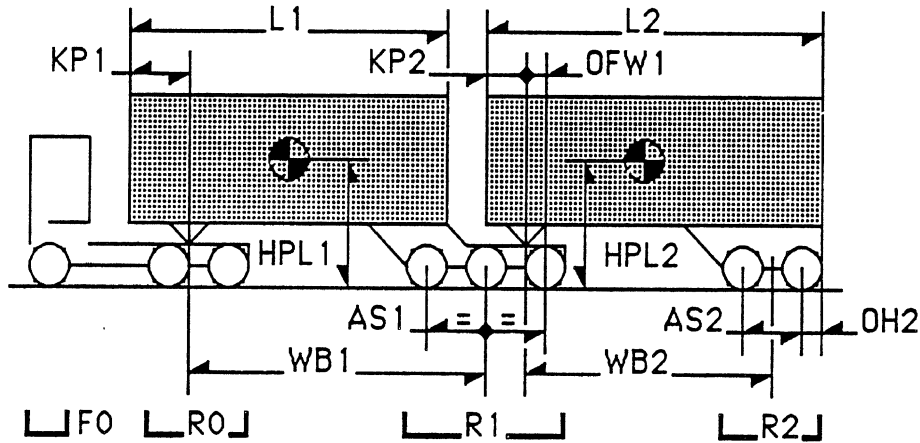
- 1) This configuration combines the front 48' semi of 2.4 with the rear 27' trailer of 2.2.
- 2) In the reversed order case, a tandem dolly is used, as is understood to be the case when the order is switched, and trailer payloads are kept as close to reference values as practical -- otherwise repeating variation 2) of configuration 2.3.

RTAC SIMULATION MATRIX 2.5

VEHICLE VARIATIONS	PERFORMANCE MEASURES				
	a(1)	a(3)	b(1,2)	c(1)	e
1.00) <u>Reference Vehicle</u>	A	A,C	A,C	A,C	A
1.01) Ref. Vehicle - Empty	-	-	-	-	A
2.00) <u>Reversed Order of Semi's:</u> w/Turnpike-Doubles Dolly &: F0= 4.5, R0=12.0 [Tonnes] R1= 9.0 [Tonnes] (single axle) F2= R2= 15.0 [Tonnes] (tandem)	A	A	A	-	A
3.00) <u>High Payload</u> HPL=105[in.]	A	A,C	A,C	-	A

Category 3. B-TRAIN DOUBLES

Configuration 3.1 - Baseline B-Train



<u>Weights:</u> [Tonnes]		<u>Axle Loads:</u> [Tonnes]	
GCW	56.5	F0	5.5
Semitrailer #	1 2	R0	15.0
Tare	6.8 4.3	R1	21.0
Payload	~18.6 ~18.6	R2	15.0

<u>Semitrailer Dimensions:</u>		#1	#2
HPL#	Payload C.G. Height	~78"	~78"
WB#	Wheelbase	280"	246"
AS1	Tridem Axle Spreads	48+48"	--
KP#	Kingpin Setback	60"	24"
L#	Bed/Van Length	27'	27'
OH#	Rear Overhang	--	30"
OFW#	Fifth Wheel Offset	0"	--

(*) OFW# > 0 when fifth-wheel CL is ahead of last-axle CL.

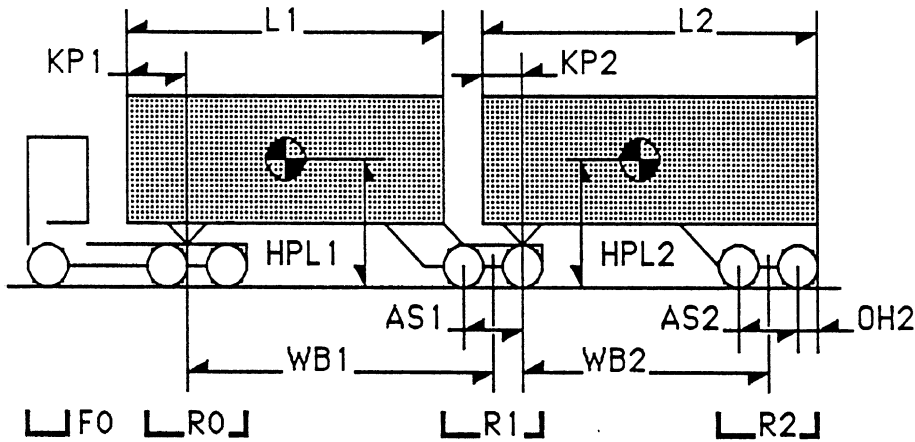
NOTES

- 1) Rear fifth wheel reference location on the front semi is assumed to be exactly over this semi's rearmost axle, closely approximating the generally most common locations used in practice. A large kingpin setback of 60" is used for the front semitrailer, reflecting the general practice of attempting to shift load forward from this semi's axles (the "center group") to the tractor's, in order to avoid overloading the center group. It is to be noted that, as opposed to all other semitrailers examined, the front semitrailer in a B-train is always custom-designed and built for use in this role, as reflected also by the non-standard kingpin setback. Tridem geometry is as assumed in the reference case of configuration 1.2.
- 2) Bed (and hence wheelbase) lengths (20' to 40') are varied within common practice limits.
- 3) Rear fifth wheel location is varied relative to the center group position, with all other geometric and payload parameters held at reference values (resulting in axle load variation).
- 4) Axle loads presume good axle allowance utilization, achieved by some payload bias. Increased axle load variations, including some abnormally high front axle loads (achievable through the use of wide-base tires) reflect continued good axle utilization under proportionally higher allowances, as is typical for this high GCW, "tridem center-group" configuration.
- 5) Partial and bias loading -- see variation 5) of configuration 2.1.
- 6) The compensating rear fifth wheel uncouples the roll moments of the two semitrailers, hence affecting the static and dynamic roll-over threshold levels.
- 7) The case of air-suspension all-around reflects a growing popularity of this equipment, mostly in specialized hauling such as tankers, etc.

RTAC SIMULATION MATRIX 3.1

<u>VEHICLE VARIATIONS</u>	<u>PERFORMANCE MEASURES</u>			
	<u>a(1.3)</u>	<u>b(1.2)</u>	<u>c(1)</u>	<u>e</u>
1.00) <u>Reference Vehicle</u>	Y	Y	Y	-
2) <u>Length of Units [ft.]</u>				
2.1) - <u>Equal Bed Lengths:</u>				
2.11) L1 = L2 = 22	Y	Y	Y	-
2.12) L1 = L2 = 32	Y	Y	Y	-
2.13) L1 = L2 = 40	Y	Y	Y	-
2.2) - <u>Unequal Bed Lengths:</u>				
2.21) L1/L2 = 32/22	Y	Y	Y	-
2.22) L1/L2 = 22/32	Y	Y	Y	-
3) <u>Rear Fifth Wheel Location [in.]</u>				
3.01) OFW1 = 24.	Y	Y	Y	-
3.02) OFW1 = 12.	Y	Y	Y	-
3.03) OFW1 = -12.	Y	Y	Y	-
3.04) OFW1 = -24.	Y	Y	Y	-
4) <u>Axle Loads F0/R0/R1/R2 [Tonnes]</u> (w/wide-base front tires)				
4.01) 6.5/17.0/24.0/17.0	Y	Y	-	-
4.02) 7.5/20.0/30.0/20.0	Y	Y	-	-
5) <u>Partial & Bias Loading</u>				
5.10) Trailer#1 Empty	Y	Y	-	-
5.2) - 0.5 Payloads @:				
5.21) 0.25*L1/0.75*L2	Y	Y	-	-
5.22) 0.75*L1/0.25*L2	Y	Y	-	-
6.00) <u>Compensating Rr 5th Wheel</u>	Y	Y	-	-
7.00) <u>Air Suspension All-Around</u>	Y	Y	-	-
8.00) <u>High Payload HPL =105[in.]</u>	Y	Y	-	-

Configuration 3.2 - Tandem Front Semi B-Train



Weights: [Tonnes]		Axle Loads: [Tonnes]	
GCW	53.5	F0	5.5
Semitrailer #	1	R0	16.0
Tare	6.0	R1	16.0
Payload	~17.5	R2	16.0
	2		
	4.3		
	~17.5		

Semitrailer Dimensions:		#1	#2
HPL#	Payload C.G. Height	~77"	~77"
WB#	Wheelbase	304"	246"
AS#	Tandem Spread	48"	48"
KP#	Kingpin Setback	60"	24"
L#	Bed/Van Length	27'	27'
OH#	Rear Overhang	--	30"
OFW#	Fifth Wheel Offset (*)	0"	--

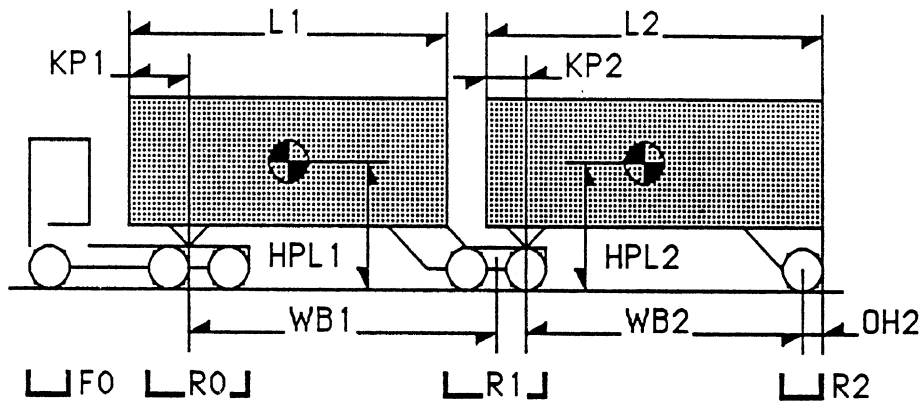
NOTES

- 1) Tandem geometry is as assumed in the reference case of configuration 1.1.
- 2) Equal tandem loads along the train necessitate some bias loading, and may reflect many "tailored" designs (tankers in particular).

RTAC SIMULATION MATRIX 3.2

VEHICLE VARIATIONS	PERFORMANCE MEASURES			
	a(1.3)	b(1.2)	c(1)	e
1.00) <u>Reference Vehicle</u>	Y	Y	Y	Y
1.01) Ref. Vehicle - Empty	-	-	-	Y
2) <u>Axle Loads F0/R0/R1/R2 [Tonnes]</u>				
2.01) 4.5/14.0/14.0/14.0	Y	Y	-	Y
2.02) 5.5/20.0/20.0/20.0	Y	Y	-	Y
3.00) <u>High Payload HPL =105[in.]</u>	Y	Y	-	Y

Configuration 3.3 - Single-Axle Rear Semi B-Train



<u>Weights: [Tonnes]</u>			<u>Axle Loads: [Tonnes]</u>	
GCW	41.5		F0	4.5
Semitrailer #	1	2	R0	13.0
Tare	6.0	3.2	R1	15.0
Payload	~12.1	~12.0	R2	9.0
<u>Semitrailer Dimensions:</u>			#1	#2
HPL#	Payload C.G. Height		~75"	~75"
WB#	Wheelbase		304"	270"
KP#	Kingpin Setback		60"	24"
L#	Bed/Van Length		27'	27'
OH#	Rear Overhang		--	30"

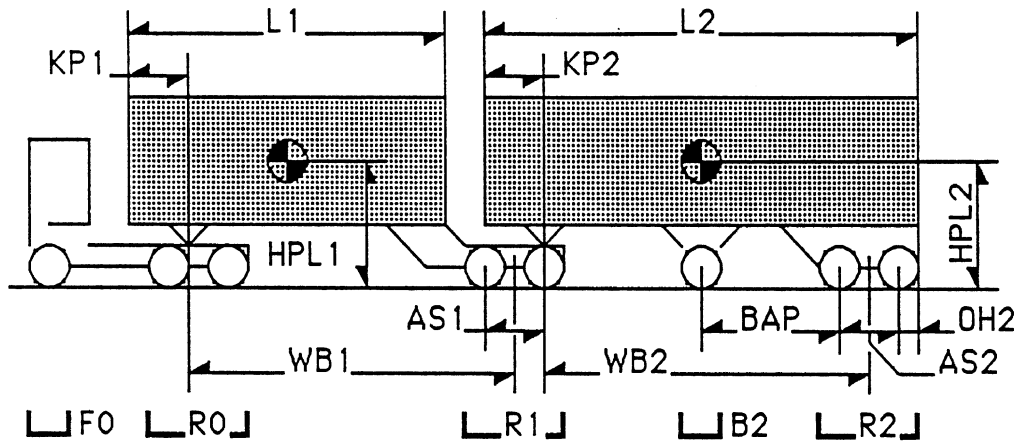
NOTES

- 1) Reference payloads are assumed to be mildly-biased, equal density general freight, yielding under-utilization of tractor's tandem. This rather uncommon axle configuration is perceived as the field result of hardware availability rather than load optimization.
- 2) Axle loading variations are aimed at illustrating cases of better, more uniform axle load allowances, enabled by biased payloads.

RTAC SIMULATION MATRIX 3.3

<u>VEHICLE VARIATIONS</u>	<u>PERFORMANCE MEASURES</u>			
	<u>a(1,3)</u>	<u>b(1,2)</u>	<u>c(1)</u>	<u>e</u>
1.00) <u>Reference Vehicle</u>	Y	Y	Y	Y
1.01) <u>Ref. Vehicle - Empty</u>	-	-	-	Y
2) <u>Axle Loads F0/R0/R1/R2 [Tonnes]</u>				
2.01) 5.0/15.0/18.0/ 9.0	Y	Y	-	Y
2.02) 5.5/18.0/20.0/10.0	Y	Y	-	Y
3.00) <u>High Payload HPL =105[in.]</u>	Y	Y	-	Y

Configuration 3.4 - Belly-Axle B-Train



<u>Weights: [Tonnes]</u>		<u>Axle Loads: [Tonnes]</u>	
GCW	61.5	F0	5.5
Semitrailer #	1	R0	16.0
Tare	6.3	R1	16.0
Payload	~17.0	B2	8.0
		R2	16.0

<u>Semitrailer Dimensions:</u>		<u>#1</u>	<u>#2</u>
HPL#	Payload C.G. Height	~75"	~75"
WB#	Wheelbase	294"	294"
AS#	Tandem Spread	48"	48"
OH#	Rear Overhang	--	30"
KP#	Kingpin Setback	36"	36"
L#	Bed/Van Length	26'	32'
BAP	Belly-Axle Position	--	126"

NOTES

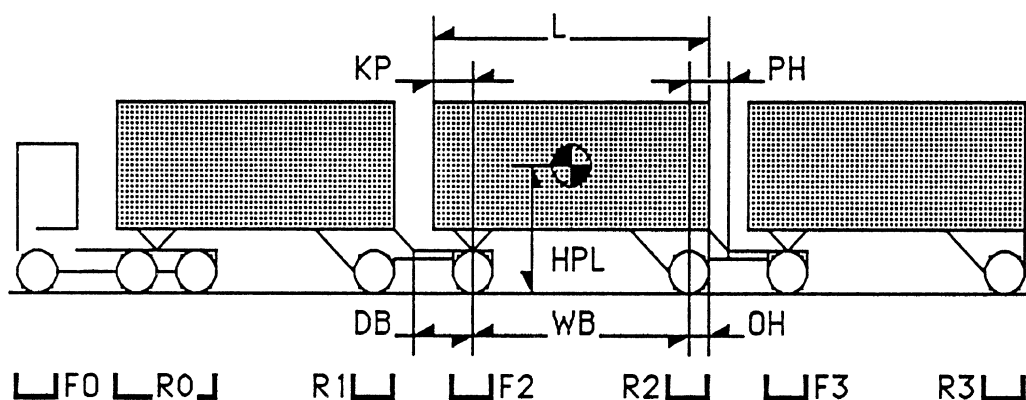
- 1) Trailer lengths are set to allow a "reversed order" condition in which the belly-axle location is the only actual distinguishing parameter. In other words, the 32' and 26' semitrailers have identical values for wheelbases (294") and kingpin setbacks (60"), and only one semi has a "midships" located belly axle.
- 2) When the belly-axle load is varied, the sum of this load plus the two equal loads on both adjacent tandems is held constant -- see note 2) for configuration 1.4.
- 3) When moving the belly axle from one semi to the other, axle loads are not varied, so that payloads are adjusted accordingly.
- 4) "Lo" and "Hi" self-steer properties are the same as selected above in configuration 2.1.7).

RTAC SIMULATION MATRIX 3.4

<u>VEHICLE VARIATIONS</u>	<u>PERFORMANCE MEASURES</u>			
	<u>a(1.3)</u>	<u>b(1.2)</u>	<u>c(1.2)</u>	<u>e</u>
1.00) <u>Reference Vehicle</u>	Y	Y	Y(1)	Y
2) <u>Axle Loads R1/B2/R2 [Tonnes]</u>				
2.01) 18/ 4/18	Y	Y	-	-
2.02) 17/ 6/17	Y	Y	-	-
2.03) 15/10/15	Y	Y	-	-
3.00) <u>Belly Axle on Semi #1</u>	Y	Y	Y	-
4) <u>Belly Axle Steer Enabled</u>				
4.01) Steering Friction - Low	Y(3)	Y	Y(2)	-
4.02) Steering Friction - High	Y(3)	Y	Y(2)	-
4.03) Steering Stiffness - Low	Y(3)	Y	Y(2)	-
4.04) Steering Stiffness - High	Y(3)	Y	Y(2)	-
5.00) <u>High Payload HPL =105[in.]</u>	Y	Y	-	-

Category 4. A & C-TRAIN TRIPLES

Configuration 4.1 - Baseline Triples



<u>Weights: [Tonnes]</u>		<u>Axle Loads: [Tonnes]</u>	
GCW	55.0	F0	4.5
Dollies' Tare	1.1	R0	10.5
Semis' Tare	3.2	R1, R2, R3	8.0
Semis' Payload	~11.7	F2, F3	8.0

<u>Semitrailer Dimensions:</u>		(#1, 2, 3)
HPL	Payload C.G. Height	~75."
WB	Wheelbase	270."
KP	Kingpin Setback	24."
L	Bed/Van Length	27.'
OH	Rear Overhang	30."
PH	Pintle Hook Location	30."

<u>Converter Dolly:</u>		
DB	Drawbar Length	72."

B-Dolly Data (in C-Train Configuration): (See Configuration 2.1)

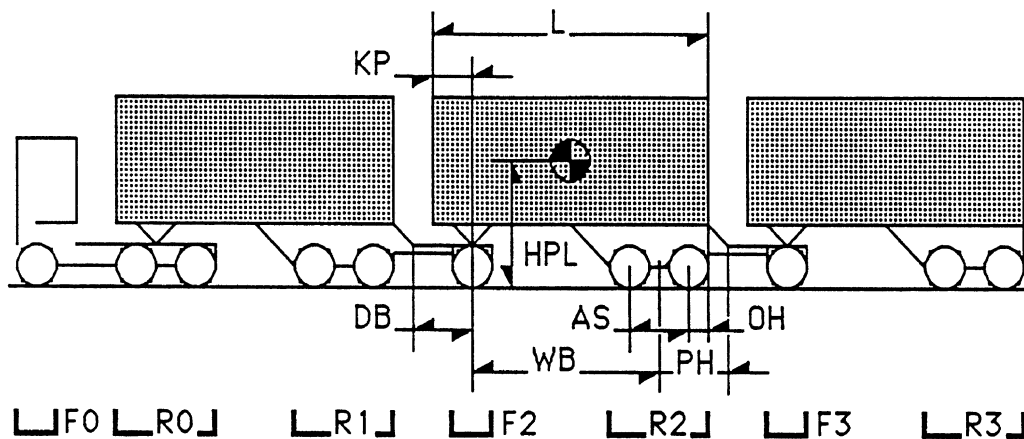
NOTES

- 1) thru 6): Generally, all notes referring to A & C-train doubles pertain to triples as well -- especially the schemes used for setting and varying trailer size, pintle-hook location, dolly drawbar lengths and B-dolly properties.
- 7) The partial and bias loading variations 7.1) & 7.2) are aimed at highlighting all extreme yaw/roll and braking behavior cases, except such that may be regarded as "degenerate".

RTAC SIMULATION MATRIX 4.1

<u>VEHICLE VARIATIONS</u>	<u>PERFORMANCE MEASURES</u>			
	<u>a(3)</u>	<u>b(1,2)</u>	<u>e</u>	<u>f</u>
1.00) <u>Reference Vehicle</u>	A,C	A,C	A	A
1.01) Ref. Vehicle - Empty	-	-	A	-
2) <u>Semitrailer Lengths</u> [ft.]				
2.01) L = 22.	A,C	A,C	A	A
2.02) L = 24.	A,C	A,C	A	A
2.03) L = 30.	A,C	A,C	A	A
3) <u>Hitch & Bogie Location</u> [in.]				
3.1) - Drawbar Length:				
3.11) DB = 96.	A,C	A,C	A	A
3.12) DB = 120.	A,C	A,C	A	A
3.2) - Hitch Location (DB=108"):				
3.21) PH = 0.	A,C	A,C	A	A
3.22) PH = 60.	A,C	A,C	A	A
4) <u>Axle Loading</u> [Tonnes]				
4.01) F2= F3= R1= R2= R3 = 6.	A,C	A,C	A	-
4.02) F2= F3= R1= R2= R3 = 10.	A,C	A,C	A	-
5.00) <u>High Payload</u> HPL= 105[in.]	A,C	A,C	A	-
6) <u>B-Dolly Characteristics</u>				
6.01) Steering Friction - Low	-	C	-	-
6.02) Steering Friction - High	-	C	-	-
6.03) Steering Stiffness - Low	-	C	-	-
6.04) Steering Stiffness - High	-	C	-	-
6.05) Hitch Lash (Yaw) - 6. deg.	C	C	-	-
6.06) Hitch Roll Stiffness - Low	-	C	-	-
6.07) Hitch Roll Stiffness - High	-	C	-	-
6.08) Free-Castering Dolly Axles	C	C	-	-
6.09) Dolly Axle Steer Disabled	C	C	-	-
7) <u>Partial & Bias Loading</u>				
7.1) - Reference Payloads, with:				
7.11) Trailer #1 Empty	A,C	A,C	A	-
7.12) Trailers #1 & 2 Empty	A,C	A,C	A	-
7.13) Trailer #3 Empty	A,C	A,C	A	-
7.2) - 0.5 Payloads (all) @:				
7.21) .25*L (all three)	A,C	A,C	A	-
7.22) .75*L (all three)	A,C	A,C	A	-
7.23) .75*L1/.25*L2/.75*L3	A,C	A,C	A	-
7.24) .25*L1/.75*L2/.25*L3	A,C	A,C	A	-
7.25) .75*L1/.75*L2/.25*L3	A,C	A,C	A	-

Configuration 4.2 - Tandem Axle Triples



<u>Weights:</u> [Tonnes]		<u>Axle Loads:</u> [Tonnes]	
GCW	63.5	F0	4.5
Dollys' Tare	1.1	R0	11.0
Semis' Tare	4.3	R1, R2, R3	10.0
Semis' Payload	~13.6	F2, F3	9.0

<u>Semitrailer Dimensions:</u>		(#1, 2, 3)
HPL	Payload C.G. Height	~76."
WB	Wheelbase	246."
AS	Tandem Spread	48."
KP	Kingpin Setback	24."
L	Bed/Van Length	27.'
OH	Rear Overhang	30."
PH	Pintle Hook Location	54."

NOTES

- 1) This configuration's loading is limited by the single-axle dollies, as well as by GCW allowances. Its existence is considered to be merely a result of fleet hardware flexibility and freight volume (rather than weight) requirements. Hence, payloads are assumed to be centered or only slightly biased, and tandems are grossly under-utilized.

RTAC SIMULATION MATRIX 4.2

<u>VEHICLE VARIATIONS</u>	<u>PERFORMANCE MEASURES</u>			
	<u>a(3)</u>	<u>b(1,2)</u>	<u>e</u>	<u>f</u>
1.00) <u>Reference Vehicle</u>	A,C	A,C	A	A
1.01) Ref. Vehicle - Empty	-	-	A	-
2) <u>Axle Loading</u> [Tonnes]				
2.01) R1 = R2 = R3 = 9.	A,C	A,C	A	-
2.02) R1 = R2 = R3 = 12.	A,C	A,C	A	-
3.00) <u>High Payload</u> HPL=105[in.]	A,C	A,C	A	-

APPENDIX E

DEMONSTRATION TEST PROGRAM

APPENDIX E

DEMONSTRATION TESTS

1.0 Introduction

A series of full-scale vehicle tests were conducted by the staff of The University of Michigan Transportation Research Institute (UMTRI) using the facilities of the Chrysler Proving Grounds in Chelsea, Michigan. The tests were intended, primarily, to provide direct demonstration of certain response characteristics of selected vehicles which are of interest in the overall study of truck weights and dimensions being sponsored by the Canroad Transportation Research Corporation (CTRC). While the test results are meant to supplement a corresponding set of simulation results also being produced for the study vehicles, the test cases represent only a small subset of the cases being studied through simulation. Also, the test vehicles do not match, precisely, the vehicles which are simulated, since each test configuration contains certain suspension, steering, brake, and inertial elements which have not been specifically characterized through laboratory measurement. Nevertheless, for the most part, the test vehicles have been judged to reasonably approximate the corresponding vehicles which were simulated.

Each test vehicle was instrumented so that responses could be quantified in terms of engineering measures which UMTRI has developed. Additionally, the critical vehicle responses which speak directly to safety problems were covered on video tape. Test procedures were tailored for each vehicle configuration and setup condition according to our general understanding of the stability and control problems which were expected to prevail in each case. The rationale behind the selection of procedures for each vehicle is discussed in conjunction with the test results later in this document.

The test plan is organized to provide, in sections 2 and 3, the respective descriptions of vehicle setup and test procedures. The results are then presented and discussed in section 4.

2.0 Description of Test Vehicles

Three truck combinations were included in the test schedule, all of which employed a Kenworth tractor having the following specifications:

Conventional cab with 60-inch sleeper

400-horsepower Caterpillar diesel engine

235-inch wheelbase

Tandem, air-suspended rear axles with 60-inch spread

Fifteen-speed transmission (10 speeds are used in normal operation)

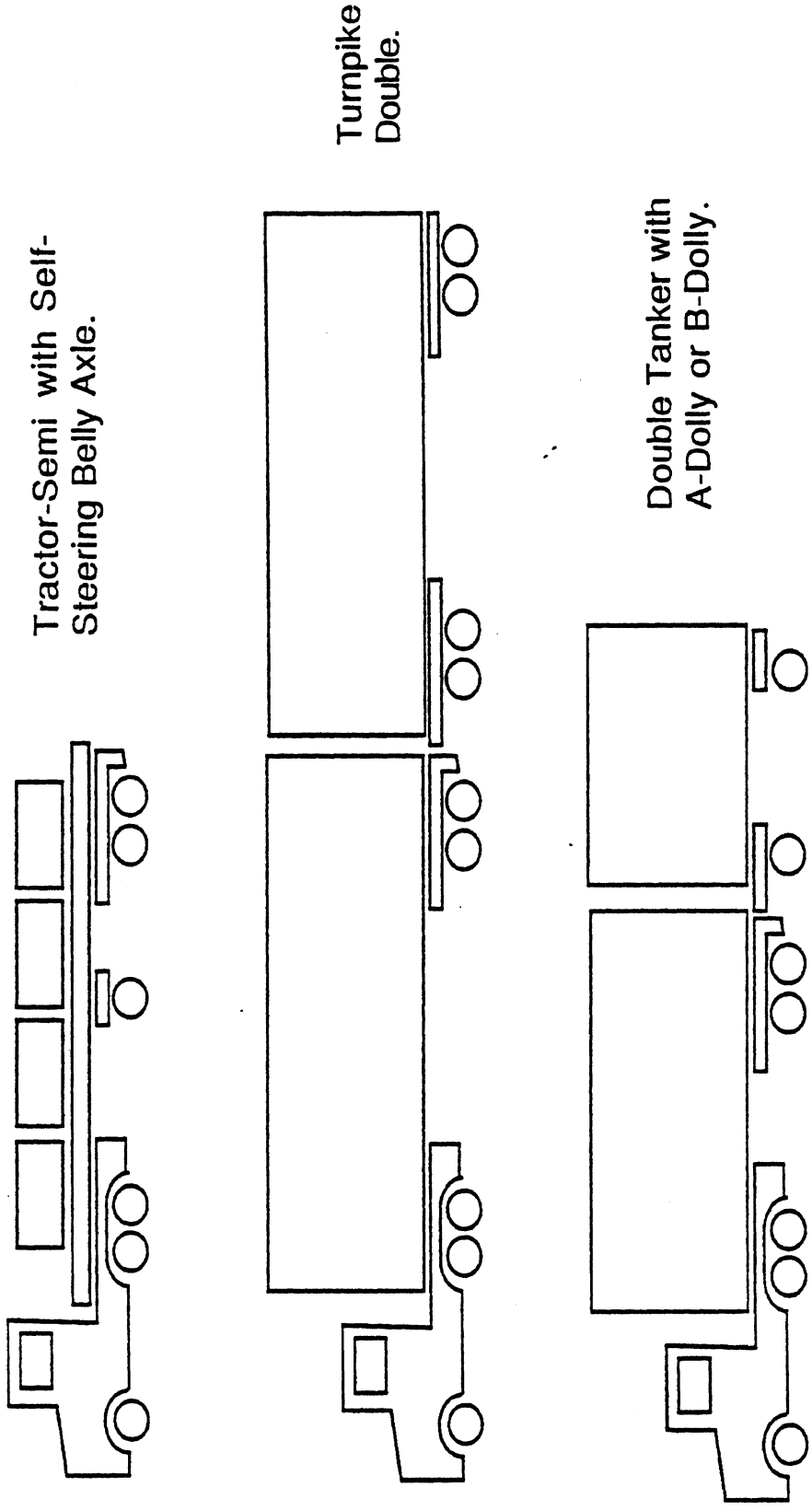
The tractor and all trailers were outfitted with new Michelin 11R 22.5 radial tires. All trailers had a nominal width of 2.6 m (102 in). A schematic of each vehicle is provided in Figure 1. Below is a brief description of each vehicle, including the resulting Gross Vehicle Weight (GVW).

1. Tractor-Semitrailer with self-steering belly axle. This vehicle had six axles and a GVW of 45,500 Kg (100,300 lbs). A CESCHI steerable belly-axle was mounted at the approximate mid-wheelbase position on the semitrailer and the semitrailer tandem axle was in the full-rearward position. The single trailer was a 13.7-m (45-ft) long flat-bed, loaded with steel weights such that the vertical center of gravity of the payload was approximately 80 inches above the ground.

2. Turnpike Double. This vehicle had 9 axles and a GVW of 69,500 kg (153,200 lbs). The two trailers were each 13.7 m (45 ft) long, with van-type bodies, and were coupled by means of a convention tandem-axle A-dolly. The trailers were loaded with steel weights such that the vertical center of gravity of the payload was approximately 2 m (80 in) above the ground.

3. Double Tanker with A-dolly. This vehicle had 7 axles and a GVW of 53,500 kg (117,950 lbs). The front trailer was 10.4m (34 ft) long and the rear trailer was 6.1 m (20 ft) long. Both trailers were configured as tankers for the transport of bulk petroleum products. The front trailer had two out of four compartments filled with water with the other two compartments empty. The rear trailer was designed with only two compartments, but incorporated baffles approximately 1.1m (44 in) from the each end of the vessel. In order to obtain a reasonable weight distribution using water as the loading fluid, these baffles were sealed and pressurized with air. The resulting water loading on the overall vehicle approximated normal operation with a full load of gasoline.

The rear trailer was connected to the front trailer using two different dollies; a conventional single-axle A-dolly, and a Westank-Willock turntable-style B-dolly. The B-dolly connects to the front trailer with two pintle hitches, and its axle steer mechanism



Tractor-Semi with Self-Steering Belly Axle.

Turnpike Double.

Double Tanker with A-Dolly or B-Dolly.

Figure 1

employs a rather light centering device which permits the centering force to near zero when the dolly axle is steered off of its center detent.

3.0 Description of Maneuvers.

A total of six basic maneuvers were performed with the four truck/trailer combinations. These maneuvers included various steering and braking experiments. Not all tests were performed with all vehicles, however, since certain maneuvers are intended to demonstrate phenomena which are evident only for certain vehicles. A complete test matrix is shown on Table 1.

All of the experiments were performed at the Chrysler Proving Grounds in Chelsea, Michigan. The steering maneuvers (no. 1 and 2) were conducted on either the Vehicle Dynamics Area or the High-Speed Oval, both with a dry, asphalt surface. One additional steering maneuver (no. 5) was a very slow speed turn over a wet, slippery surface, which was performed on the Skid Traction Facility. The braking tests (no. 3 and 4) were conducted on the Skid Traction Facility. All braking experiments were conducted with wet surfaces. The following paragraphs briefly describe each maneuver.

1. Sinusoidal Steer. To investigate the rearward amplification phenomenon for the double-trailer combinations tested in this program, a sinusoidal steer input was used. This maneuver allows investigation of the rearward amplification phenomenon and dynamic rollover tendencies of the vehicle, as well as any oscillatory motion of the vehicle prevailing after the steering angle is returned to zero.

The sine-wave steering consists of the driver turning the steering wheel from an initially straight-running condition such that the steering-wheel angle varies as a sine wave. The sine wave lasts for one period, after which the steering angle is returned to zero. Three values for the period of the sine wave were used: 2, 3, and 4 seconds. Using the period value yielding peak amplification (which was 2 seconds for all vehicles), the amplitude of the steering sine wave was then increased during successive runs until the rear trailer exhibited rollover. Additional runs with a period of 3 seconds and large steering values were made for the double tanker configuration.

The sinusoidal steering maneuvers for the turnpike double were performed on the High-Speed Oval, at a nominal speed of 100 km/h (63 mph). The sinusoidal steering maneuvers for the double tanker combinations were performed on the Vehicle Dynamics Area at a nominal speed of 70 km/h (44 mph). The original plan called for all sinusoidal

TABLE 1 - Test Matrix

	TRACTOR-SEMITRAILER WITH SELF-STEERING BELLY AXLE.	TURNPIKE DOUBLE.	DOUBLE TANKER WITH A-DOLLY AND B-DOLLY.
TRAPEZOIDAL STEERS	A,D	A	A,D,F
SINUSOIDAL STEERS	A,D	A	A,D,F
SPLIT-FRICTION BRAKING	B,D	-	B,D,F
BRAKING IN A TURN	B,D	-	B,D,F
UNDULATING ROAD	A,C	-	A,C,E
TIGHT RADIUS TURNS OVER A LOW-FRICTION SURFACE	B,D	-	-

- A. Loaded only
- B. Loaded and unloaded
- C. Steerable axle - unlocked only
- D. Steerable axle - locked and unlocked
- E. B-dolly only
- F. B-dolly and A-dolly

steering experiments to be performed at 100 kilometers per hour on the High-Speed Oval. However, the double tanker with the B-dolly installed exhibited such an oscillatory response at 70 km/hr that the higher speed value was felt to be possible unsafe.

2. Trapezoidal Steer. Transient responses to an abrupt steering input and steady-turning responses were examined using the trapezoidal steering maneuver. This maneuver was performed when the driver turns the steering wheel from a zero angle to some specified value of steer angle as quickly as possible, and holds that angle constant for the duration of the maneuver. The amplitude of the steer angle is controlled by mechanical stops located on the steering column.

This maneuver began by accelerating the vehicle to a speed slightly greater than the test speed. The driver puts the transmission in neutral, and lets the vehicle coast until it has slowed to the test speed, after which the steer input is applied. Successive runs are made at increasing steering wheel angle until the steer angle which results in rollover is found.

The trapezoidal steer maneuvers for all vehicles were performed on the Vehicle Dynamics Area at a nominal speed of 70 km/h (44 mph).

3. Straight-Line Braking on Split-Friction Surface. Straight braking experiments are intended to examine the possibility of anomalous behavior of the self-steering axles during braking. A substantial angle of axle steer as a result of braking forces could lead to jackknife or trailer swing. Large angles of axle steer as a result of braking forces was hypothesized to be of concern relative to jackknife or trailer swing responses.

The tests were carried out by bringing the vehicle to the test speed on dry asphalt pavement, and then proceeding onto a wetted pair of differential friction surfaces and applying the brakes. The split-friction condition was arranged such that one side of the self-steering axle traveled on a more slippery surface than the other side. The brake pressure applied during the tests was regulated so that the pressure could be chosen before a given run, and kept constant during the braking maneuver. Brake pressures from 10 psi up to wheel lockup, or the maximum attainable by the vehicle brake system, were used in successive runs.

The Skid Traction Facility was used for the straight-line braking tests. The high-friction side of the track was coarse concrete, while the other side was an epoxy-coated concrete. ASTM skid numbers for the high- and low-friction surfaces were on the order of

75 and 20, respectively. Both sides of the split-friction condition were wetted for all braking tests. The nominal speed upon application of the brakes was 40 km/h (25 mph).

4. Braking in a Turn. As with straight-line braking, the braking-in-a-turn experiments were intended to examine any unusual behavior as a result of imbalanced braking forces on the self-steering axle, which could cause a yaw instability leading to jackknife or trailer swing.

The braking-in-a-turn tests were carried out by bringing the vehicle to the test speed on dry asphalt pavement, then proceeding onto a wetted, low friction surface. The wet test surface was a jennite coated strip, having an ASTM skid number of approximately 30. After entering the wetted, jennite surface, the driver steered a curved path by following a line of traffic cones, and the brakes were applied. The curved path was an arc of 87 m (27 ft) radius, yielding a nominal lateral acceleration level of 0.15 g at the test speed of 40 km/h (25 mph). The brake pressure applied during the tests was regulated so that a pressure could be chosen and held constant for the duration of a given run. Brake pressures from 10 psi up to the maximum attainable by the vehicle brake system were employed.

5. Tight Turn onto Low-Friction Surface. This maneuver was performed only on the tractor-semitrailer with belly axle. The purpose of the test is to determine whether the presence of a non-steering belly axle can cause a jackknife phenomenon as the tractor rear wheels are entering a low-friction surface during a very tight turn.

The experiment began by bringing the vehicle at a very low test speed onto a dry asphalt pavement. The driver then steered the vehicle in a tight-radius turn. The path of the vehicle was chosen such that the tractor entered the low-friction surface while the trailer tires were still on the asphalt surface. The radius of the turn was the smallest radius that the vehicle was capable of achieving. These tests were carried out on the Skid Traction Facility on the epoxy surface, which will be wetted prior to the run. The nominal speed of the vehicle was 5 km/h (3 mph).

6. Undulating Road. This maneuver was intended to demonstrate any anomalous behavior of a self-steering axle when the vehicle is traveling over an undulating road. The selected vehicles were driven over several undulating roads while the measurements were recorded. Large chuck holes were the only type of undulation which resulted in any significant steering from the self-steering axle. The nominal speed for these tests was 30 km/h (18.8).

4.0 Results of the Experiments

The test matrix shown in Table 1 identifies the three vehicle combinations and the test procedures selected for examining the response issues which pertain to each vehicle. The results of the experimental procedures listed for each vehicle in Table 1 are discussed below.

A. Tractor-Semitrailer with Steerable Belly Axle

a. *Trapezoidal Steer* The trapezoidal steering maneuvers for the tractor-semitrailer were performed to investigate the response of the vehicle during a steady turn, such as would be encountered on a freeway exit ramp, and to examine the rollover tendency of the vehicle. The issue that was of particular interest with this vehicle involves the difference in response when the self-steering belly axle is locked as opposed to unlocked.

The initial experiment was performed with a steering-wheel angle of 80 degrees. The steering-wheel angle was increased in increments of 10 degrees in successive runs until the tires of the outriggers touched down on the pavement (the absence of the outriggers would result in a rollover of the vehicle), which was used as the criterion for rollover.

The steering-wheel angle for touchdown for both cases, self-steering axle locked and unlocked, was 150 degrees. Figures 2 and 3 show the lateral acceleration and the roll angle, respectively, of the rear trailer with a steer angle of 150 degrees for both cases. Notice from Figure 2 that rollover occurred at a lateral acceleration slightly above 0.4 g's for both cases.

For a steering-wheel angle of 150 degrees, which resulted in rollover, the response of the vehicle was somewhat different between cases with the self-steering axle locked and unlocked. The case with the axle locked was a very smooth maneuver, similar to runs at lesser steer angles. With the self-steering axle unlocked, the vehicle motion was not smooth. After the vehicle had rolled to a degree where the wheels on one side of the self-steering axle had left the ground, the axle steered at somewhat larger angles, approximately 11 degrees, which is shown in Figure 4. At this point the trailer exhibited a vertical oscillatory motion as a result of the rear axles of the trailer sliding sideways. The oscillatory motion is evident in the lateral acceleration response shown in Figure 2. This motion did not significantly affect the rollover threshold of the vehicle, since the oscillations only became evident right at the rollover condition.

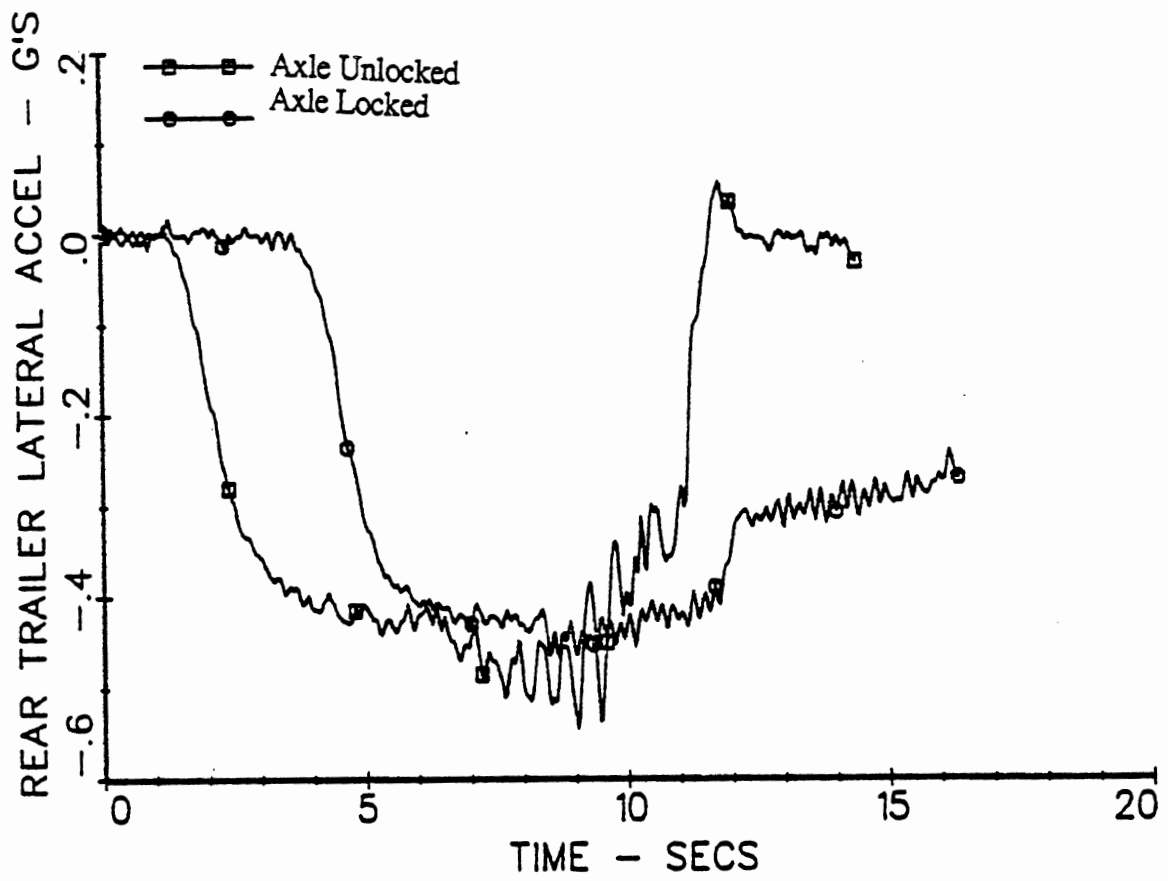


Figure 2

Trapezoidal steer responses of tractor semitrailer test vehicles

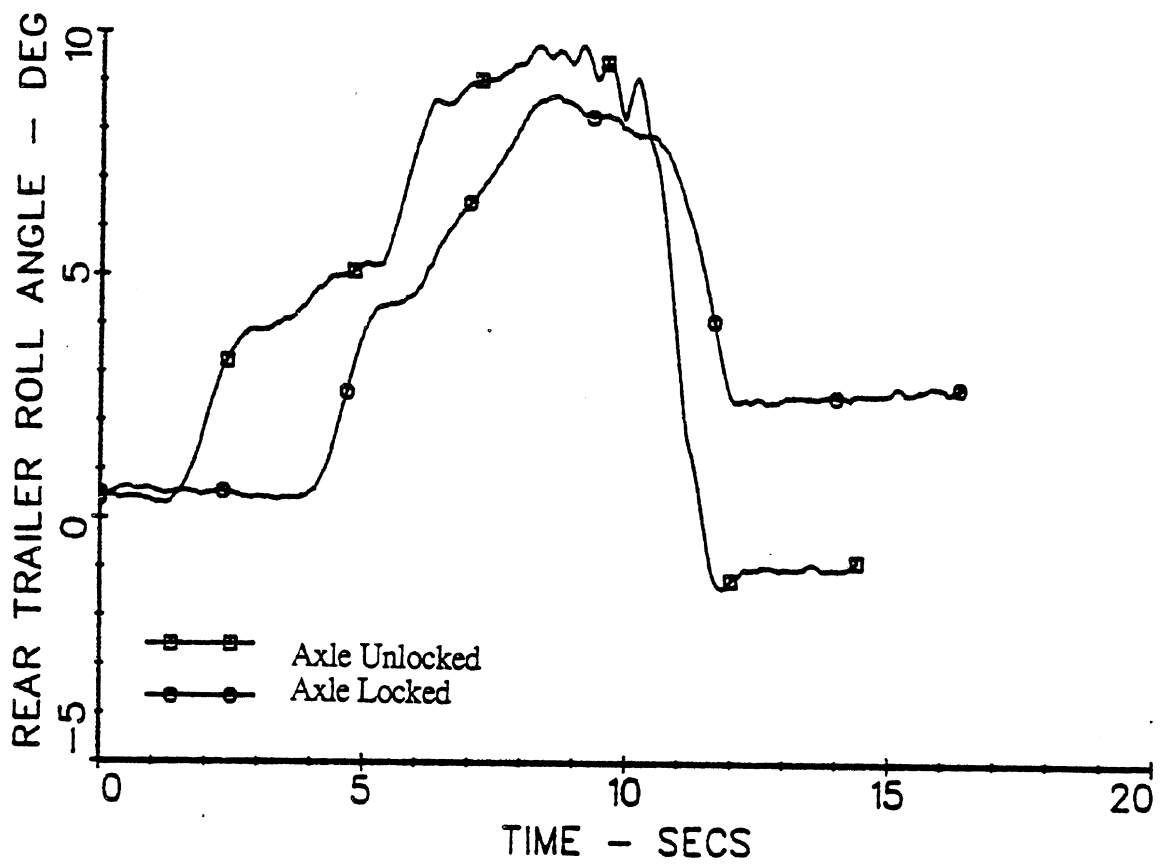


Figure 3

Trapezoidal steer responses of tractor semitrailer test vehicles

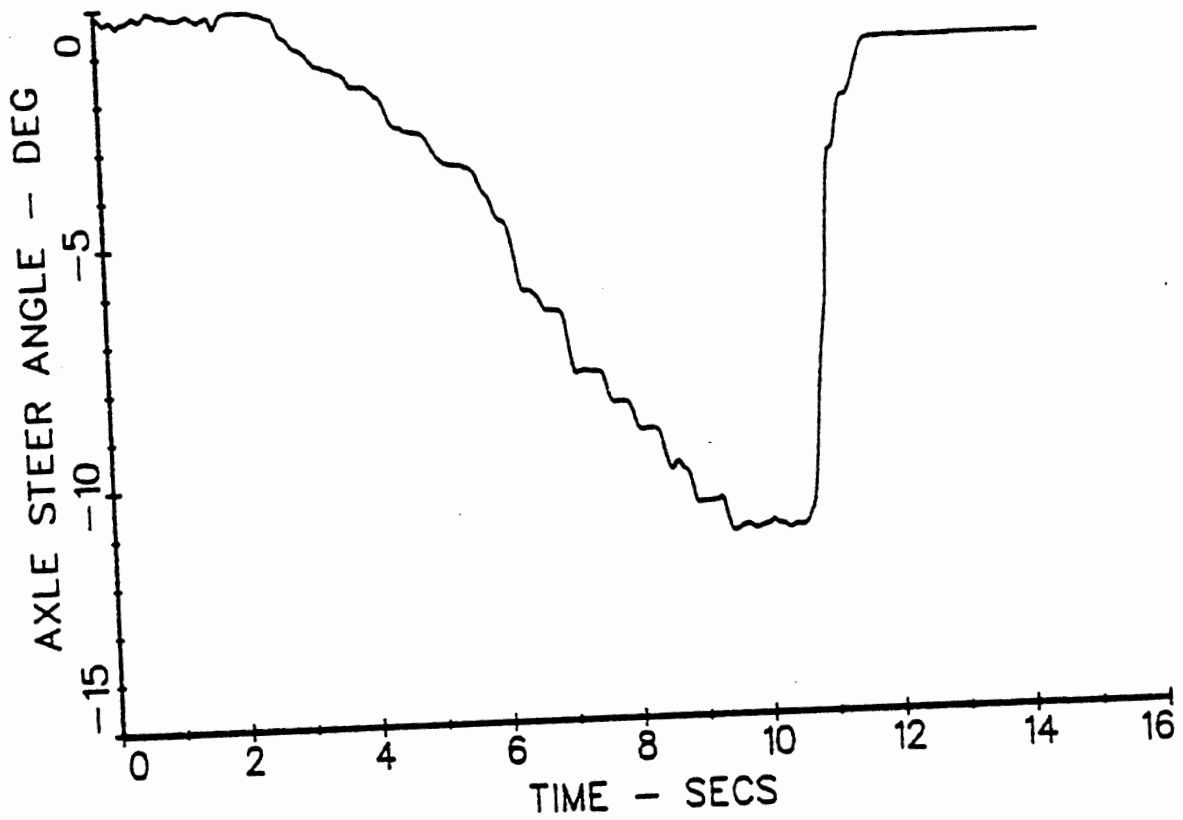


Figure 4

Steer angle response of self-steering belly axle on tractor semitrailer test vehicle

b. *Straight-line Braking.* The straight-line braking experiments were performed under the split-friction surface condition. The right/left difference in the surface friction was intended to induce a moment on the self-steering belly axle when the brakes were applied, resulting in large steer angles and possibly a significant yaw disturbance. The experiments with the vehicle fully-loaded using the rough concrete and epoxy surfaces produced small but detectable responses with the self-steering axle unlocked. The vehicle came to a stop with virtually zero articulation angle between tractor and semitrailer. The repeat run with the self-steering axle locked and full brake pressure did not show any yaw response of significance.

The straight-line braking tests were repeated with the vehicle unloaded, also using the rough concrete and epoxy surfaces. For brake pressures of 20 psi and greater, the self-steering axle steered rapidly to full displacement, and remained in this orientation until the vehicle came to a stop. With brake pressures of 20 psi and greater, the wheels on the rough concrete kept rolling, while the wheels on the other side were locked. The tractor yaw response with the brake pressure at the maximum level is shown in Figure 5, for cases with the self-steering axle locked and unlocked. The steer angle at the self-steering axle is shown in Figure 6. Notice in Figure 5 that the maximum yaw rate was a minimal 3.5 degrees per second for both cases. The yaw disturbance is shown to damp out faster with the axle locked, however. Runs with lesser brake pressures showed similar results to a lesser degree.

c. *Braking in a Turn.* The braking-in-a-turn maneuver was intended to determine whether large steer angles of the self-steering belly axle would occur during braking and lead to a yaw instability. Runs were made with the self-steering belly axle locked and unlocked.

The maneuver was performed by steering the test vehicle onto the wet, jennite-coated surface, following a line of traffic cones outlining the desired curved path. Once the vehicle was in a steady turn and all wheels were on the jennite surface, the brakes were applied and held at constant pressure until the vehicle stopped. When the experiment was performed with the vehicle fully loaded and the self-steering belly axle unlocked, the vehicle did jackknife, but not until a high level of brake pressure caused lockup of the tractor tandem axles. The steer angle of the self-steering belly axle reached a maximum value of 7 degrees. Runs made with the self-steering axle locked showed that the vehicle again jackknifed only when the brake input attained the maximum pressure value, at which lockup of the tractor tandem axles occurred.

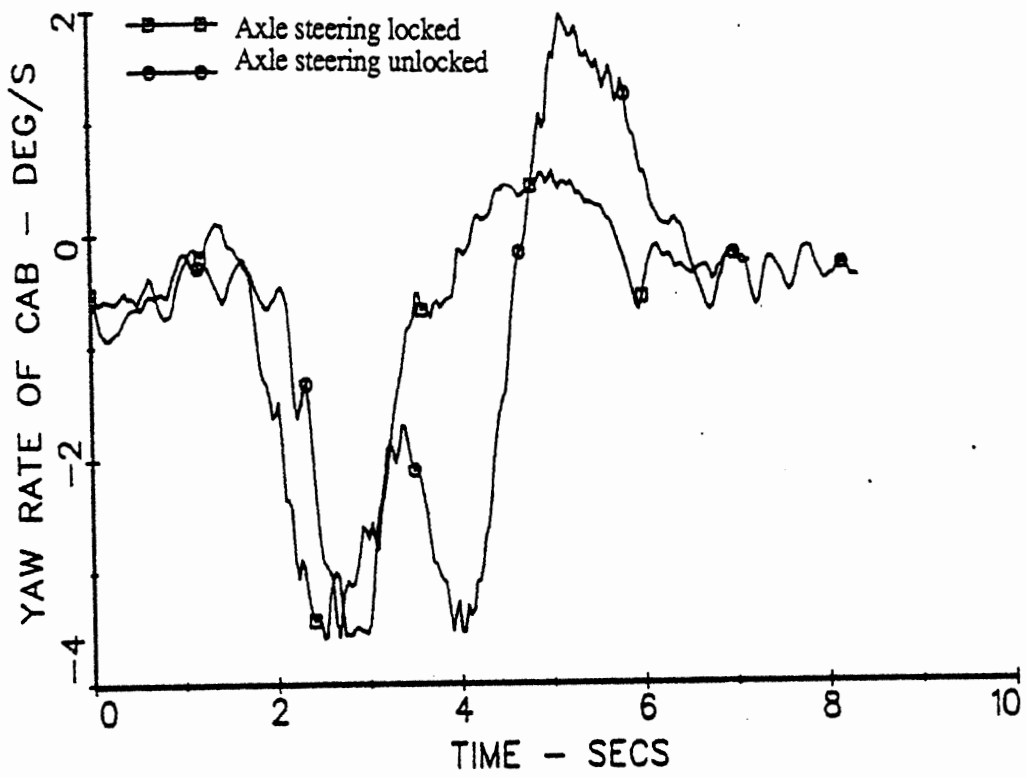


Figure 5

Tractor yaw rate response in straight line, split-friction braking

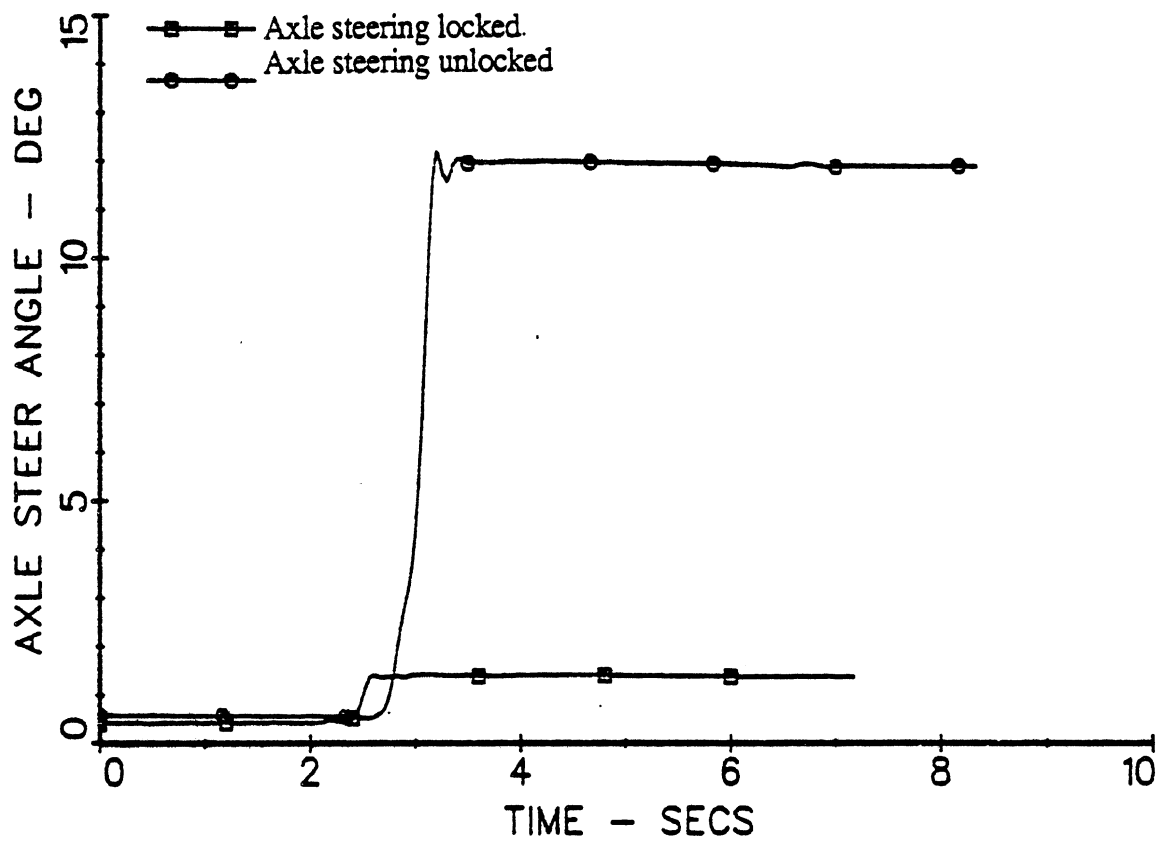


Figure 6

Steer angle response at self-steer belly axle during split-friction braking maneuver

The experiments were repeated with the vehicle unloaded. The results of the tests with the self-steering axle unlocked show that the vehicle will jackknife at very low braking pressures, starting at 20 psi, simply as a result of lockup of the tractor tandem axles. The yaw rate of the tractor and the angle of the self-steering axle are given in Figures 7 and 8, respectively. Notwithstanding that the steer angle at the self-steering axle reaches a value of 4.5 degrees in the "steer unlocked" case, in Figure 8, the tractor yaw rate responses are nearly identical in the respective locked and unlocked cases, in Figure 7. These results indicate that the steer-centering properties of the belly axle do not have a significant affect on stability in this maneuver.

d. *Tight-Radius Turns.* Tight radius turns were performed on the Skid Traction Facility and were intended to determine the jackknife tendency at very low speeds. With the self-steering axle locked, the yaw moment needed to turn the trailer is very large, as a result of the belly axle being located far forward of the rear tandem axles. It was expected that once the rear tractor wheels had entered the low-friction surface, the rear tires on the tractor would approach a saturation level of lateral force, perhaps resulting in a vehicle jackknife.

The experiments with the self-steering axle locked and unlocked showed that the vehicle did not exhibit a jackknife tendency under the stated conditions. The experiments were performed with the vehicle loaded and unloaded with the same result of no jackknifing. The experiments were also repeated at higher speeds, approximately 15 km/h (9 mph), with the same result.

Unfortunately, the experiment was inconclusive to the degree that the available epoxy surface appeared to yield a rather high peak friction condition for this near-zero-speed maneuver. It is likely, however, that the maximum friction force produced by snow- or iced-covered roads that would be encountered in service would lead to the hypothesized jackknife result.

e. *Undulated Road.* The purpose of this maneuver was to test the tendency of the self-steering belly axle to steer to a substantial angle when one side of the axle proceeds over a bump or hole in the road, while the other side stays on a smooth surface.

The vehicle was driven over several roads, each with a different type of undulation. The surfaces used were cobblestones, irregular bumps, and regularly-spaced, uniform chuck holes. The vehicle proceeded over each of these types of undulation successively at speeds of 10 and 20 km/h (6 to 12 mph). The cobblestones and the irregular-spaced bumps did

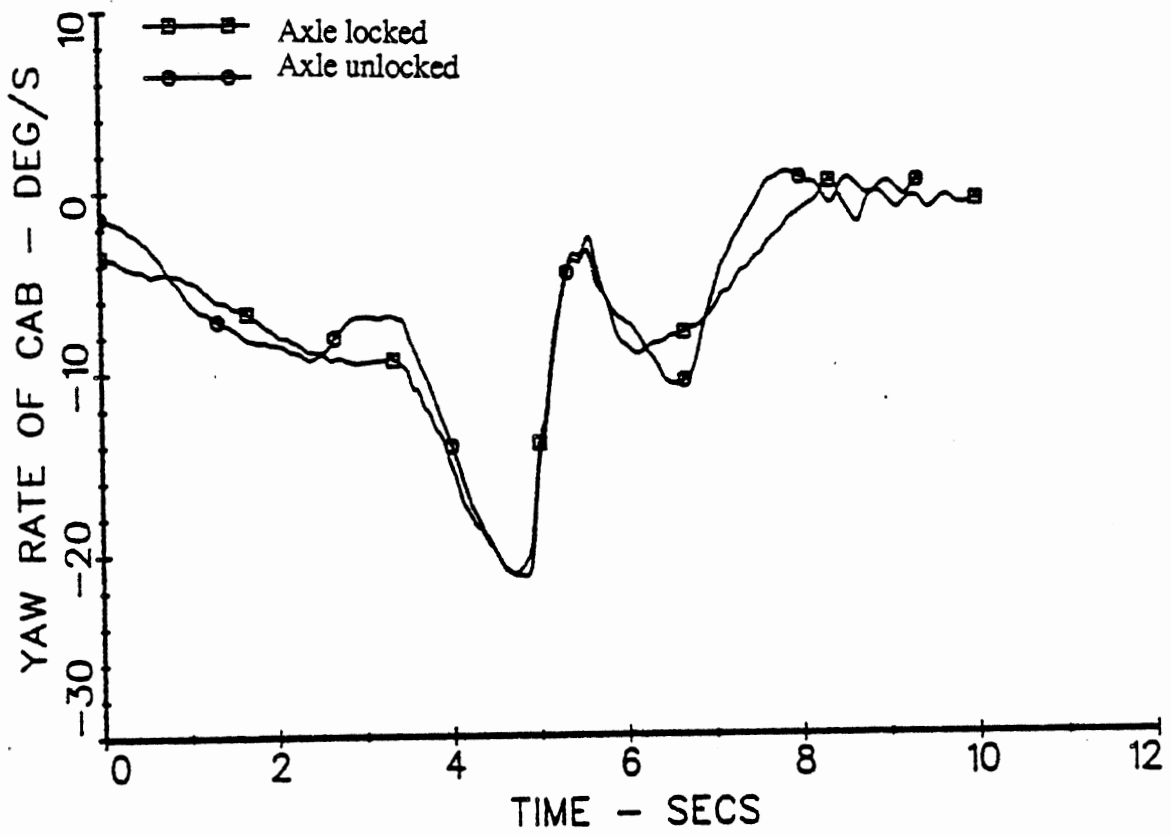


Figure 7

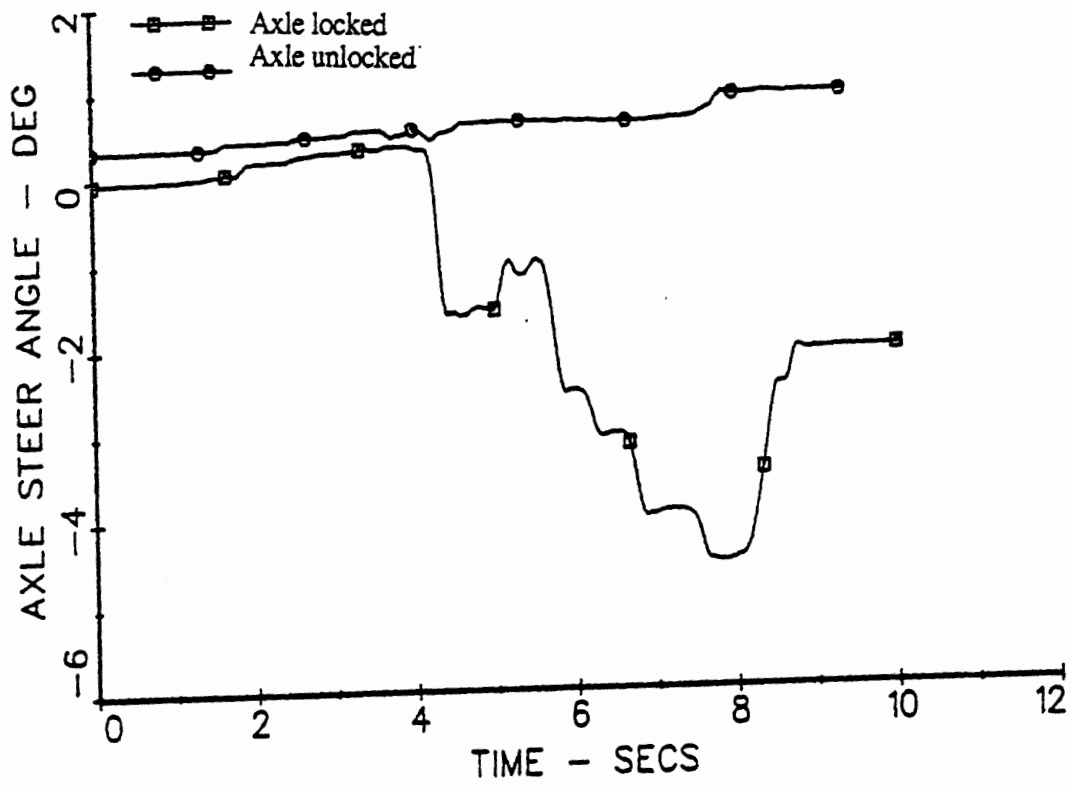


Figure 8

not produce any significant steer angle of the self-steering belly axle at either speed. Accordingly, the overall vehicle yaw response was also very small. The chuck holes, which were approximately 0.3 m (12 in) wide and 0.6 m (4 in) deep, did produce an approximate 3-degree steer angle of the self-steering belly axle. The axle steered to this angle only momentarily, and then returned quickly to a zero steer angle. The yaw response appeared likewise short-lived. The yaw rate and the self-steering axle angle for this maneuver are shown in Figures 9 and 10.

Conclusions From Tests with Tractor and Belly-Axle Semitrailer

Moreover, the sum of the experiments conducted on the belly-axle-semitrailer indicated the steering freedom of this centrally mounted belly axle did not significantly influence the performance of the vehicle combination. This basic finding was also confirmed by means of the simulation exercise conducted in this study. The belly-axle mechanism is incapable of altering the overall response of the vehicle because (a) the parent 5-axle tractor semitrailer on which the belly-axle has been mounted is basically a very yaw-stable and well-damped vehicle and (b) the belly-axle is installed at a position which is very near the trailer mass center--that is, with virtually no lever arm for imposing dynamic moments influencing the yaw response of the trailer. Nevertheless, supportive analysis in Volume I indicates that the tendency toward producing a tractor jackknife during tight-radius turning on a slippery surface is certainly exaggerated with the very widely-spread belly-axle installation.

B. Turnpike Double.

a. Trapezoidal Steer. The trapezoidal steer maneuvers were performed with this vehicle to examine the response of the vehicle in a steady turn, such as would be experienced on a freeway exit ramp, and to examine the rollover tendency of the vehicle in a sustained turn. The vehicle was fully loaded for these experiments.

The initial experiment was performed at a steer angle of 80 degrees. The steering-wheel angle was increased in successive runs until a rollover condition was achieved. Rollover was again represented by touch-down of the outriggers, which occurred in this maneuver when the steering-wheel angle was 150 degrees. The lateral acceleration and the roll angle of the second trailer are shown in Figures 11 and 12, respectively, for the critical steer angle of 150 degrees. As is evident in Figures 11 and 12, the vehicle motion for the rollover case was smooth, with no unexpected motion. This was true for all steer angles tested.

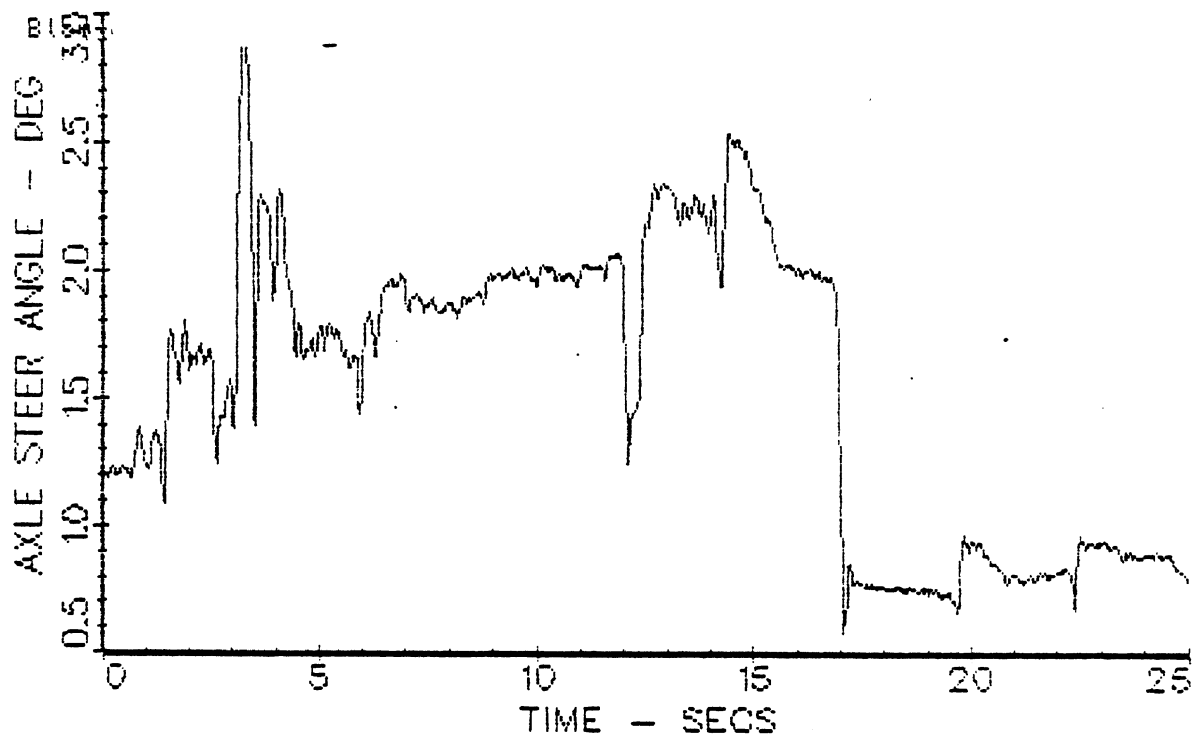


Figure 9

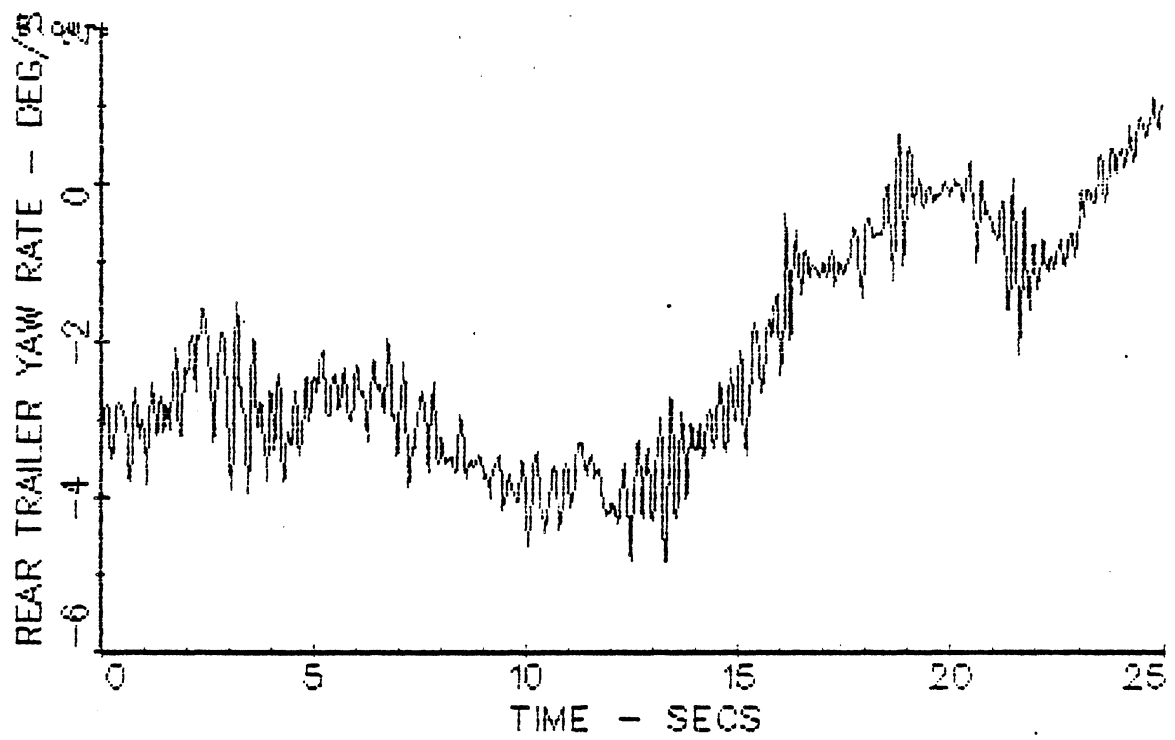


Figure 10

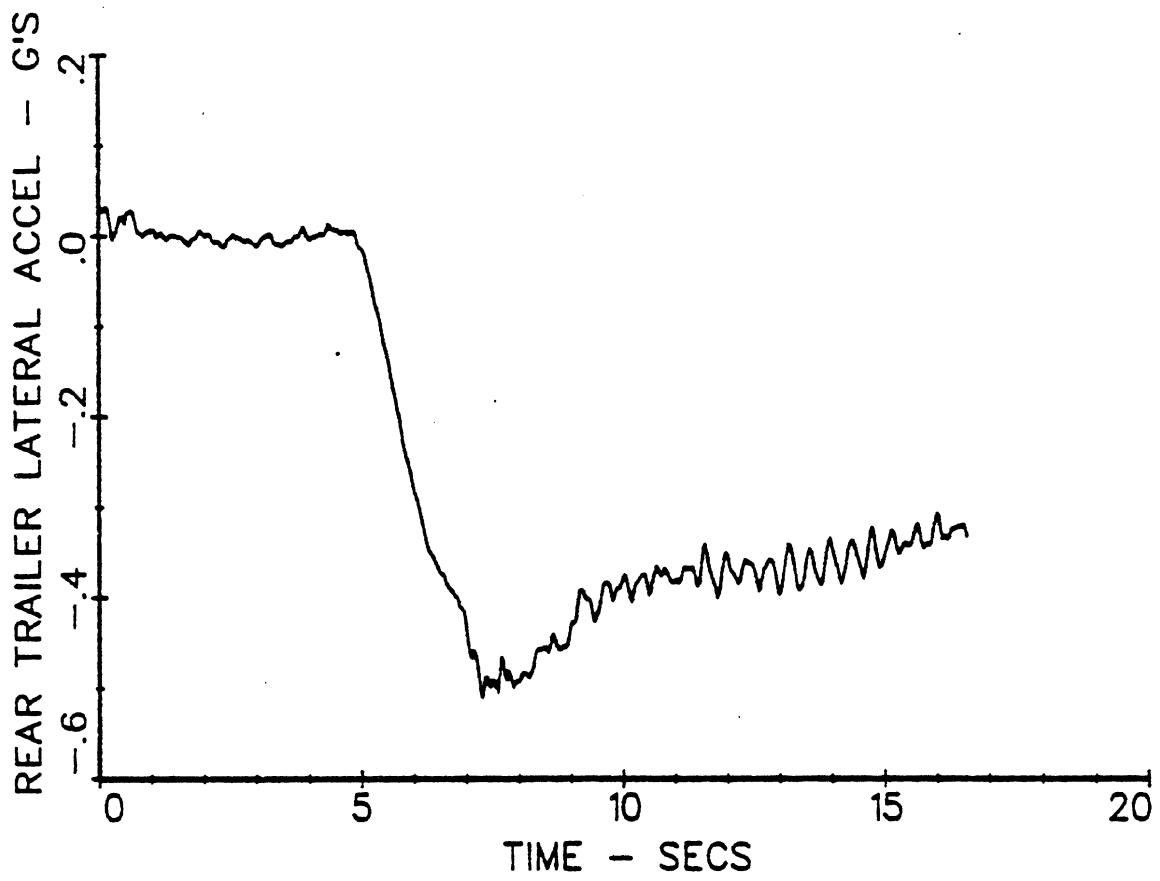


Figure 11

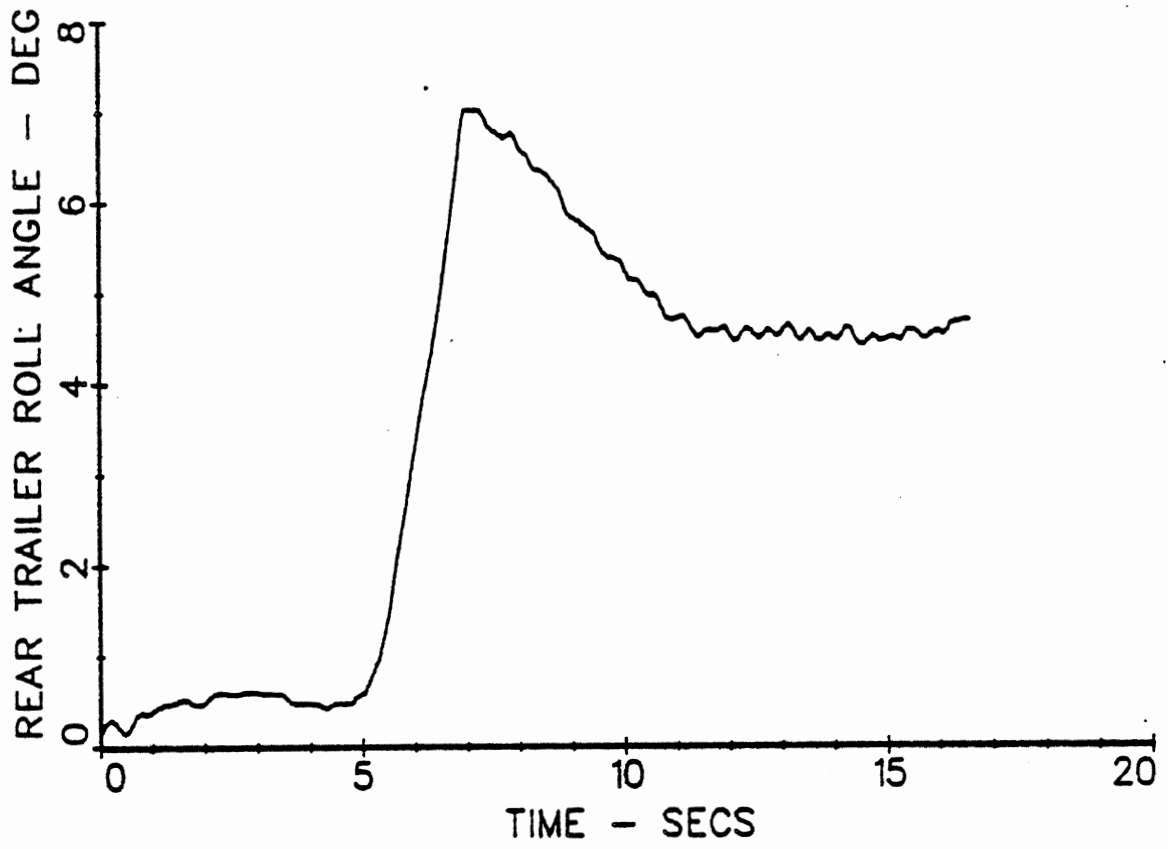


Figure 12

The steering wheel angle of 150 degrees resulted in a lateral acceleration of 0.47 g at the center of gravity of the second trailer.

b. Sinusoidal Steer . The sinusoidal steer maneuvers were performed with this vehicle to investigate the rearward amplification of lateral acceleration at the rear trailer. All of the sinusoidal steer tests were performed on the High-Speed Oval Facility at the Chrysler Proving Grounds at a speed of approximately 100 kilometers per hour.

Both the period and the amplitude of the sine wave, which represents the steering-wheel angle, were varied. Initial experiments were run with the relatively low steering amplitude of 80 degrees using three different values of period, i.e., 2 sec., 3 sec., and 4 sec. The results of the initial experiments were then used to determine which period had the largest value of rearward amplification. The highest amplification response was seen to be 1.30 for a period of 2 seconds. Using a period of 2 seconds, the amplitude was increased in successive runs until the rear trailer exhibited rollover. The lateral acceleration of the tractor and the second trailer are shown in Figure 13 for the case when the vehicle exhibited rollover. Note in Figure 13 that the rear trailer rolls over in the maneuver in which the tractor experiences a lateral acceleration level of 0.30 g.

Conclusions from Tests with Turnpike Double

The turnpike double was observed, as expected, to exhibit no undesirable anomalies of response in steady turns and rapid path-change maneuvers. The vehicle is rather heavily damped in yaw response and exhibits the smallest levels of rearward amplification of all A-train combinations. These results confirm previous studies and the extensive simulation results produced in this project. Thus, although the Turnpike double makes very large demands on the available space at roadway intersections and other tight-radius curves, it compares favorably with the 5-axle tractor semitrailer in dynamic behavior.

C. Double Tanker with A- and B-Dolly.

a. Trapezoidal Steer . The trapezoidal steer tests were performed with this vehicle to determine whether the self-steering axle on the B-dolly would steer to significant angles , resulting in an uncontrollable motion of the vehicle. Duplicate runs were made with the self-steering axle locked and unlocked, and with an A-dolly installed instead of the B-dolly. The vehicle configurations were identical except for the switching of the dollies. All the trapezoidal steer maneuvers were performed on the Vehicle Dynamics Area at a nominal speed of 70 km/h (44mph) and the vehicle fully-loaded.

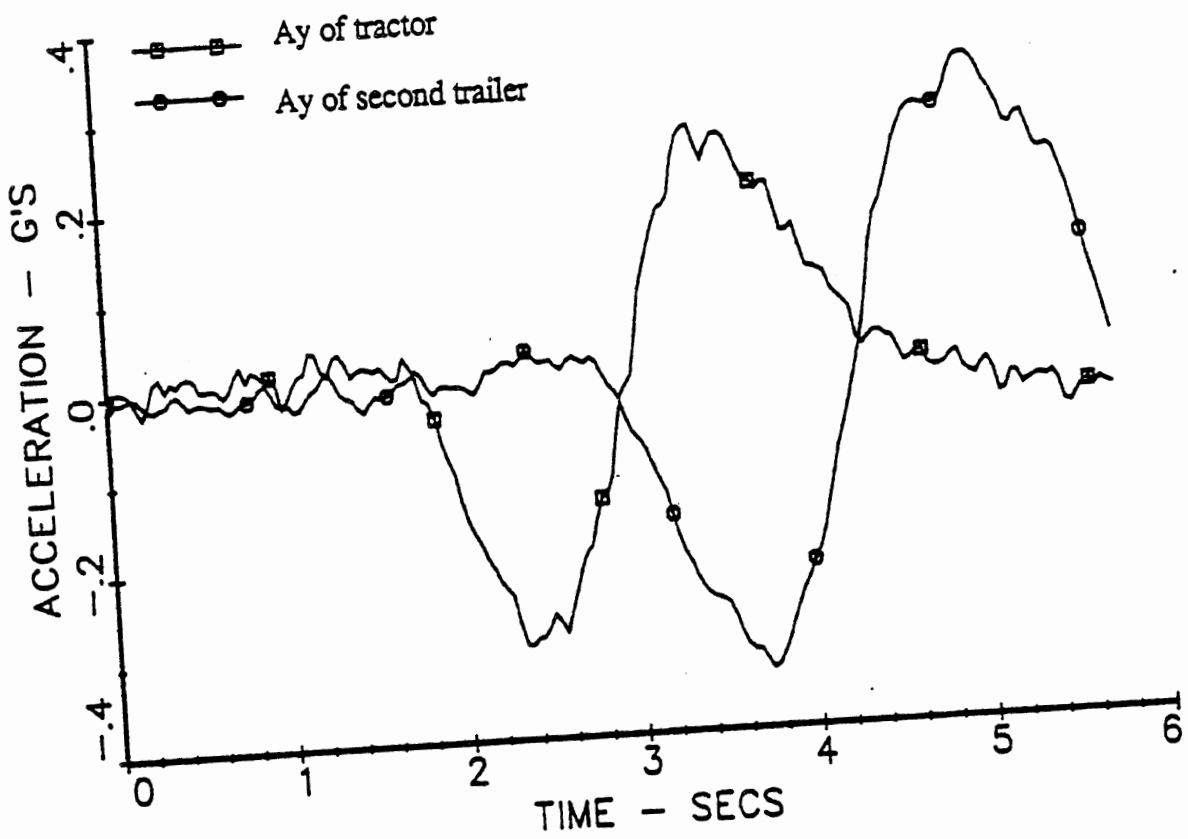


Figure 13

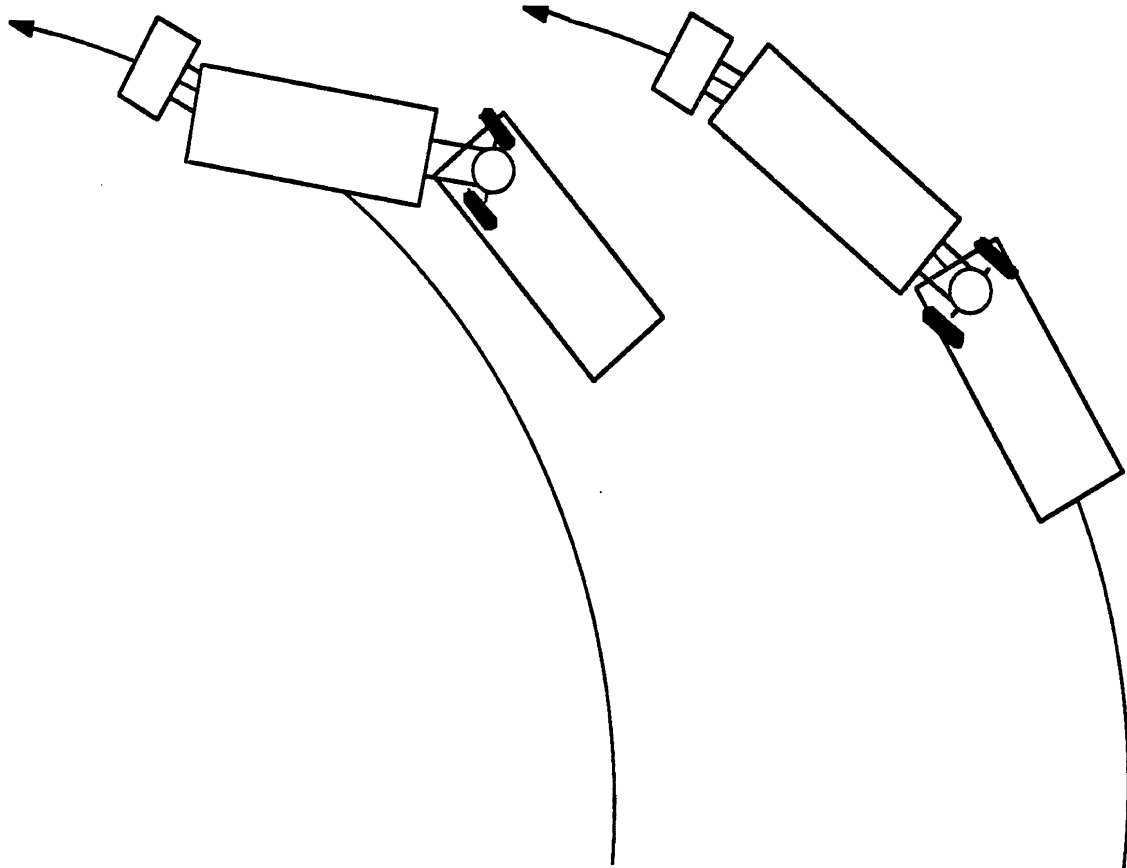
Initial runs were made with the B-dolly installed and the self-steering axle unlocked. The initial steering-wheel angle was 80 degrees. Although this steering-wheel angle causes the vehicle to turn very gradually in a large radius curve, the vehicle with the self-steering axle unlocked exhibited an anomalous motion that became more evident with increasing steering-wheel angles. Due to insufficient side force levels being generated at the dolly axle, the rear of the lead trailer exhibited a large degree of high-speed, outboard offtracking, such as shown qualitatively in Figure 14. Further, the entire vehicle exhibited a distinctly oscillatory yawing motion. The same runs made with the self-steering axle locked did not exhibit these motion anomalies.

The experiments with the A-dolly installed were similar to the results with the B-dolly having the self-steering axle locked. The yaw rate response of the tractor is shown in Figure 15 for cases with the B-dolly installed and the self-steering axle locked and unlocked, and with the A-dolly installed. The oscillatory nature of the B-dolly configuration is evident in Figure 15.

The amplitude of the self-steer angle during the trapezoid steer maneuver which resulted in rollover is shown in Figure 16. The indicated peak steer angle value near 5 degrees is, indeed, large and implies a large excursion in outboard offtracking--in excess of 3.5 m (11.5 ft). Moreover, although the experiments showed that rollover occurred with a lateral acceleration level of 0.4 g regardless of the dolly configuration, the key problem revealed in these tests involved the excessive tendency of the steerable B-dolly toward outboard offtracking and an oscillatory transient response involving all three units of this double combination.

b. Sinusoidal Steer. The sinusoidal steer tests were performed with this vehicle to determine the response of the vehicle in a lane-change maneuver with various degrees of abruptness. Again the focus was upon the difference in response with the self-steering axle locked and unlocked. The maneuver was made for two different steer input periods; 2 sec and 3 sec. For each period, the amplitude of the input to the steering wheel was increased for successive runs until rollover was achieved.

Initial runs were made with the B-dolly installed and the self-steering axle unlocked. These runs were repeated with the axle locked and with the A-dolly replacing the B-dolly. The lateral acceleration of both the tractor and the second trailer are shown in Figure 17 with the B-dolly installed and the self-steering axle unlocked, and Figure 18 with the A-dolly installed. Similar results for a period of 3 seconds are shown in Figures 19 and 20.



a. B-dolly axle steer unlocked

b. B-dolly axle steer locked

Figure 14.

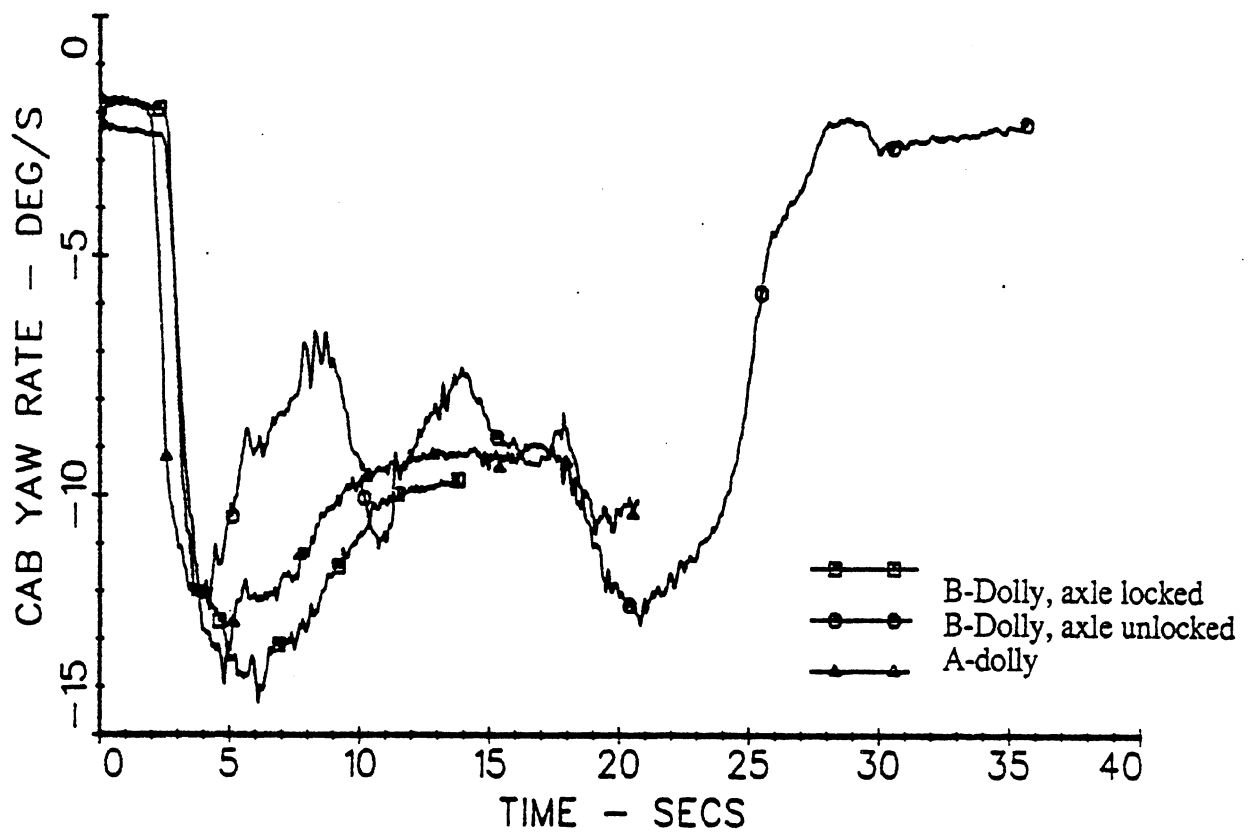


Figure 15

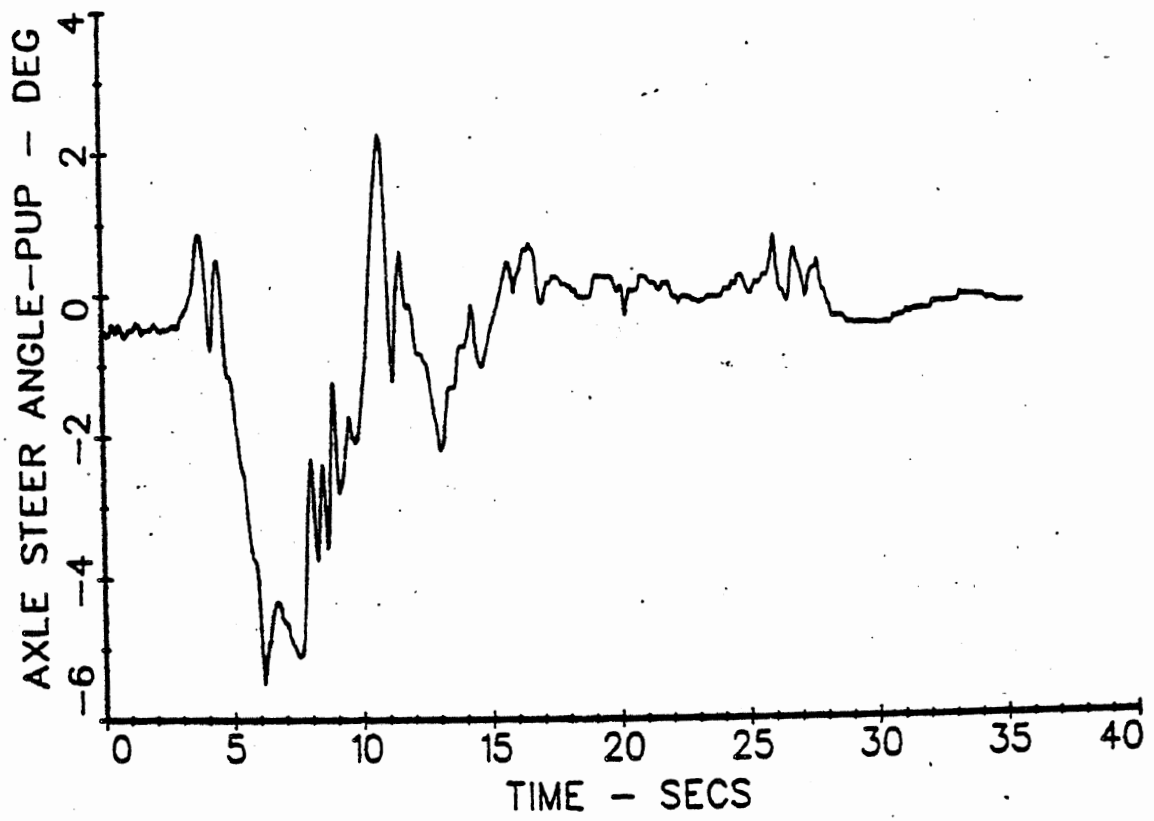
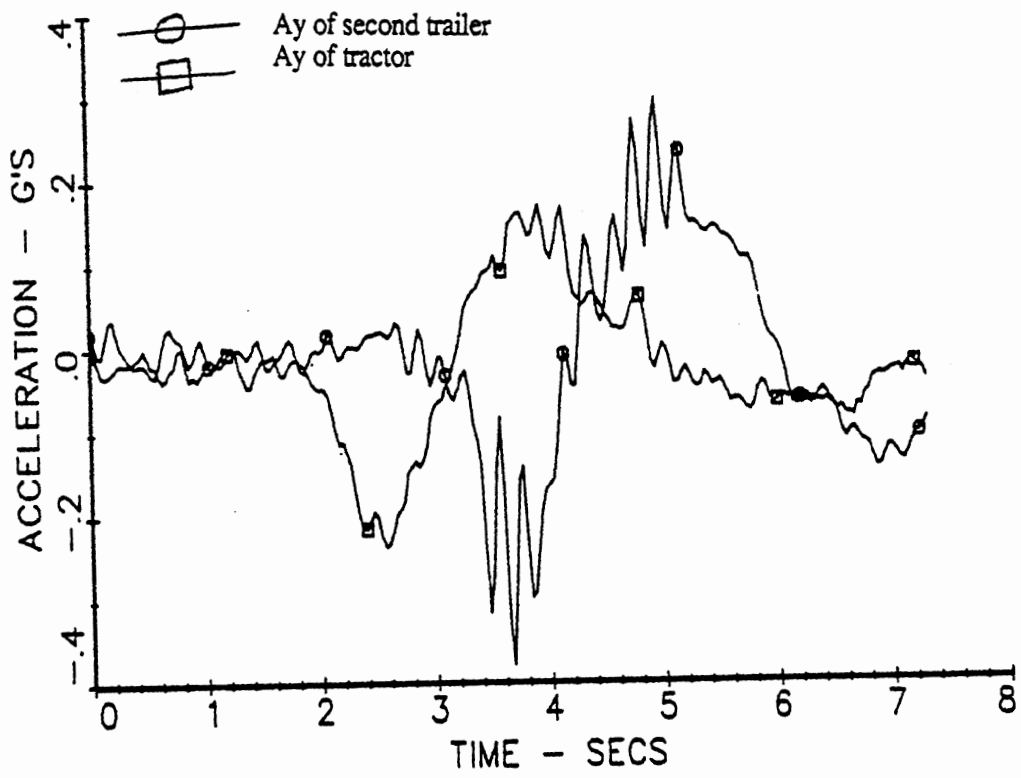
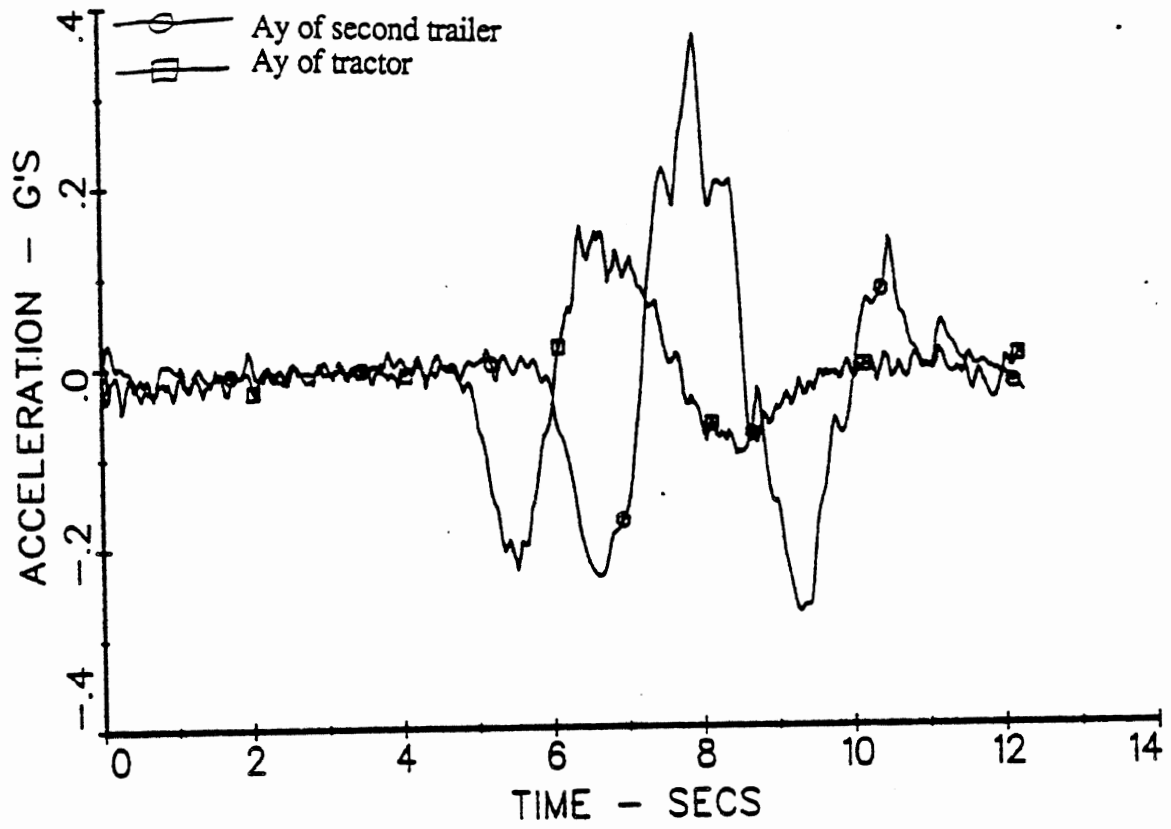


Figure 16



B-Dolly, unlocked

Figure 17



A-Dolly

Figure 18

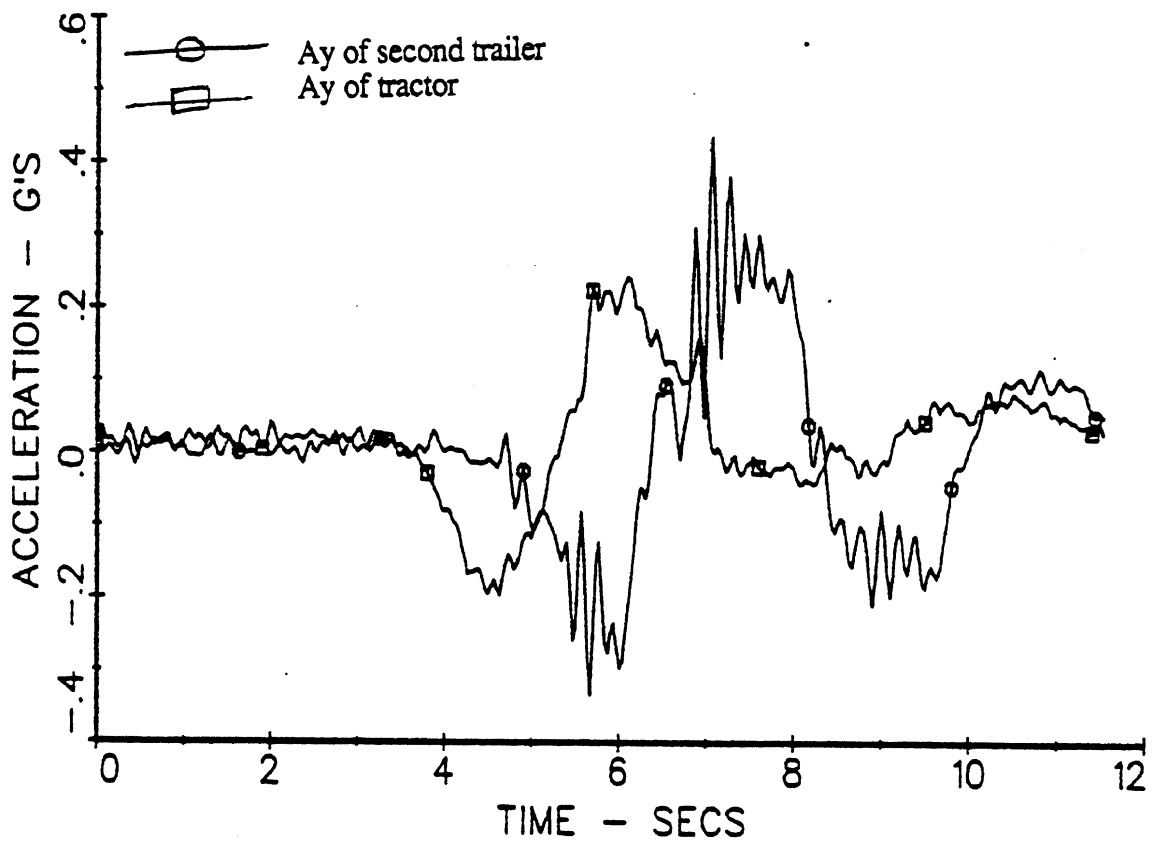


Figure 19

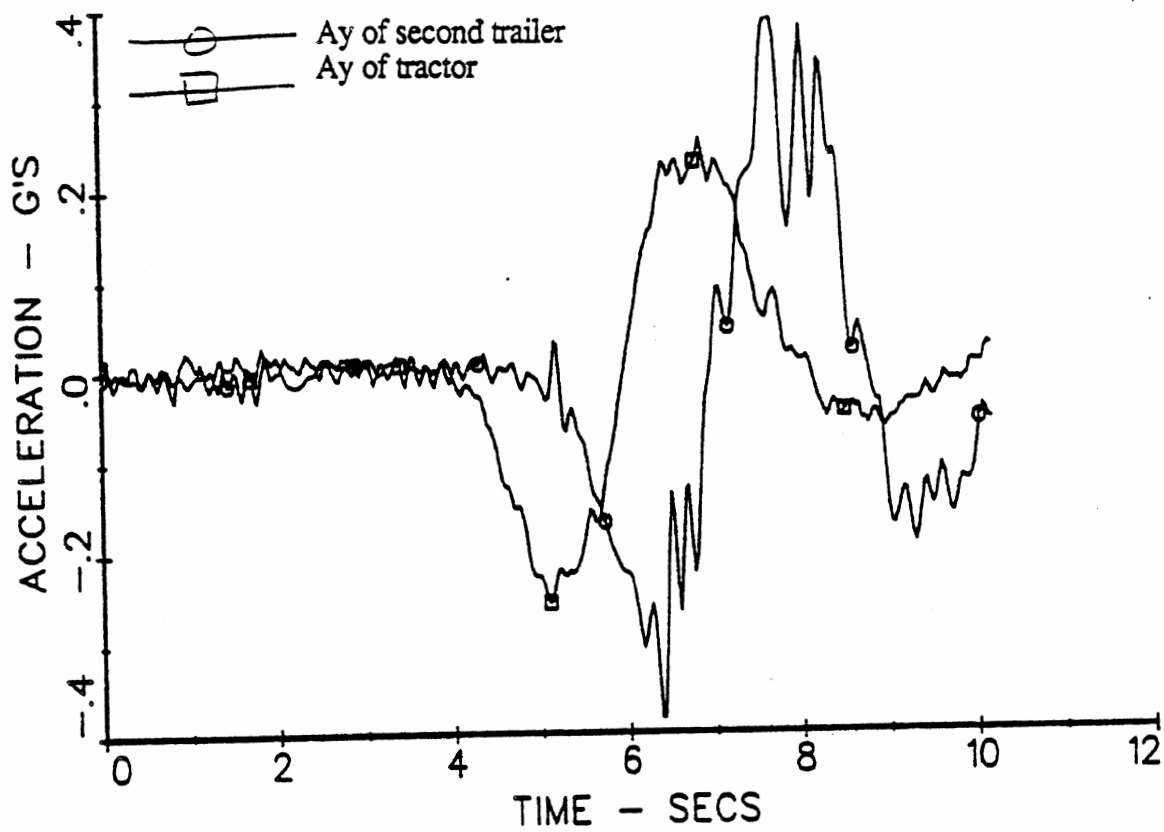


Figure 20

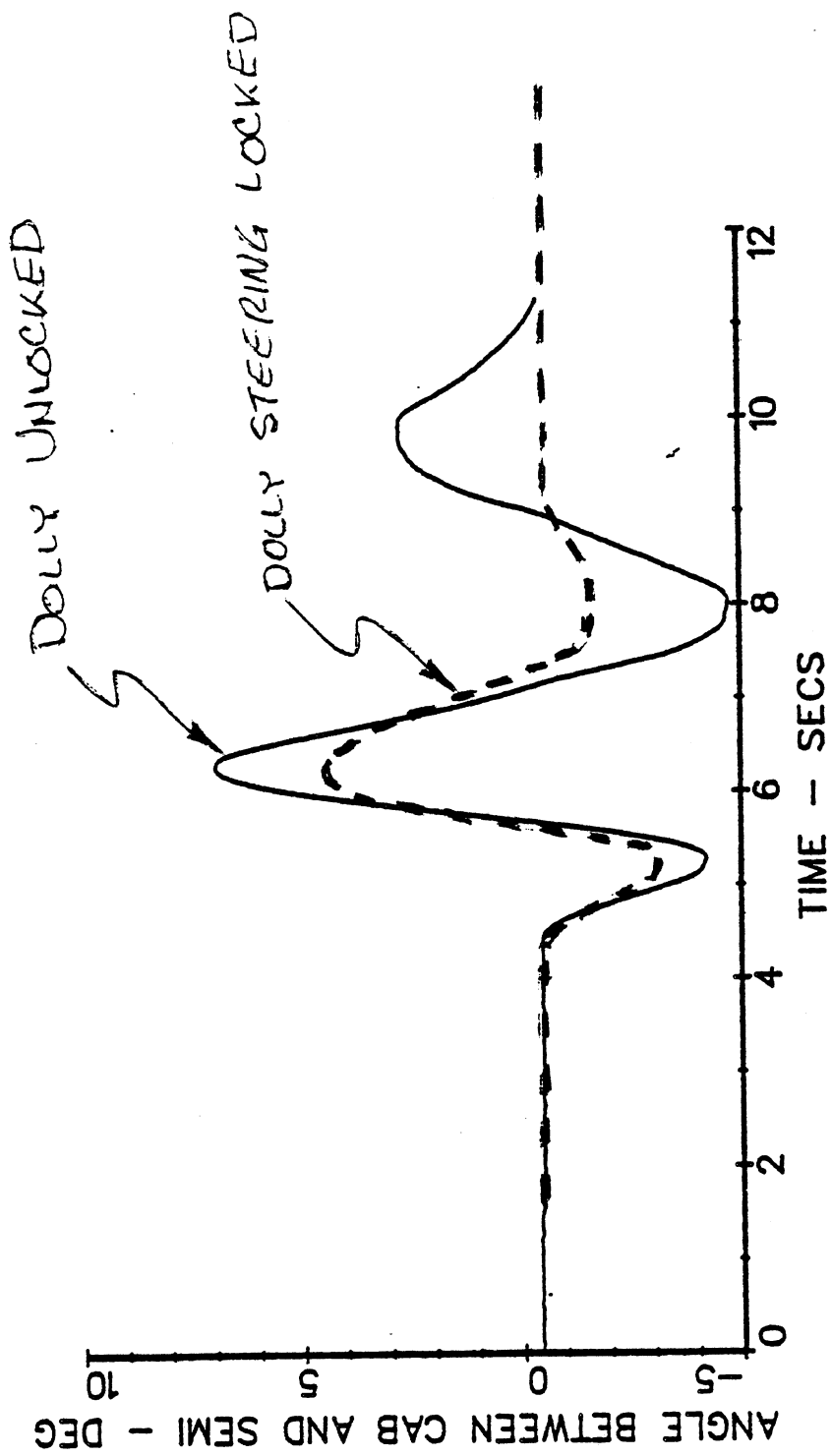
For a period of 2 seconds, rollover occurred with a maximum steering-wheel angle of 130 degrees, and for a 3-second period, rollover occurred at an angle of 110 degrees.

The data reveal that the vehicle with steerable-axle B-dolly exhibits a nominal level of rearward amplification equal to 1.3--and the amplification response is rather flat over both steer-input frequencies. By contrast, the A-double exhibits an amplification level slightly above 2.0 in response to a steer input having a 2-second period and a value of 1.4 at a period of 3 seconds. These results are quite in line with simulation results seen for similar vehicles. That is, the B-dolly definitely introduces a reduction in rearward amplification relative to the A-dolly (while also affording the benefit of roll coupling which is not characterized through the rearward amplification measure).

Although the B-dolly provided a substantial improvement in rearward amplification behavior, a lightly-damped transient decay was seen to follow the conclusion of the nominal lane-change motion. Indeed, the yaw response of both trailers and the tractor continued for several periods after conclusion of the steer input. Shown in Figure 21, for example, is the articulation angle response between the tractor and first trailer. With the dolly steering mechanism unlocked, the articulation response is seen to be markedly oscillatory in this 2.0-second maneuver at 70 km/h (44 mph). Although the data collection time cut the transient short in Figure 22, it is apparent that even less damping of the articulation response was evident in a sine-steer maneuver having a 3.0-second period.

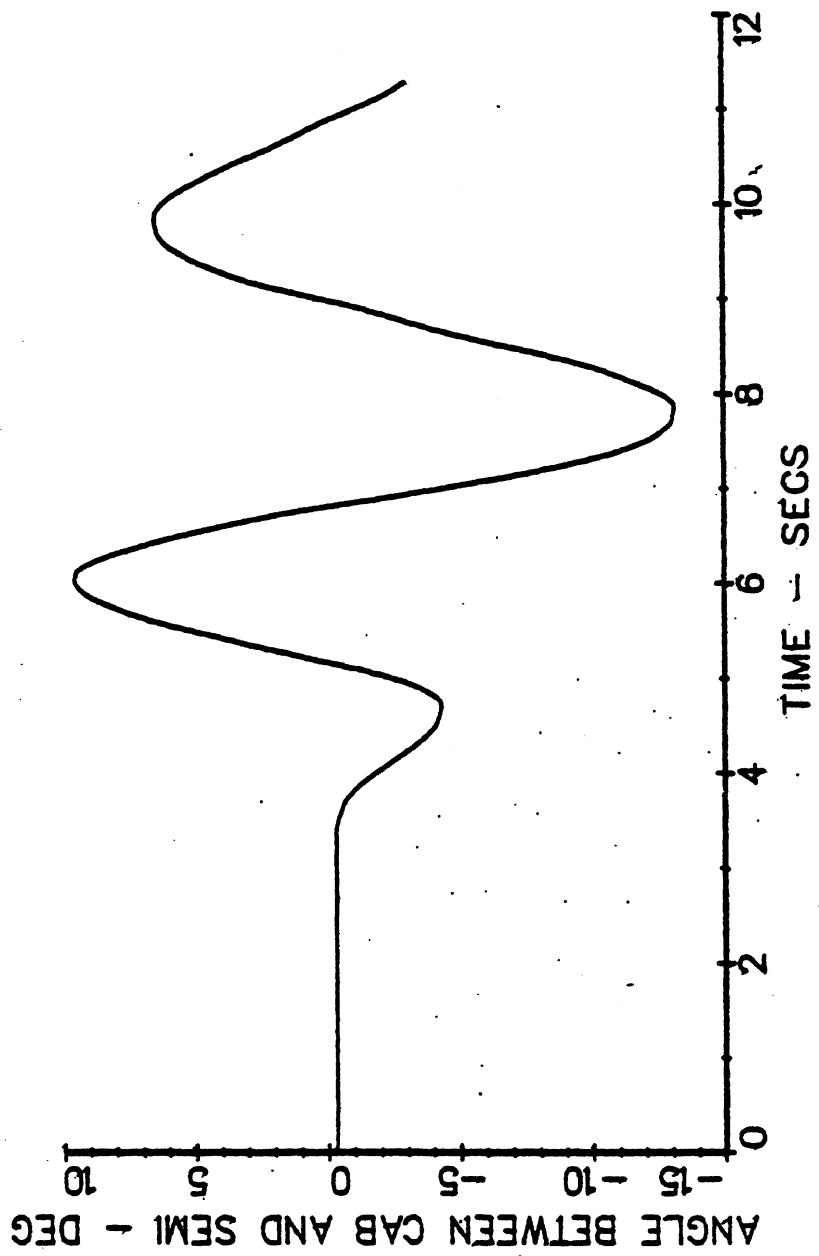
Simulations involving an analogous case to this almost freely-steering B-dolly showed similar results, namely, that the C-train combination as a whole can exhibit very lightly damped motion responses when the steer-centering properties are insufficiently stiff (and when the distance from the lead trailer axle to the dolly axle is rather long, as in the tested case). Further, when such vehicle configurations are operated at higher speeds, a divergent yaw oscillation is possible. For fear of being unable to control the vehicle in a test scenario which incited such a divergency, tests at a speed of 100 km/h (63 mph) were abandoned.

c. Straight-Line Braking. The straight-line braking tests were performed on the Skid Traction Facility. As with the tractor-semitrailer combination, the maneuver with the double tankers was performed on the rough concrete and epoxy-coated surface, with both surfaces wetted. These tests were intended to demonstrate the tendency of the self-steering axle on the B-dolly to steer when the brakes are applied. Tests with the self-steering axle on the B-dolly locked and with the A-dolly were performed for some conditions to compare with the results of the unlocked tests.



09/27/85 11:46:44 DT-SS-U-F
70-130DEG-2SEC

Figure 21



09/27/85 11:22:12 DT-SS-U-F
70-110DEG-3SEC

Figure 22

The tests began at a low brake pressure of 20 psi, and the brake pressure was increased until all wheels on the vehicle were locked. With the vehicle unloaded, the self-steering axle steered completely to maximum amplitude at a brake pressure of 30 psi, and remained in that configuration until the vehicle stopped. The tractor yaw response for this situation showed a minimal disturbance, as seen in Figure 23. At higher brake pressures, the self-steering axle steered more abruptly, and the yaw response was larger, but still far short of the level needed to incite a jackknife response. The axles on the rear trailer tended to slide sideways somewhat as a result of lockup of these axles, resulting in an articulation angle of approximately 5 degrees between the rear trailer and the front trailer. The articulation angle between the tractor and the front trailer was small, around 2 degrees. The tests were repeated with the self-steering axle locked. The yaw response for this case is also shown in Figure 23. The yaw rates for the case with the self-steering axle locked were smaller than with the axle unlocked, however, the final articulation angles were approximately the same. Hence, although the self-steering axle steered to a large angle, these responses of the B-dolly did not create a significant motion disturbance for the overall vehicle combination.

d. *Braking in a Turn.* The braking-in-a-turn experiments were performed on the jennite-coated strip on the Skid Traction Facility, as were the similar tests with the tractor-semitrailer combination. This maneuver was intended to determine whether large steer angles of the self-steering axle would occur during braking, and produce anomalous motion disturbances of the overall vehicle.

The tests were performed with the vehicle unloaded. With the self-steering axle unlocked, the tests show that the vehicle will jackknife at the low brake pressures of 30 psi simply as a result of lockup of the rear tandem axles on the tractor. The steer angle at the dolly axle reached values as large as 10 degrees in this test. Tests with the self-steering axle locked in the zero-steer attitude show, of course, that the vehicle would jackknife also at the low brake pressure of 30 psi. The yaw rate responses for both cases are shown in Figure 24. Again, the self-steering axle did not significantly affect the performance for the braking-in-a-turn maneuver for any condition.

e. *Undulated Road.* This maneuver was intended to demonstrate any anomalous behavior of the self-steering axle as the one side of the axle proceeds through an obstruction in the road while the other side remains on smooth pavement. The results of the experiments with the tractor-semitrailer showed that the only type of undulation which

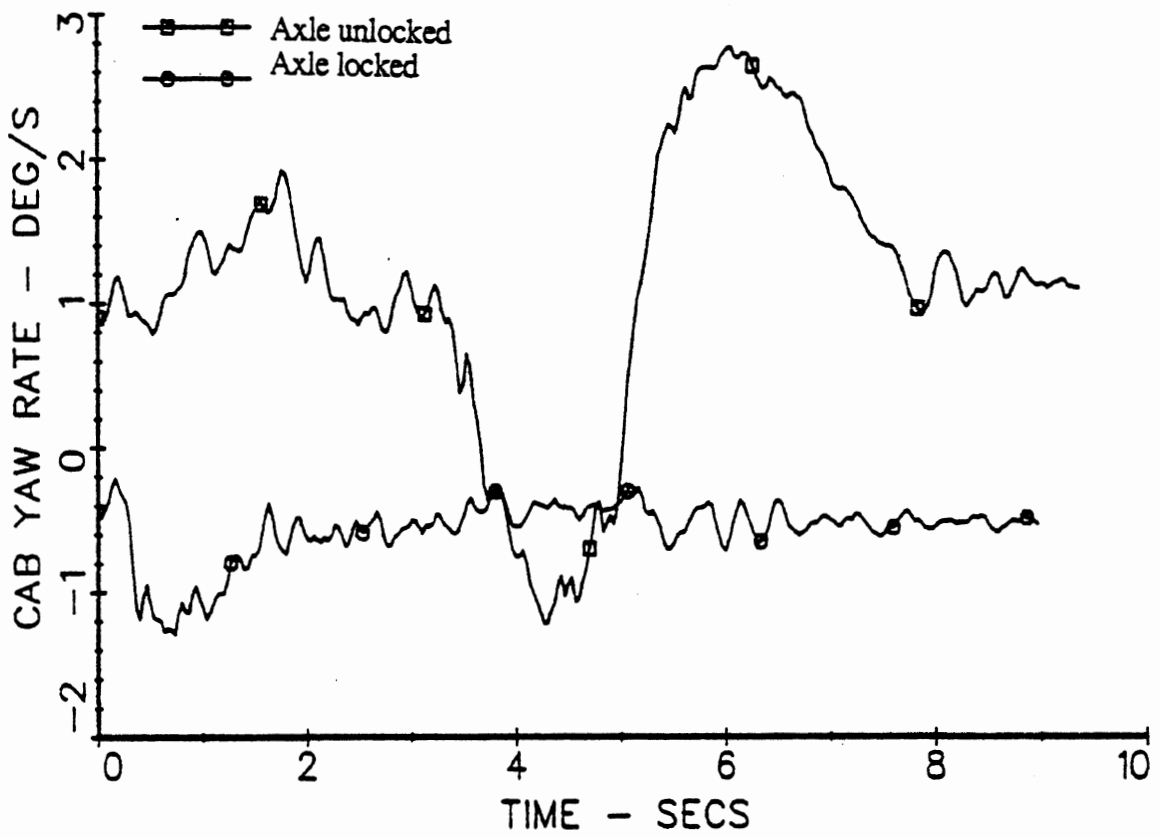


Figure 23

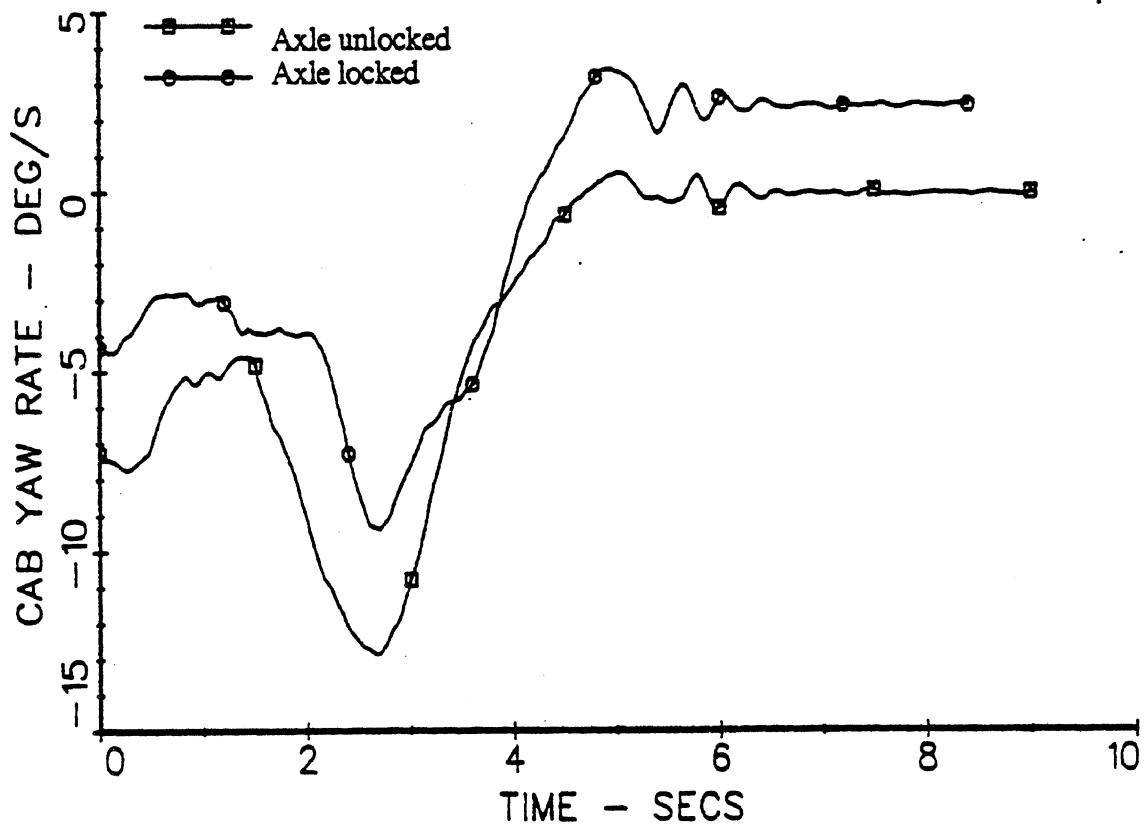


Figure 24

had any significant effect on the self-steering axle were the large chuck holes. Hence, only this type of undulation was investigated for the double tanker.

The vehicle was driven over a single chuck hole at a low speed of approximately 10 km/h (6 mph). The chuck hole was approximately 0.3 m (12 in) wide and 0.1 m (4 in) deep. As the self-steering axle was exiting the chuck hole, it steered rapidly until it reached its maximum displacement. The axle returned to the forward position after it had proceeded onto the level pavement. The yaw rate of the second trailer and the angle of the self-steering axle are given in Figures 25 and 26. The yaw disturbance created by the chuck hole, shown in Figure 23, is large, but short-lived, and did not produce a significant overall motion disturbance.

Conclusions from Tests with Double Tanker

Although this vehicle combination exhibited a reasonable level of static rollover threshold, when operated in a steady turn maneuver, the ability of the dolly axle to steer toward the outside in a moderate-severity turn produced an exceedingly large excursion in outboard offtracking. This response confirms a primary finding of the simulation study, namely that an insufficiently-centered steering axle on a B-dolly can yield grossly undesirable levels of high-speed offtracking.

The test data showed that the B-dolly provided the expected improvement in rearward amplification response over the A-dolly, but introduced an anomalous tendency toward lightly damped transient oscillations. The effective level of damping declined with increased maneuver amplitude and involved gross yaw motions responses at both articulation points. It is clear that such behavior derived from the deficient steer-centering behavior in the dolly's steerable-axle mechanism. Such a deficiency, together with the long dolly drawbar incorporated into this combination, would be expected to yield a divergent oscillation if excited by means of a modest steering disturbance while at legal highway speed.

Even with the low level of steer-centering behavior, negligible sensitivities to differential right/left braking and to traversal of discrete pot-hole disturbances were observed. It is apparent that anomalous steering due to brake imbalance and momentary road disturbances are unlikely to produce significant disturbances in the response of an overall doubles combination. It may be, however, that a vehicle of this type would suffer a substantial disturbance if it departed from the roadway such that the wheels on one side of the dolly axle encountered soft soil and the associated drag forces which would sustain a steer deflection at that axle. Such a possibility was not explored here, however.

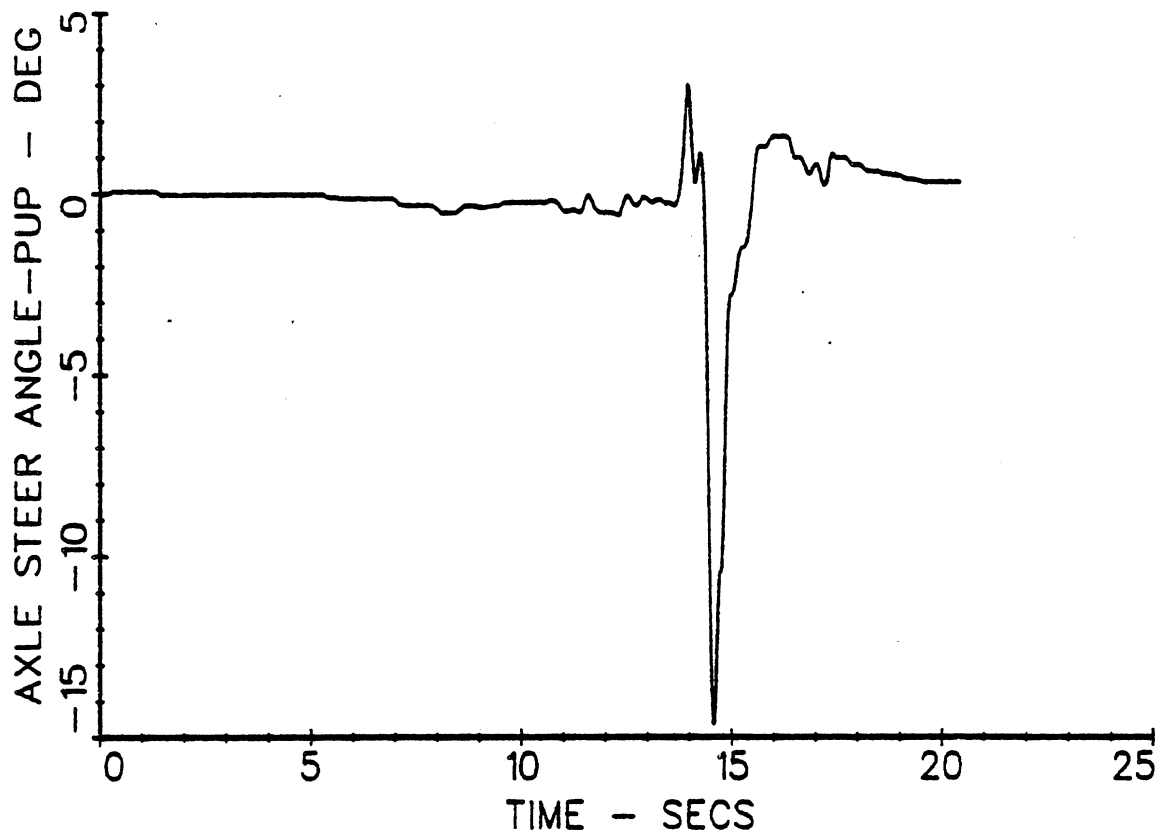


Figure 25

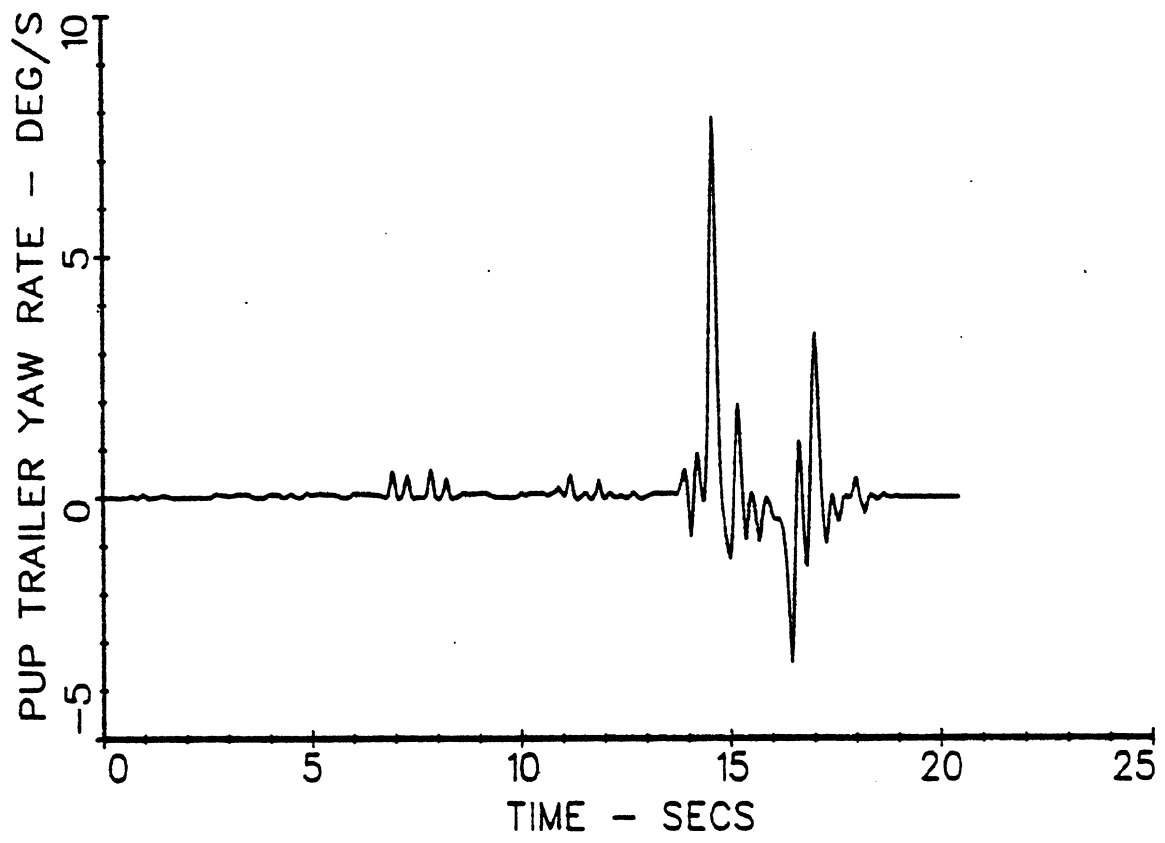


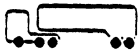
Figure 26

APPENDIX F

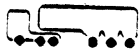
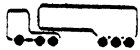
DATA-BASE OF SIMULATION RESULTS

This appendix contains a complete tabulated display of all the performance measures computed for all the vehicle configurations and variations, as defined in the simulation matrix presented in Appendix D. The tables are in a corresponding matrix format to that of the simulation matrix, in that the vehicle configuration and variation numbers are labelled vertically on the left in the same order as before, while the performance measures are labelled across the top of each table, again in the same order. In addition, the first row of each vehicle configuration is indexed by a schematic vehicle picture for quick reference.

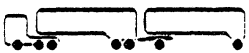
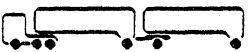
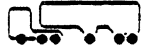
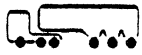
Static Rollover Threshold



Configuration	Variation	Train Type	Critical Unit	Rollover Threshold (g's)
1.1	1.00	B	1	0.437
1.1	2.11	B	1	0.427
1.1	2.12	B	1	0.441
1.1	2.13	B	1	0.45
1.1	2.21	B	1	0.399
1.1	2.22	B	1	0.448
1.1	2.23	B	1	0.456
1.1	3.11	B	1	0.436
1.1	3.12	B	1	0.436
1.1	3.13	B	1	0.436
1.1	3.14	B	1	0.437
1.1	3.15	B	1	0.438
1.1	3.16	B	1	0.436
1.1	3.21	B	1	0.384
1.1	3.22	B	1	0.386
1.1	3.23	B	1	0.386
1.1	4.11	B	1	0.418
1.1	4.12	B	1	0.46
1.1	4.13	B	1	0.455
1.1	4.21	B	1	0.423
1.1	4.22	B	1	0.415
1.1	5.11	B	1	0.438
1.1	5.12	B	1	0.354
1.1	5.13	B	1	0.416
1.1	5.20	B	1	0.467
1.1	5.30	B	1	0.408
1.1	6.01	B	1	0.455
1.1	6.02	B	1	0.418
1.1	6.03	B	1	0.401
1.1	6.04	B	1	0.385
1.1	7.01	B	1	0.315
1.1	7.02	B	1	0.337
1.1	8.01	B	1	0.485
1.1	8.02	B	1	0.498
1.1	9.11	B	1	0.443
1.1	9.12	B	1	0.442
1.1	9.21	B	1	0.453
1.1	9.22	B	1	0.457
1.1	10.00	B	1	0.474
1.2	1.00	B	1	0.418
1.2	2.01	B	1	0.468
1.2	2.02	B	1	0.402
1.2	2.03	B	1	0.374
1.2	3.00	B	1	0.323
1.3	1.00	B	1	0.376
1.3	2.01	B	1	0.42
1.3	2.02	B	1	0.351
1.3	3.01	B	1	0.373
1.3	3.02	B	1	0.373



Static Rollover Threshold



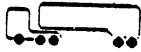
Configuration	Variation	Train Type	Critical Unit	Rollover Threshold (g's)
1.3	3.03	B	1	0.374
1.3	3.04	B	1	0.374
1.3	4.00	B	1	0.304
1.4	1.00	B	1	0.332
1.4	2.01	B	1	0.305
1.4	3.00	B	1	0.3
1.5	1.00	B	1	0.399
1.5	2.01	B	1	0.398
1.5	2.02	B	1	0.396
1.5	2.03	B	1	0.396
1.5	3.01	B	1	0.397
1.5	3.02	B	1	0.395
1.5	3.03	B	1	0.393
1.5	4.01	B	1	0.409
1.5	4.02	B	1	0.417
1.5	5.00	B	1	0.314
2.1	1.00	A	2	0.434
2.1	2.01	A	1	0.464
2.1	2.02	A	1	0.494
2.1	3.11	A	2	0.432
2.1	3.12	A	2	0.432
2.1	3.13	A	2	0.432
2.1	3.14	A	2	0.43
2.1	3.21	A	2	0.434
2.1	3.22	A	2	0.434
2.1	3.23	A	2	0.435
2.1	3.24	A	2	0.437
2.1	3.25	A	2	0.45
2.1	3.26	A	2	0.442
2.1	3.31	A	2	0.432
2.1	3.32	A	2	0.432
2.1	3.33	A	2	0.432
2.1	4.01	A	1	0.402
2.1	4.02	A	1	0.355
2.1	4.03	A	1	0.295
2.1	4.04	A	1	0.257
2.1	5.22	A	2	0.498
2.1	6.00	A	1	0.47
2.1	9.00	A	1	0.365
2.2	1.00	A	2	0.446
2.2	2.01	A	2	0.48
2.2	2.02	A	2	0.407
2.2	4.00	A	2	0.311
2.3	1.00	A	1	0.354
2.3	2.00	A	1	0.379
2.3	3.00	A	1	0.319

Static Rollover Threshold



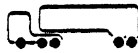
Configuration	Variation	Train Type	Critical Unit	Rollover Threshold (a's)
2.4	1.00	A	1	0.539
2.4	2.01	A	1	0.496
2.4	2.02	A	1	0.459
2.4	2.03	A	1	0.481
2.4	3.00	A	1	0.365
2.5	1.00	A	1	0.472
2.5	2.00	A	2	0.396
2.5	3.00	A	1	0.329
3.1	1.00	B	1	0.418
3.1	2.11	B	1	0.393
3.1	2.12	B	1	0.462
3.1	2.21	B	1	0.438
3.1	2.22	B	1	0.415
3.1	3.01	B	1	0.423
3.1	3.02	B	1	0.423
3.1	3.03	B	1	0.417
3.1	3.04	B	1	0.417
3.1	4.01	B	1	0.359
3.1	4.02	B	1	0.291
3.1	6.00	B	1	0.416
3.1	7.00	B	1	0.385
3.1	8.00	B	1	0.347
3.2	1.00	B	1	0.418
3.2	2.01	B	1	0.487
3.2	2.02	B	1	0.345
3.2	3.00	B	1	0.336
3.3	1.00	B	1	0.466
3.3	2.01	B	1	0.43
3.3	2.02	B	1	0.378
3.3	3.00	B	1	0.342
3.4	1.00	B	1	0.406
3.4	2.01	B	1	0.397
3.4	2.02	B	1	0.402
3.4	2.03	B	1	0.415
3.4	3.00	B	1	0.413
3.4	4.01	B	1	0.409
3.4	4.02	B	1	0.402
3.4	4.03	B	1	0.409
3.4	4.04	B	1	0.401
3.4	5.00	B	1	0.338

Understeer Coefficient

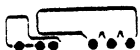


Configuration	Variation	Train Type	UC at .25 g's (deg/g)
1.1	1.00	B	1.8909
1.1	4.11	B	3.7245
1.1	4.12	B	0
1.1	4.13	B	0.0573
1.1	5.11	B	2.865
1.1	5.12	B	5.9592
1.1	5.13	B	2.4639
1.1	5.20	B	1.6617
1.1	5.30	B	2.292
1.1	6.01	B	2.9796
1.1	6.02	B	1.146
1.1	6.03	B	0.6876
1.1	6.04	B	0.1146
1.1	7.01	B	-0.5157
1.1	7.02	B	0.1719
1.1	9.11	B	2.1774
1.1	9.12	B	0.2292
1.1	9.21	B	0.4011
1.1	9.22	B	-0.9168
1.1	10.00	B	2.5785

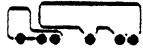
Steady State High-Speed Offtracking



Configuration	Variation	Train Type	Offtracking (m)
1.1	1.00	B	-0.303
1.1	2.11	B	-0.285
1.1	2.12	B	-0.307
1.1	2.13	B	-0.321
1.1	2.21	B	-0.31
1.1	2.22	B	-0.29
1.1	2.23	B	-0.271
1.1	3.11	B	-0.306
1.1	3.12	B	-0.31
1.1	3.13	B	-0.318
1.1	3.14	B	-0.322
1.1	3.15	B	-0.302
1.1	3.16	B	-0.301
1.1	3.21	B	-0.396
1.1	3.22	B	-0.406
1.1	3.23	B	-0.411
1.1	4.11	B	-0.291
1.1	4.12	B	-0.316
1.1	4.13	B	-0.313
1.1	4.21	B	-0.31
1.1	4.22	B	-0.319
1.1	4.23	B	-0.323
1.1	5.11	B	-0.33
1.1	5.12	B	-0.341
1.1	5.13	B	-0.345
1.1	5.20	B	-0.236
1.1	5.30	B	-0.255
1.1	6.01	B	-0.275
1.1	6.02	B	-0.33
1.1	6.03	B	-0.359
1.1	6.04	B	-0.387
1.1	7.01	B	-0.371
1.1	7.02	B	-0.346
1.1	8.01	B	-0.211
1.1	8.02	B	-0.24
1.1	9.11	B	-0.187
1.1	9.12	B	-0.534
1.1	9.21	B	-0.302
1.1	9.22	B	-0.362
1.1	10.00	B	-0.287
1.2	1.00	B	-0.304
1.2	2.01	B	-0.264
1.2	2.02	B	-0.321
1.2	2.03	B	-0.364
1.2	3.00	B	-0.356
1.3	1.00	B	-0.4
1.3	2.01	B	-0.34



Steady State High-Speed Offtracking

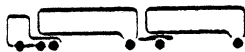


Configuration	Variation	Train Type	Offtracking (m)
1.3	2.02	B	-0.442
1.3	3.01	B	-0.409
1.3	3.02	B	-0.418
1.3	3.03	B	-0.427
1.3	3.04	B	-0.435
1.3	4.00	B	-0.45
1.4	1.00	B	-0.485
1.4	2.01	B	-0.538
1.4	3.00	B	-0.5
1.5	1.00	B	-0.36
1.5	2.01	B	-0.356
1.5	2.02	B	-0.355
1.5	2.03	B	-0.36
1.5	3.01	B	-0.354
1.5	3.02	B	-0.347
1.5	3.03	B	-0.34
1.5	4.01	B	-0.373
1.5	4.02	B	-0.422
1.5	5.00	B	-0.4
2.1	1.00	A	-0.431
2.1	2.01	A	-0.382
2.1	2.02	A	-0.453
2.1	2.03	A	-0.458
2.1	3.11	A	-0.449
2.1	3.12	A	-0.456
2.1	3.13	A	-0.464
2.1	3.14	A	-0.485
2.1	3.21	A	-0.44
2.1	3.22	A	-0.451
2.1	3.23	A	-0.481
2.1	3.24	A	-0.424
2.1	3.25	A	-0.414
2.1	3.26	A	-0.407
2.1	3.31	A	-0.424
2.1	3.32	A	-0.459
2.1	3.33	A	-0.498
2.1	4.01	A	-0.477
2.1	4.02	A	-0.552
2.1	4.03	A	-0.575
2.1	4.04	A	-0.79
2.1	5.10	A	-0.379
2.1	5.21	A	-0.362
2.1	5.22	A	-0.368
2.1	6.00	A	-0.654
2.1	9.00	A	-0.49
2.1	1.00	C	-0.488

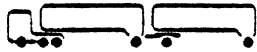
Steady State High-Speed Offtracking



Configuration	Variation	Train Type	Offtracking (m)
2.1	2.01	C	-0.477
2.1	2.02	C	-0.539
2.1	2.03	C	-0.547
2.1	3.11	C	-0.517
2.1	3.12	C	-0.555
2.1	3.13	C	-0.524
2.1	3.14	C	-0.555
2.1	3.21	C	-0.508
2.1	3.22	C	-0.571
2.1	3.24	C	-0.48
2.1	3.25	C	-0.458
2.1	3.26	C	-0.452
2.1	3.31	C	-0.491
2.1	3.32	C	-0.527
2.1	3.33	C	-0.565
2.1	4.01	C	-0.527
2.1	4.02	C	-0.574
2.1	4.03	C	-0.699
2.1	4.04	C	-0.868
2.1	5.10	C	-0.543
2.1	5.21	C	-0.362
2.1	5.22	C	-0.412
2.1	6.00	C	-0.696
2.1	7.11	C	-0.507
2.1	7.12	C	-0.43
2.1	7.13	C	-0.635
2.1	7.14	C	-0.469
2.1	7.15	C	-0.498
2.1	7.16	C	-0.498
2.1	7.17	C	-0.492
2.1	7.18	C	-0.74
2.1	7.19	C	-0.424
2.1	7.21	C	-0.55
2.1	7.22	C	-0.454
2.1	7.23	C	-0.565
2.1	7.24	C	-0.505
2.1	7.25	C	-0.524
2.1	7.26	C	-0.531
2.1	7.27	C	-0.553
2.1	7.28	C	-0.848
2.1	7.29	C	-0.453
2.1	8.00	C	-0.498
2.1	9.00	C	-0.535
2.2	1.00	A	-0.478
2.2	2.01	A	-0.426
2.2	2.02	A	-0.54
2.2	3.10	A	-0.405
2.2	3.21	A	-0.375

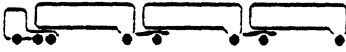


Steady State High-Speed Offtracking



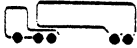
Configuration	Variation	Train Type	Offtracking (m)
2.2	3.22	A	-0.385
2.2	4.00	A	-0.57
2.2	1.00	C	-0.563
2.2	2.01	C	-0.488
2.2	2.02	C	-0.633
2.2	3.10	C	-0.602
2.2	3.21	C	-0.364
2.2	3.22	C	-0.427
2.2	4.00	C	-0.655
2.3	1.00	A	-0.509
2.3	2.00	A	-0.480
2.3	3.00	A	-0.579
2.3	1.00	C	-0.552
2.3	2.00	C	-0.550
2.3	3.00	C	-0.613
2.4	1.00	A	-0.453
2.4	2.01	A	-0.519
2.4	2.02	A	-0.591
2.4	2.03	A	-0.702
2.4	3.00	A	-0.53
2.5	1.00	A	-0.496
2.5	2.00	A	-0.491
2.5	3.00	A	-0.585
2.5	1.00	C	-0.578
2.5	3.00	C	-0.687
3.1	1.00	B	-0.421
3.1	2.11	B	-0.39
3.1	2.12	B	-0.433
3.1	2.13	B	-0.371
3.1	2.21	B	-0.403
3.1	2.22	B	-0.42
3.1	3.01	B	-0.406
3.1	3.02	B	-0.414
3.1	3.03	B	-0.434
3.1	3.04	B	-0.445
3.1	4.01	B	-0.488
3.1	4.02	B	-0.659
3.1	5.10	B	-0.359
3.1	5.21	B	-0.344
3.1	5.22	B	-0.355
3.1	6.00	B	-0.421
3.1	7.00	B	-0.351
3.1	8.00	B	-0.459
3.2	1.00	B	-0.435

Steady State High-Speed Offtracking

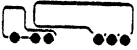


Configuration	Variation	Train Type	Offtracking (m)
3.2	2.01	B	-0.391
3.2	2.02	B	-0.585
3.2	3.00	B	-0.486
3.3	1.00	B	-0.408
3.3	2.01	B	-0.447
3.3	2.02	B	-0.524
3.3	3.00	B	-0.469
3.4	1.00	B	-0.496
3.4	2.01	B	-0.483
3.4	2.02	B	-0.502
3.4	2.03	B	-0.587
3.4	3.00	B	-0.513
3.4	4.01	B	-0.529
3.4	4.02	B	-0.478
3.4	4.03	B	-0.509
3.4	4.04	B	-0.497
3.4	5.00	B	-0.584
4.1	1.00	A	-0.577
4.1	2.01	A	-0.541
4.1	2.02	A	-0.564
4.1	2.03	A	-0.584
4.1	3.11	A	-0.618
4.1	3.21	A	-0.581
4.1	7.11	A	-0.522
4.1	7.12	A	-0.469
4.1	7.13	A	-0.497
4.1	7.21	A	-0.486
4.1	7.22	A	-0.487
4.1	7.23	A	-0.484
4.1	7.24	A	-0.463
4.1	7.25	A	-0.473
4.1	6.04	C	-0.606
4.1	6.05	C	-0.711
4.1	7.23	C	-0.492
4.1	7.25	C	-0.485
4.2	1.00	A	-0.529
4.2	2.01	A	-0.502
4.2	3.00	A	-0.585

Response to Rapid Steering Reversals



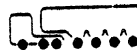
Configuration	Variation	Train Type	Critical Unit	LTR	RM	Overshoot *	Period (sec)	Time (sec)
1.1	1.00	B	1	0.384	---	0.298	3.00	3.30
1.1	5.20	B	1	0.384	---	0.237	3.00	3.30
1.1	5.30	B	1	0.407	---	0.263	3.00	3.30
1.1	7.01	B	1	0.548	---	0.405	3.00	3.40
1.1	7.02	B	1	0.511	---	0.374	3.00	3.40
1.1	10.00	B	1	0.360	---	0.282	3.00	3.30



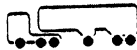
1.2	1.00	B	1	0.408	---	0.318	3.00	3.40
1.2	2.01	B	1	0.364	---	0.266	3.00	3.30
1.2	2.02	B	1	0.420	---	0.335	3.00	3.40
1.2	2.03	B	1	0.442	---	0.379	3.00	3.50
1.2	3.00	B	1	0.540	---	0.395	3.00	3.50



1.3	1.00	B	1	0.475	---	0.463	3.00	3.50
1.3	2.01	B	1	0.436	---	0.386	3.00	3.40
1.3	2.02	B	1	0.508	---	0.519	3.00	3.50
1.3	3.01	B	1	0.486	---	0.482	3.00	3.50
1.3	3.02	B	1	0.495	---	0.509	3.00	3.50
1.3	3.03	B	1	0.506	---	0.539	3.00	3.50
1.3	3.04	B	1	0.517	---	0.571	3.00	3.50
1.3	4.00	B	1	0.596	---	0.553	3.00	3.50



1.4	1.00	B	1	0.625	---	0.772	3.00	3.60
1.4	2.01	B	1	0.692	---	0.878	3.00	3.70
1.4	3.00	B	1	0.692	---	0.825	3.00	3.60



1.5	1.00	B	1	0.478	---	0.436	3.00	3.40
1.5	2.01	B	1	0.463	---	0.412	3.00	3.40
1.5	2.02	B	1	0.447	---	0.392	3.00	3.40
1.5	2.03	B	1	0.433	---	0.384	3.00	3.40
1.5	3.01	B	1	0.467	---	0.413	3.00	3.40
1.5	3.02	B	1	0.457	---	0.392	3.00	3.40
1.5	3.03	B	1	0.447	---	0.372	3.00	3.40
1.5	4.01	B	1	0.473	---	0.431	3.00	3.40
1.5	4.02	B	1	0.438	---	0.443	3.00	3.45
1.5	5.00	B	1	0.608	---	0.519	3.00	3.50



2.1	1.00	A	2	0.795	---	0.783	2.50	3.60
2.1	2.01	A	2	0.931	---	0.927	2.50	3.50
2.1	2.02	A	2	0.634	---	0.671	2.50	3.60

* This measure is termed "Transient High-Speed Offtracking" in the text (meters)



Response to Rapid Steering Reversals

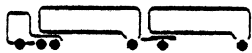
Configuration	Variation	Train Type	Critical Unit	LTR	RM	Overshoot *	Period (sec)	Time (sec)
2.1	2.03	A	2	0.484	---	0.559	3.00	4.00
2.1	3.11	A	2	0.799	---	0.817	2.50	3.60
2.1	3.12	A	2	0.804	---	0.830	2.50	3.70
2.1	3.13	A	2	0.804	---	0.839	2.50	3.70
2.1	3.14	A	2	0.787	---	0.850	2.50	3.70
2.1	3.21	A	2	0.841	---	0.843	2.50	3.60
2.1	3.22	A	2	0.917	---	0.962	2.50	3.60
2.1	3.23	A	2	1.000	0.642	1.192	2.50	4.80
2.1	3.24	A	2	0.809	---	0.790	2.50	3.60
2.1	3.25	A	2	0.839	---	0.819	2.50	3.50
2.1	3.26	A	2	0.949	---	0.801	2.00	4.50
2.1	3.31	A	2	0.720	---	0.731	2.50	3.60
2.1	3.32	A	2	0.792	---	0.826	2.50	3.70
2.1	3.33	A	2	0.865	---	0.926	2.50	3.80
2.1	4.01	A	2	0.864	---	0.901	2.50	3.70
2.1	4.02	A	2	0.970	---	1.132	3.00	5.50
2.1	4.03	A	2	1.000	0.321	1.324	3.00	4.70
2.1	4.04	A	2	1.000	0.000	Rollover	2.40	4.20
2.1	5.10	A	2	0.720	---	0.637	2.50	3.50
2.1	5.21	A	2	0.708	---	0.598	2.50	3.50
2.1	5.22	A	2	0.639	---	0.621	2.50	3.40
2.1	6.00	A	2	0.920	---	1.330	3.00	4.00
2.1	8.00	A	2	0.795	---	0.783	2.50	3.60
2.1	9.00	A	2	1.000	0.300	0.942	3.00	4.40
2.1	1.00	C	1	0.436	---	0.753	3.00	3.60
2.1	2.01	C	1	0.527	---	0.980	3.00	3.60
2.1	2.02	C	1	0.337	---	0.610	3.00	3.60
2.1	2.03	C	1	0.258	---	0.489	3.00	3.70
2.1	3.11	C	1	0.423	---	0.812	3.00	3.60
2.1	3.12	C	1	0.413	---	0.834	3.00	3.60
2.1	3.13	C	1	0.431	---	0.855	3.00	3.70
2.1	3.14	C	1	0.424	---	0.886	3.00	3.70
2.1	3.21	C	1	0.472	---	0.818	3.00	3.60
2.1	3.22	C	1	0.515	---	1.012	3.00	3.60
2.1	3.23	C	1	0.817	---	4.298	3.00	6.90
2.1	3.24	C	1	0.443	---	0.768	3.00	3.60
2.1	3.25	C	1	0.479	---	0.760	3.00	3.60
2.1	3.26	C	1	0.517	---	0.829	3.00	3.60
2.1	3.31	C	1	0.435	---	0.758	3.00	3.60
2.1	3.32	C	1	0.426	---	0.844	3.00	3.70
2.1	3.33	C	1	0.421	---	0.880	3.00	3.70
2.1	4.01	C	1	0.499	---	0.894	3.00	3.60
2.1	4.02	C	1	0.564	---	1.070	3.00	3.70
2.1	4.03	C	1	0.655	---	1.237	3.00	3.80
2.1	4.04	C	1	0.728	---	1.495	3.00	3.90
2.1	5.10	C	1	0.357	---	0.586	3.00	3.70
2.1	5.21	C	1	0.370	---	0.508	3.00	3.40
2.1	5.22	C	1	0.426	---	0.617	3.00	3.50
2.1	6.00	C	1	0.475	---	1.188	3.00	3.80
2.1	7.11	C	1	0.439	---	0.894	3.00	3.70
2.1	7.12	C	1	0.450	---	0.647	3.00	3.50
2.1	7.13	C	1	0.418	---	0.971	3.00	3.70
2.1	7.14	C	1	0.445	---	0.704	3.00	3.60
2.1	7.15	C	1	0.436	---	0.753	3.00	3.60
2.1	7.16	C	1	0.433	---	0.776	3.00	3.60

* This measure is termed "Transient High-Speed Offtracking" in the text (meters)

Response to Rapid Steering Reversals



Configuration	Variation	Train Type	Critical Unit	LTR	RM	Overshoot *	Period (sec)	Time (sec)
2.1	7.17	C	1	0.443	---	0.706	3.00	3.60
2.1	7.18	C	1	0.441	---	1.265	3.00	4.10
2.1	7.19	C	1	0.449	---	0.636	3.00	3.50
2.1	7.21	C	1	0.436	---	0.893	3.00	3.60
2.1	7.22	C	1	0.438	---	0.695	3.00	3.60
2.1	7.23	C	1	0.390	---	1.052	3.00	3.80
2.1	7.24	C	1	0.432	---	0.765	3.00	3.60
2.1	7.25	C	1	0.431	---	0.855	3.00	3.70
2.1	7.26	C	1	0.433	---	0.824	3.00	3.60
2.1	7.27	C	1	0.415	---	0.825	3.00	3.60
2.1	7.28	C	1	0.436	---	1.556	3.00	4.30
2.1	7.29	C	1	0.436	---	0.682	3.00	3.60
2.1	8.00	C	1	0.436	---	0.753	3.00	3.60
2.1	9.00	C	1	0.569	---	0.878	3.00	3.60



2.2	1.00	A	2	0.785	---	0.852	2.50	3.60
2.2	2.01	A	2	0.692	---	0.725	2.50	3.50
2.2	2.02	A	2	0.859	---	1.052	3.00	3.90
2.2	3.10	A	2	0.687	---	0.653	2.50	3.50
2.2	3.21	A	2	0.640	---	0.571	2.50	3.60
2.2	3.22	A	2	0.607	---	0.575	2.50	3.40
2.2	4.00	A	2	1.000	0.189	1.089	3.00	4.80
2.2	1.00	C	1	0.387	---	0.743	3.00	3.60
2.2	2.01	C	1	0.372	---	0.634	3.00	3.50
2.2	2.02	C	1	0.408	---	0.863	3.00	3.60
2.2	3.10	C	1	0.323	---	0.518	3.00	3.90
2.2	3.21	C	1	0.330	---	0.457	3.00	3.40
2.2	3.22	C	1	0.374	---	0.520	3.00	3.50
2.2	4.00	C	1	0.531	---	0.908	3.00	3.70



2.3	1.00	A	2	0.813	---	0.999	3.00	3.90
2.3	2.00	A	2	0.811	---	0.850	3.00	4.10
2.3	3.00	A	2	1.000	0.000	Rollover	3.00	3.90
2.3	1.00	C	1	0.513	---	0.913	3.00	3.50
2.3	2.00	C	1	0.422	---	0.770	2.50	3.40
2.3	3.00	C	1	0.526	---	0.897	2.50	3.40



2.4	1.00	A	2	0.408	---	0.453	3.00	4.00
2.4	2.01	A	2	0.483	---	0.566	3.00	4.00
2.4	2.02	A	2	0.526	---	0.633	3.00	4.10
2.4	2.03	A	2	0.609	---	0.793	3.00	4.20
2.4	3.00	A	2	0.668	---	0.631	3.00	4.10

* This measure is termed "Transient High-Speed Offtracking" in the text (meters)

Response to Rapid Steering Reversals



Configuration	Variation	Train Type	Critical Unit	LTR	RM	Overshoot *	Period (sec)	Time (sec)
2.5	1.00	A	2	0.649	---	0.684	3.00	4.00
2.5	2.00	A	2	0.573	---	0.693	3.00	3.90
2.5	3.00	A	2	0.983	---	0.965	3.00	4.10
2.5	1.00	C	1	0.285	---	0.522	3.00	3.60
2.5	3.00	C	1	0.398	---	0.676	3.00	3.70



3.1	1.00	B	1	0.501	---	0.608	3.00	3.50
3.1	2.11	B	1	0.625	---	0.708	3.00	3.40
3.1	2.12	B	1	0.392	---	0.524	3.00	3.50
3.1	2.13	B	1	0.292	---	0.358	3.00	3.50
3.1	2.21	B	1	0.477	---	0.569	3.00	3.50
3.1	2.22	B	1	0.519	---	0.641	3.00	3.40
3.1	3.01	B	1	0.500	---	0.581	3.00	3.50
3.1	3.02	B	1	0.502	---	0.599	3.00	3.50
3.1	3.03	B	1	0.505	---	0.640	3.00	3.50
3.1	3.04	B	1	0.506	---	0.663	3.00	3.50
3.1	4.01	B	1	0.572	---	0.722	3.00	3.50
3.1	4.02	B	1	0.719	---	0.960	3.00	3.70
3.1	5.10	B	1	0.488	---	0.492	3.00	3.60
3.1	5.21	B	1	0.406	---	0.449	3.00	3.40
3.1	5.22	B	1	0.445	---	0.458	3.00	3.40
3.1	6.00	B	1	0.510	---	0.643	3.00	3.50
3.1	7.00	B	1	0.493	---	0.497	3.00	3.40
3.1	8.00	B	1	0.613	---	0.703	3.00	3.50



3.2	1.00	B	1	0.477	---	0.599	3.00	3.50
3.2	2.01	B	1	0.423	---	0.528	3.00	3.50
3.2	2.02	B	1	0.603	---	0.839	3.00	3.70
3.2	3.00	B	1	0.597	---	0.694	3.00	3.60



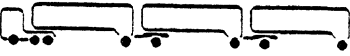
3.3	1.00	B	1	0.401	---	0.533	3.00	3.40
3.3	2.01	B	1	0.443	---	0.595	3.00	3.50
3.3	2.02	B	1	0.517	---	0.735	3.00	3.50
3.3	3.00	B	1	0.566	---	0.663	3.00	3.60



3.4	1.00	B	1	0.501	---	0.728	3.00	3.60
3.4	2.01	B	1	0.499	---	0.678	3.00	3.60
3.4	2.02	B	1	0.509	---	0.694	3.00	3.60
3.4	2.03	B	1	0.492	---	0.772	3.00	3.60
3.4	3.00	B	1	0.515	---	0.859	3.00	3.50
3.4	4.01	B	1	0.500	---	0.754	3.00	3.60
3.4	4.02	B	1	0.532	---	0.733	3.00	3.60
3.4	4.03	B	1	0.499	---	0.718	3.00	3.60

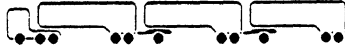
* This measure is termed "Transient High-Speed Offtracking" in the text (meters)

Response to Rapid Steering Reversals

Configuration	Variation	Train Type	Critical Unit	LTR	RM	Overshoot *	Period (sec)	Time (sec)
3.4	4.04	B	1	0.518	---	0.731	3.00	3.60
3.4	5.00	B	1	0.595	---	0.843	3.00	3.70
								
4.1	1.00	A	3	1.000	0.473	1.620	2.50	4.40
4.1	2.01	A	3	1.000	0.000	Rollover	3.00	4.00
4.1	2.02	A	3	1.000	0.000	Rollover	2.00	6.50
4.1	2.03	A	3	0.886	---	1.414	2.50	4.20
4.1	3.11	A	3	1.000	0.474	1.716	2.50	4.60
4.1	3.12	A	3	0.980	---	1.454	2.00	4.20
4.1	3.21	A	3	0.931	---	1.468	2.50	5.60
4.1	3.22	A	3	1.000	0.000	Rollover	2.50	6.80
4.1	4.01	A	3	0.865	---	1.145	2.50	4.00
4.1	4.02	A	3	1.000	0.000	Rollover	2.50	4.20
4.1	5.00	A	3	1.000	0.000	Rollover	2.00	3.95
4.1	7.11	A	3	0.897	---	1.336	2.50	4.10
4.1	7.12	A	3	0.814	---	1.009	2.50	4.00
4.1	7.13	A	3	0.752	---	1.150	2.50	4.10
4.1	7.21	A	3	0.921	---	1.081	2.00	3.70
4.1	7.22	A	3	0.788	---	0.985	2.50	4.20
4.1	7.23	A	3	0.873	---	1.040	2.50	4.00
4.1	7.24	A	3	0.817	---	1.031	2.50	4.00
4.1	7.25	A	3	0.774	---	0.997	2.50	4.00
4.1	1.00	C	1	0.294	---	1.003	3.00	3.90
4.1	2.01	C	1	0.405	---	1.279	3.00	3.80
4.1	2.02	C	1	0.352	---	1.156	3.00	3.80
4.1	2.03	C	1	0.249	---	0.870	3.00	3.90
4.1	3.11	C	1	0.280	---	1.078	3.00	4.00
4.1	3.12	C	1	0.263	---	1.154	3.00	4.10
4.1	3.21	C	1	0.290	---	1.028	3.00	3.90
4.1	3.22	C	1	0.256	---	1.200	3.00	4.50
4.1	4.01	C	1	0.267	---	0.733	3.00	3.60
4.1	4.02	C	1	0.345	---	1.350	3.00	4.10
4.1	5.00	C	1	0.431	---	1.264	3.00	4.00
4.1	6.01	C	1	0.341	---	1.439	3.00	4.20
4.1	6.02	C	1	0.347	---	0.872	3.00	3.80
4.1	6.03	C	1	0.265	---	1.071	3.00	3.90
4.1	6.04	C	1	0.329	---	0.921	3.00	3.80
4.1	6.05	C	1	0.318	---	1.377	3.00	4.20
4.1	6.06	C	1	0.295	---	1.018	3.00	3.90
4.1	6.07	C	1	0.196	---	0.650	2.00	3.30
4.1	6.08	C	1	0.380	---	2.895	3.00	4.50
4.1	6.09	C	1	0.347	---	0.872	3.00	3.80
4.1	7.11	C	1	0.274	---	0.657	2.50	3.70
4.1	7.12	C	1	0.672	---	0.347	2.00	6.50
4.1	7.13	C	1	0.283	---	0.747	2.50	3.40
4.1	7.21	C	1	0.230	---	0.591	2.50	3.40
4.1	7.22	C	1	0.283	---	0.717	2.50	3.60
4.1	7.23	C	1	0.254	---	0.644	2.50	3.50
4.1	7.24	C	1	0.240	---	0.656	2.50	3.40
4.1	7.25	C	1	0.284	---	0.682	2.50	3.40

* This measure is termed "Transient High-Speed Offtracking" in the text (meters)

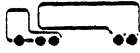
Response to Rapid Steering Reversals



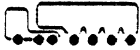
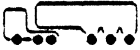
Configuration	Variation	Train Type	Critical Unit	LTR	RM	Overshoot *	Period (sec)	Time (sec)
4.2	1.00	A	3	1.000	0.000	Rollover	3.00	6.40
4.2	2.01	A	3	1.000	0.448	1.502	2.50	7.10
4.2	2.02	A	3	1.000	0.000	Rollover	2.00	6.20
4.2	3.00	A	3	1.000	0.000	Rollover	2.00	3.90
4.2	1.00	C	1	0.332	---	1.218	3.00	4.00
4.2	2.01	C	1	0.308	---	1.166	3.00	4.00
4.2	2.02	C	1	0.378	---	1.336	3.00	4.30
4.2	3.00	C	1	0.444	---	1.433	3.00	4.00

* This measure is termed "Transient High-Speed Offtracking" in the text (meters)

Low-Speed Offtracking



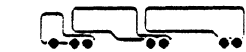
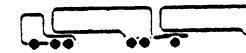
Configuration	Variation	Train Type	Offtracking (meters)
1.1	1.00	B	5.906
1.1	2.11	B	5.673
1.1	2.12	B	6.046
1.1	2.13	B	6.355
1.1	2.21	B	4.557
1.1	2.22	B	6.961
1.1	2.23	B	8.043
1.1	3.11	B	5.904
1.1	3.12	B	5.897
1.1	3.13	B	5.899
1.1	3.14	B	5.905
1.1	3.15	B	5.894
1.1	3.16	B	5.927
1.1	3.21	B	5.902
1.1	3.22	B	5.900
1.1	3.23	B	5.904
1.1	4.21	B	5.560
1.1	4.22	B	5.052
1.1	4.23	B	4.550
1.2	1.00	B	5.577
1.3	1.00	B	4.942
1.3	3.01	B	4.793
1.3	3.02	B	4.651
1.3	3.03	B	4.511
1.3	3.04	B	4.383
1.4	1.00	B	4.166
1.5	1.00	B	5.492
1.5	2.01	B	5.576
1.5	2.02	B	5.668
1.5	2.03	B	5.766
1.5	3.01	B	5.478
1.5	3.02	B	5.471
1.5	3.03	B	5.483
1.5	4.01	B	5.716
1.5	4.02	B	5.892
2.1	1.00	A	4.293
2.1	2.01	A	3.094
2.1	2.02	A	5.641
2.1	2.03	A	7.719
2.1	3.21	A	4.069
2.1	3.22	A	3.753
2.1	3.23	A	3.405
2.1	3.24	A	4.100
2.1	3.25	A	3.860



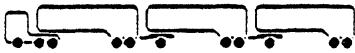
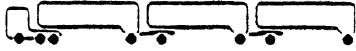
Low-Speed Offtracking



Configuration	Variation	Train Type	Offtracking (meters)
2.1	3.26	A	3.633
2.1	3.31	A	4.538
2.1	3.32	A	4.544
2.1	3.33	A	4.461
2.1	1.00	C	4.113
2.1	2.01	C	2.846
2.1	2.02	C	5.511
2.1	2.03	C	7.620
2.1	3.21	C	3.852
2.1	3.22	C	3.487
2.1	3.23	C	3.057
2.1	3.24	C	3.906
2.1	3.25	C	3.658
2.1	3.26	C	3.451
2.1	3.31	C	4.124
2.1	3.32	C	4.024
2.1	3.33	C	3.882
2.2	1.00	A	4.881
2.2	3.10	A	4.886
2.2	3.21	A	4.890
2.2	3.22	A	4.885
2.2	1.00	C	4.753
2.2	3.10	C	5.251
2.2	3.21	C	5.098
2.2	3.22	C	4.750
2.3	1.00	A	4.593
2.3	1.00	C	4.407
2.4	1.00	A	10.207
2.5	1.00	A	7.606
2.5	1.00	C	7.489
3.1	1.00	B	4.473
3.1	2.11	B	3.245
3.1	2.12	B	5.830
3.1	2.13	B	7.906
3.1	2.21	B	4.609
3.1	2.22	B	4.530
3.1	3.01	B	4.489
3.1	3.02	B	4.484
3.1	3.03	B	4.459
3.1	3.04	B	4.442
3.2	1.00	B	4.754
3.3	1.00	B	5.061

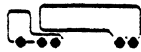


Low-Speed Offtracking

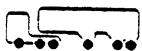
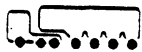
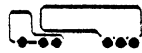


Configuration	Variation	Train Type	Offtracking (meters)
3.4	1.00	B	5.051
3.4	3.00	B	5.167
4.1	1.00	A	6.791
4.1	2.01	A	5.310
4.1	2.02	A	5.873
4.1	2.03	A	7.705
4.1	3.11	A	6.962
4.1	3.12	A	7.172
4.1	3.21	A	6.986
4.1	3.22	A	6.980
4.2	1.00	A	6.172

Friction Demand in a Tight Radius Turn

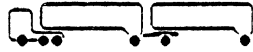


Configuration	Variation	Train Type	Mu	Articulation Angle (deg) *
1.1	1.00	B	0.031	42.899
1.1	2.11	B	0.057	44.615
1.1	2.12	B	0.023	10.252
1.1	2.13	B	0.043	24.678
1.1	2.21	B	0.026	9.051
1.1	2.22	B	0.037	45.397
1.1	2.23	B	0.043	47.43
1.1	3.11	B	0.027	13.052
1.1	3.12	B	0.033	22.322
1.1	3.13	B	0.056	40.788
1.1	3.14	B	0.07	42.683
1.1	3.15	B	0.026	31.013
1.1	3.16	B	0.059	42.454
1.1	3.21	B	0.042	12.97
1.1	3.22	B	0.074	35.043
1.1	3.23	B	0.09	36.998
1.1	4.11	B	0.034	41.883
1.1	4.12	B	0.044	26.355
1.1	4.13	B	0.038	32.149
1.1	4.21	B	0.029	12.923
1.1	4.22	B	0.025	13.433
1.1	4.23	B	0.023	12.479
1.1	8.01	B	0.042	42.441
1.1	8.02	B	0.031	14.628
1.2	1.00	B	0.051	39.931
1.3	1.00	B	0.217	42.392
1.3	2.01	B	0.181	41.112
1.3	2.02	B	0.233	43.251
1.3	3.01	B	0.26	43.043
1.3	3.02	B	0.313	43.097
1.3	3.03	B	0.365	43.132
1.3	3.04	B	0.421	43.218
1.4	1.00	B	0.709	45.147
1.4	2.01	B	0.755	45.775
1.5	1.00	B	0.303	45.655
1.5	2.01	B	0.239	45.186
1.5	2.02	B	0.171	42.581
1.5	2.03	B	0.099	42.953
1.5	3.01	B	0.251	44.623
1.5	3.02	B	0.201	42.816
1.5	3.03	B	0.149	43.932
1.5	4.01	B	0.186	45.135
1.5	4.02	B	0.027	37.014
2.1	1.00	A	0.024	29.232



* Tractor Articulation Angle of Peak MU

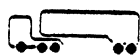
Friction Demand in a Tight Radius Turn



Configuration	Variation	Train Type	Mu	Articulation Angle (deg) *
2.1	1.00	C	0.112	32.603
2.2	1.00	C	0.047	33.695
2.3	1.00	A	0.019	20.108
2.3	1.00	C	0.093	30.628
2.4	1.00	A	0.045	43.226
2.5	1.00	C	0.041	39.072
3.1	1.00	B	0.078	31.839
3.1	2.11	B	0.106	27.392
3.1	2.12	B	0.065	35.34
3.1	2.13	B	0.057	37.31
3.1	2.21	B	0.061	31.02
3.1	2.22	B	0.112	27.575
3.1	3.01	B	0.073	31.549
3.1	3.02	B	0.076	32.239
3.1	3.03	B	0.082	32.304
3.1	3.04	B	0.086	32.341
3.4	1.00	B	0.022	12.05
3.4	3.00	B	0.145	32.856
3.4	4.01	B	0.025	11.185
3.4	4.02	B	0.025	11.765
3.4	4.03	B	0.024	13.67
3.4	4.04	B	0.027	31.087

* Tractor Articulation Angle of Peak MU









Braking Efficiencies



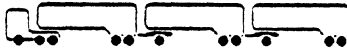
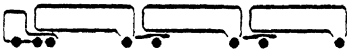
Configuration	Variation	Train Type	Efficy. at .1 g's (%)	Efficy. at .4 g's (%)
1.1	1.00	B	96.28	83.52
1.1	1.01	B	67.22	57.05
1.1	2.11	B	96.23	83.34
1.1	2.12	B	96.30	83.61
1.1	2.13	B	96.34	83.78
1.1	2.21	B	95.50	80.35
1.1	2.22	B	96.60	84.85
1.1	2.23	B	96.84	85.82
1.1	3.15	B	96.28	83.52
1.1	3.16	B	96.28	83.52
1.1	3.21	B	93.45	84.84
1.1	3.22	B	93.46	84.64
1.1	3.23	B	93.46	84.54
1.1	4.11	B	94.57	83.08
1.1	4.12	B	85.58	83.08
1.1	4.13	B	89.72	83.08
1.1	4.21	B	95.83	87.21
1.1	4.22	B	88.48	86.88
1.1	4.23	B	79.78	78.84
1.1	5.11	B	96.28	83.52
1.1	5.12	B	96.26	83.47
1.1	6.01	B	95.28	83.10
1.1	6.02	B	97.18	84.17
1.1	6.03	B	97.50	84.43
1.1	6.04	B	93.44	85.03
1.1	7.01	B	95.49	80.33
1.1	8.01	B	65.62	54.01
1.1	8.02	B	58.19	55.32
2.1	1.00	A	87.93	69.70
2.1	1.01	A	64.36	52.31
2.1	2.01	A	86.65	64.49
2.1	2.02	A	88.95	73.80
2.1	2.03	A	88.88	77.10
2.1	3.11	A	87.93	69.70
2.1	3.12	A	87.93	69.70
2.1	3.13	A	87.93	69.70
2.1	3.14	A	87.93	69.70
2.1	3.21	A	84.00	69.71
2.1	3.22	A	73.69	69.71
2.1	3.23	A	60.62	62.20
2.1	3.24	A	90.41	75.01
2.1	3.25	A	90.41	83.52
2.1	3.26	A	84.38	84.84
2.1	3.31	A	87.93	69.70
2.1	3.32	A	87.93	69.70
2.1	3.33	A	87.93	69.70
2.1	4.01	A	90.42	72.07
2.1	4.02	A	93.07	74.15
2.1	4.03	A	93.85	74.39
2.1	4.04	A	93.19	74.14
2.1	5.10	A	36.35	39.92
2.1	5.11	A	31.22	18.39



Braking Efficiencies

Configuration	Variation	Train Type	Efficy. at .1 g's (%)	Efficy. at .4 g's (%)	
	2.1	5.21	A	49.21	54.05
	2.1	5.22	A	55.00	43.01
	2.1	9.00	A	86.82	65.17
					
	2.2	1.00	A	74.64	71.05
	2.2	1.01	A	71.81	65.40
	2.2	2.01	A	74.88	70.92
	2.2	2.02	A	74.29	71.14
	2.2	3.10	A	43.73	36.36
	2.2	3.21	A	51.94	45.54
	2.2	3.22	A	51.56	47.77
	2.2	4.00	A	75.48	74.49
	2.2	3.10	C	43.73	36.36
	2.2	3.21	C	51.94	45.54
	2.2	3.22	C	51.56	47.77
					
	2.3	1.00	A	89.95	79.99
	2.3	1.01	A	61.61	57.39
	2.3	2.00	A	73.67	56.40
	2.3	3.00	A	89.40	77.86
	2.3	2.00	C	83.16	80.42
					
	2.4	1.00	A	90.43	71.14
	2.4	1.01	A	67.91	51.24
	2.4	3.00	A	91.32	74.75
					
	2.5	1.00	A	91.98	87.78
	2.5	1.01	A	69.39	62.40
	2.5	2.00	A	81.49	77.45
	2.5	3.00	A	92.06	88.06
					
	3.2	1.00	B	93.39	75.50
	3.2	1.01	B	56.00	42.14
	3.2	2.01	B	94.34	77.38
	3.2	2.02	B	92.89	74.90
	3.2	3.00	B	92.51	72.12
					
	3.3	1.00	B	86.41	85.57
	3.3	1.01	B	67.81	61.02
	3.3	2.01	B	90.37	90.19
	3.3	2.02	B	95.60	89.63
	3.3	3.00	B	87.11	88.43
					
	4.1	1.00	A	71.75	67.55
	4.1	1.01	A	77.52	69.55
	4.1	2.01	A	72.43	70.21
	4.1	2.02	A	72.10	68.93
	4.1	2.03	A	71.50	66.59
	4.1	3.11	A	71.84	67.90
	4.1	3.12	A	71.89	68.11
	4.1	3.21	A	72.10	68.94
	4.1	3.22	A	71.63	67.09
	4.1	4.01	A	88.04	84.23

Braking Efficiencies



Configuration	Variation	Train Type	Efficacy. at .1 g's (%)	Efficacy. at .4 g's (%)
4.1	4.02	A	60.51	56.17
4.1	5.00	A	72.66	71.11
4.1	7.11	A	39.85	32.15
4.1	7.12	A	44.75	26.57
4.1	7.13	A	33.71	27.71
4.1	7.21	A	74.40	64.44
4.1	7.22	A	52.00	43.26
4.1	7.23	A	52.82	46.25
4.1	7.24	A	52.00	43.26
4.1	7.25	A	52.00	43.26
4.2	1.00	A	77.91	60.80
4.2	1.01	A	69.22	56.19
4.2	2.01	A	74.13	57.10
4.2	2.02	A	84.64	67.80
4.2	3.00	A	76.60	55.83

